# Mapping Soil Physical Structure of an Agricultural Field for Assessing Potential Leaching Risk

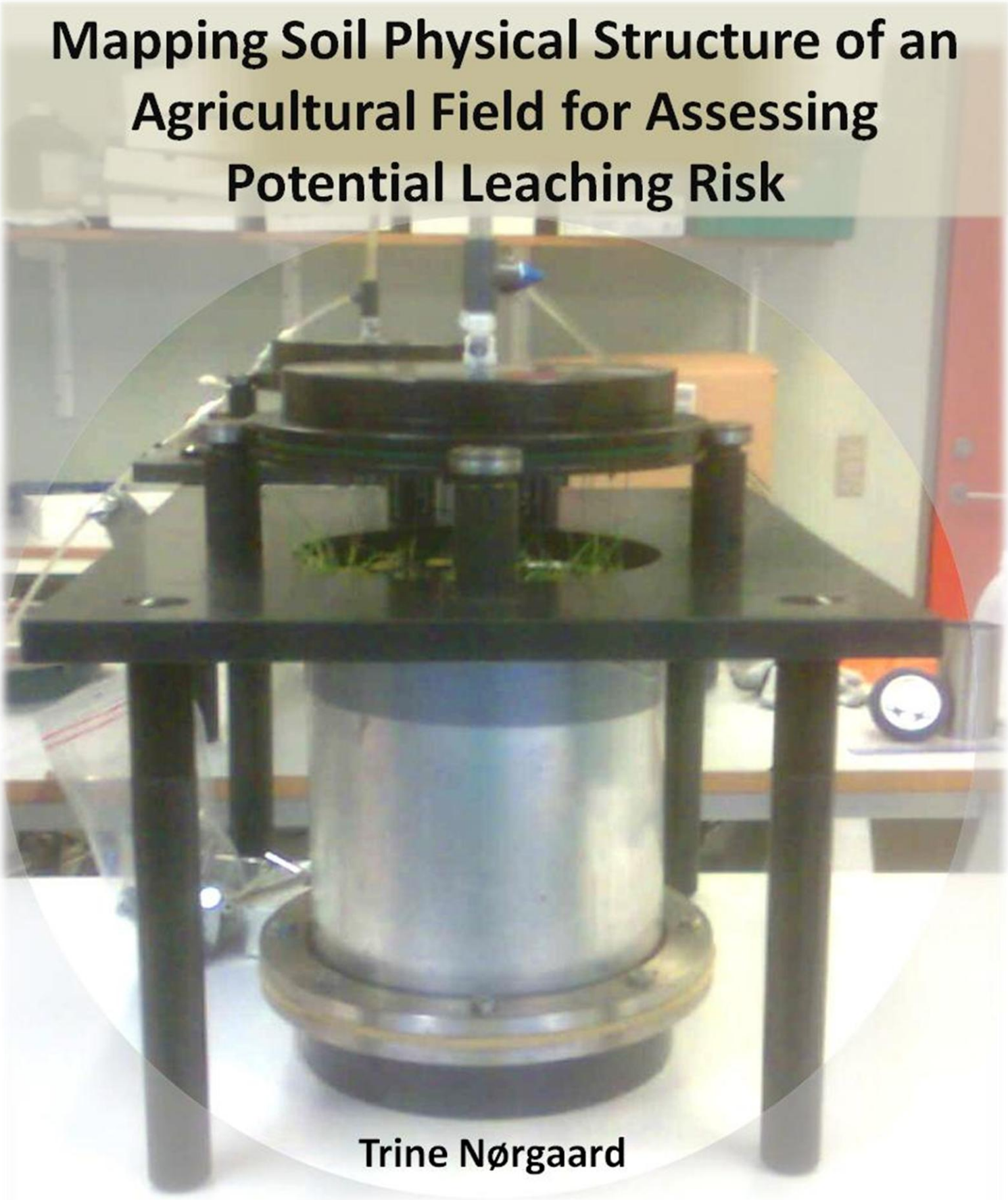

Trine Nørgaard

Master Degree Project in
Environmental Engineering
Aalborg University
September 2010 – June 2011

**Supervisors:**
Per Møldrup
Lis Wollesen de Jonge
Preben Olsen

**Title:**

# Mapping Soil Physical Structure of an Agricultural Field for Assessing Potential Leaching Risk


## Aalborg University
Department of Biotechnology, Chemistry and Environmental Engineering


**Project period:**
September 1th 2010 – June 1th 2011


**Student:**

Trine Nørgaard

**Supervisors:**
Per Møldrup (AAU)
Lis Wollesen de Jonge (DJF)
Preben Olsen (DJF)


**Copies:** 4

**Page number:** 88

**Appendixes:** 14

**Delivery date:** 01.06.2010


**Synopsis:**
The aim of the present thesis is to develop a tool for risk- and vulnerability assessments on field scale evaluating the leaching of pesticides and other contaminants applied in agriculture. The project is part of the Danish Pesticide Leaching Assessment Programme (PLAP), and focus is on a field in Silstrup in the north-western part of Jutland.

Leaching experiments is carried out on undisturbed soil columns sampled from a rectangular 15x15 m grid from the field. The columns are irrigated at an intensity of 10 mm $h^{-1}$ for ~6.5 hours. A tracer is applied to the columns as an impulse for 10 minutes to understand the transport of water through the soil, and colloid concentrations was measured in the effluent as a function of time to evaluate the colloid-facilitated transport mechanisms. Phosphorus is used as a model compound as an example of a strong sorbing contaminant.
The soil texture is determined on bulk soil sampled adjacent to the soil columns.

A large amount of colloids was leached during first flush, and the risk for colloid-facilitated transport of contaminants is enhanced by the amount of mobilised colloids and the presence of macropores.
It was possible to identify special vulnerable areas on field scale from a simple leaching setup and soil texture analyses. The highly structured soil in Silstrup allows for colloids-facilitated transport to take place, and the leaching of phosphorus was positively correlated to the leaching of particles.
Opposite other studies it was not possible to relate the leaching of particles to the clay content of the soil.
From 5% tracer arrival time, tracer mass balance and soil bulk density it was possible to characterise the soil structure within the field in Silstrup.


AALBORG UNIVERSITET

Aarhus University
Faculty of Agricultural Sciences

# Preface

This thesis is a Master Degree project from the Department of Biotechnology, Chemistry and Environmental Engineering at Aalborg University in the period from September 1th to June 1th. The thesis is made in corporation with the Faculty of Agricultural Science, Foulum, and most of the project was carried out here.

Sections, subsections, tables and figures in the report are numbered according to the order they occur. The captions of all tables are given above the tables. The captions of all figures are given below. The appendices at the end of the report are alphabetically marked. When referring to an appendix in the text the letter will be included, for example (Appendix A).
References are made inside a pair of parentheses with the name of the author(s) and the year of publications, e.g. (Lindhardt et al., 2001). More details about the references can be found in the reference list.

In November I attended the *1ST International Conference and Exploratory Workshop on Soil Architecture and Physico-Chemical Functions, "Cæsar"*. For the conference I submitted an abstract that can be seen in Appendix M and the poster I made representing this project (at an early stage) is shown in Appendix N.

According to plan I'm suppose to start a PhD on August 1th this year. The PhD will be a continuation of this master project and data/information yet not measured or treated will be considered further during that project. Additional plans for the PhD project is presented in the perspectives.

I would like to give a special thanks to the technical staff at Foulum for helping in the field and in laboratories throughout the project period. It wouldn't have been possible to obtain the large amount of data presented in this thesis without their help. Also I would like to thank Anders Lindblad Vendelboe for guidance throughout the project period, and my supervisors Preben Olsen, Lis Wollesen de Jonge and Per Møldrup.

# Table of Contents

**1 Introduction and initial problem analyses ..... 1**

1.1 Transport mechanisms in pesticide transport through the soil profile ..... 4

1.2 The Danish Pesticide Leaching Assessment Programme (PLAP) ..... 7

1.3 Silstrup ..... 8

1.3.1 Soil physical structure ..... 11

1.3.2 New pesticide findings at Silstrup ..... 12

**2 Project objective ..... 17**

2.1 Field-scale leaching experiments ..... 17

2.2 Field-scale texture analyses ..... 17

**3 Materials and methods ..... 19**

3.1 Leaching experiment ..... 19

3.1.1 Sampling procedure ..... 19

3.1.2 Leaching experiment ..... 21

3.2 Texture analyses ..... 23

3.2.1 Sampling procedure ..... 23

3.2.2 Texture analyses ..... 24

3.2.3 NIR ..... 24

**4 Results and discussion ..... 25**

4.1 Soil-air parameters: air permeability, air-connected porosity, and total air-filled porosity ..... 25

4.1.1 Air permeability ..... 25

4.1.2 Air-connected porosity ..... 26

4.1.3 Air-filled porosity ..... 26

4.1.4 Soil-air parameter correlations ..... 27

4.1.5 Highlights in soil-air parameters ..... 29

4.2 Soil texture ..... 30

4.2.1 The Dexter Index, n ..... 31

4.2.2 Highlights in soil texture ..... 32

4.3 Water transport ..... 32

4.3.1 Outflow ..... 33
4.3.2 pH ..... 33
4.3.3 Electrical conductivity ..... 33
4.3.4 Highlights in water transport ..... 34
4.4 Particle leaching ..... 34
4.4.1 Leached particle concentrations ..... 34
4.4.2 Accumulated particle leaching ..... 37
4.4.3 Particle leaching and parameter correlations ..... 41
4.4.4 Highlights in particle leaching ..... 43
4.5 Tracer (tritium) breakthrough curves ..... 43
4.5.1 5% arrival time and tritium recovery ..... 45
4.5.2 Tritium breakthrough curves and parameter correlations ..... 46
4.5.3 Highlights in tritium breakthrough curves ..... 50
4.6 Phosphorus leaching ..... 51
4.6.1 Total phosphorus and total dissolved phosphorus ..... 51
4.6.2 Particular phosphorus ..... 52
4.6.3 Particular phosphorus and parameter correlations ..... 54
4.6.4 Highlights in phosphorus leaching ..... 55

**5 Vision analyses: towards a mapping-based risk and decision tool ..... 57**

**6 Conclusions ..... 59**

**7 Perspectives for continued research ..... 61**

**8 Reference list ..... 63**

# Appendix list

**Appendix A** ..... **67**
**Appendix B** ..... **69**
**Appendix C** ..... **70**
**Appendix D** ..... **71**
**Appendix E** ..... **72**
**Appendix F** ..... **73**
**Appendix G** ..... **76**
**Appendix H** ..... **79**
**Appendix I** ..... **80**
**Appendix J** ..... **81**
**Appendix K** ..... **82**
**Appendix L** ..... **83**
**Appendix M** ..... **84**
**Appendix N** ..... **88**

# 1 Introduction and initial problem analyses

Pesticides are a class of toxic xenobiotic organic compounds applied to extensive areas of soil in both rural and urban settings in order to protect plants from unwanted weeds and deleterious organisms like insects and fungicides. Pesticides are mainly applied in order to improve the crop yield and keep roads, railways, and private gardens free of unwanted weeds. Pesticides can generally be separated up into three classes: insecticides, herbicides, fungicides (Hedemand and Strandberg, 2009). Pesticides are often toxic to humans and animals. Together with the precipitating water pesticides can leach through the soil and to the groundwater, if it is not degraded nor sorbed to organic matter or clay minerals. Most pesticides are relatively biodegradable in the environment, while others are found to be very persistent, and therefore not degradable. The upper soil layer has a natural inherent ability to degrade pesticides because of the large amount of microorganisms in this upper layer. While some pesticides are completely degraded others are only partly degraded into their degradation products. Not all degradation products are known, and often there is a lack of knowledge on how these degradation products behave in the environment. The fate of pesticides applied to the environment is described in Figure 1.

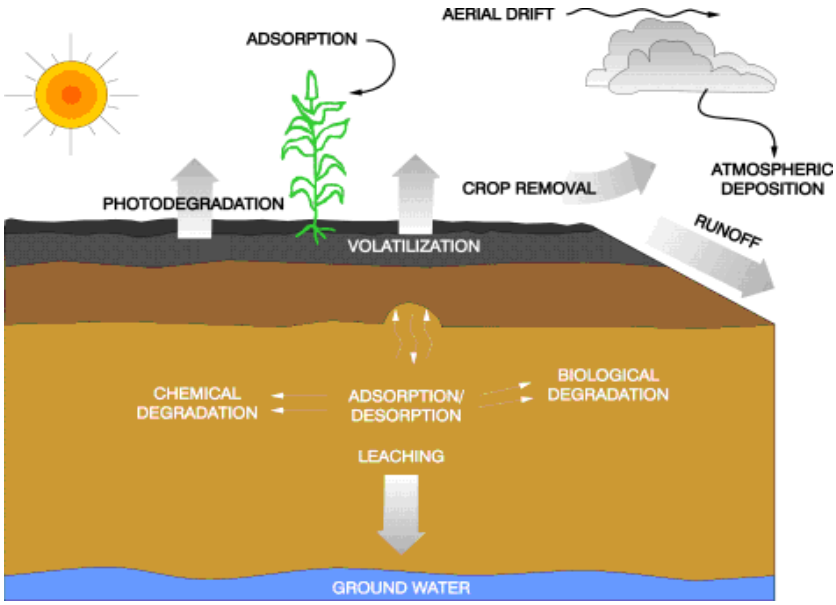


**Figure 1. General overview over the fate of pesticides in the environment (de Jonge, 2011).**

The pesticide leaching risk depends on the properties of the applied pesticide, but also on the properties of the soil whereto the pesticide is applied, and the climatic conditions while the pesticide is being applied. Sandy soil or cracked loamy soil might increase the movement of water, and solutes down to the groundwater, and even though the pesticides are sorbed it doesn't mean that they don't leach to the groundwater. The leaching is just being delayed due to slow desorption or accelerated due to colloid-facilitated transport (GEUS, 2010b).

During the nineties there was an increase in the detections of pesticides and pesticide degradation products in drinking water wells. This increase was a consequence of the fact that drinking water collected from the higher unconfined aquifers is generated after 1950, and thus it is more affected by the imprudent use of pesticides during the last 60 years. Besides that there was an increase in the amount of analyses carried out, and

an increase in the number of pesticides and degradation product analyzed for (GEUS, 2009). Figure 2 shows the development in pesticides and degradation products found in water works wells since 1993.

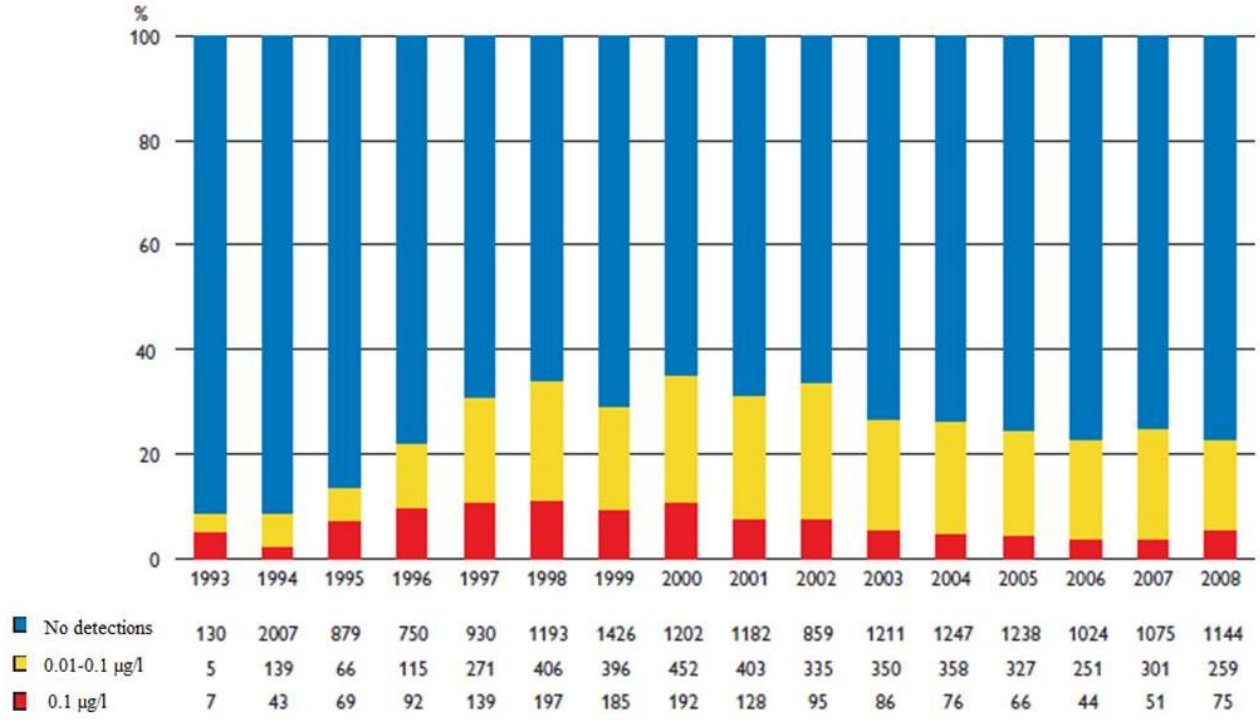


**Figure 2. Detections of pesticides and pesticide degradation products in water works wells per year in the period 1993-2008. Number of wells in each of the three classes (no findings, 0.01-0.1 µg/l and >0.1 µg/l) are listed below the figure. Modified from (GEUS, 2009).**

From 1993 to 2008 23,565 analyses were carried out from 6,632 different wells, and pesticides were found in 25 % of the wells. As seen on Figure 2, pesticide detections in water works wells during the last ten years has decreased. The decrease in pesticide findings above 0.1 µg/l is more likely due to the fact that contaminated wells are taken out of operation after the detection of pesticides more than it is because of the number of wells contaminated with pesticides has decreased (GEUS, 2009). In-situ remediation techniques like pump and treat are launched in order to contain the contamination and prevent the pesticides from spreading, but the methods are expensive and depends on the sorption properties of the contaminant, and the hydraulic conductivity of the aquifer (Loll and Moldrup, 2000) and (NIRAS, 2005).

The increase in detections of pesticides during the nineties caused several drinking water wells to shut down as shown in Figure 3. In the period from 1994 to 2001 it is assumed that approximately 100-150 drinking water wells was closed down per year (GEUS, 2009).

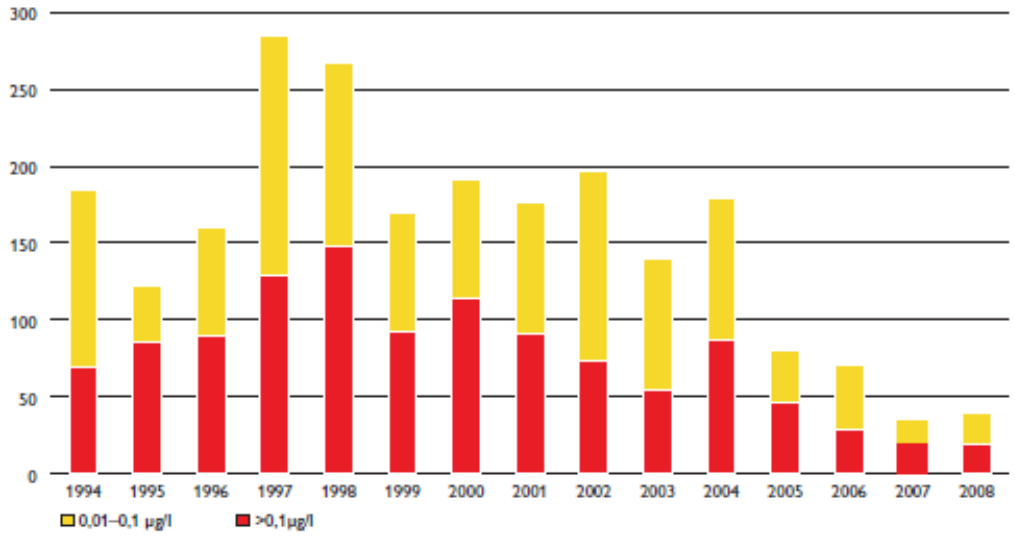


**Figure 3. Number of water wells closed because of pesticide contamination in the period from 1994-2008 (GEUS, 2009).**

The problem with increasing pesticide detections caused an increase in the public awareness about the use of pesticides and the need for thorough investigations on the area.

In order to maintain a supply of drinking water based on the extraction of clean groundwater, and no water treatment it was, and still is important to maintain surveillance by drilling controls and monitoring programs (GEUS, 2009).

The parliament convened in 1997 the Bichel-Committee in order to clarify the possibilities in reducing or phasing out the use of pesticides in agriculture. As a consequence of the conclusion made in the Bichel-committee Pesticide Action Plan II (Pesticidhandlingsplan II) was established in 2000 (mst, 2010) and later on Pesticide Action Plan 2004-2009 was established. In general the pesticide action plans aims at reducing pesticide treatment frequencies, protecting areas sensitive to pesticide leaching and expanding areas with ecological production (Miljø- og Energiministeriet, 2000).

The use of pesticides in Denmark is legislated according to Executive Order (Bekendtgørelse) no. 242 of 31/03/2011. This Order covers compounds that appear in the EU frame directive 2009/128/EF of 21/10/2009 (also called the Pesticide Directive or Plantebeskyttelsesmiddeldirektivet). The aim of the pesticide directive is to establish a sustainable frame for the use of pesticides in EU. Compounds in Executive Order no. 242 have to be approved before sale, import and use in Denmark according to Executive Order no. 878 of 26/06/2010 about chemical compounds and products. Classification, packing, labelling, sale and storage has to be carried out according to Executive Order no. 50 of 12/01/2011. The decision about whether the compound should be approved is made by the Danish EPA (Miljøministeriet). According to the Council Directive 98/83/EC of November 3$^{th}$ 1998, about water quality for human consumption, the concentration of individual pesticides (or relevant metabolites) in a groundwater sample must not exceed 0.1 µg $L^{-1}$ and the total sum of all pesticides (or metabolites) must not exceed 0.5 µg $L^{-1}$.

According to §62 in Executive Order no. 242 the Danish EPA and the Plant Directorate are responsible for supervision and control in compliance with the provisions. The municipalities assists EPA with supervision regarding use, storage and labelling; the staff handling the pesticides should have a valid certificate in handling the pesticides, and the compounds should be stored safely in a closed room in original packing with correct labelling.

Despite legislation and authorisation procedures within the area pesticides are still detected in drinking water wells. This might be due to the fact, that the legislation is not entirely updated with the knowledge that exists within the area of soil physics and pesticide leaching. The soil profile in which the pesticides exist in is complicated, as can be seen from the next section, and varies from location to location throughout the countries making it hard to formulate and practice the correct legislation.

## 1.1 Transport mechanisms in pesticide transport through the soil profile

Highly sorbing contaminants like pesticides are usually retarded by sorption in the upper soil matrix layer where they are sorbed and degraded either completely or partly into their representative degradation products. However, the release of subsurface colloids contributes to fast colloid-facilitated transport of the contaminants (de Jonge et al., 2004a). Thus, strongly sorbing contaminants may be mobilised and leached to the groundwater without any degradation.

Colloids are defined as negatively charged minerals like clay and organic matter with a particle size ranging from 1 nm to 10 µm, see Figure 4.

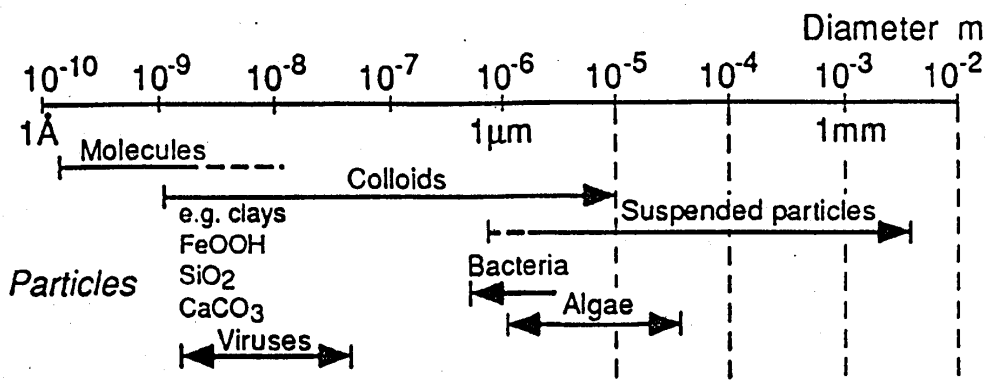


**Figure 4. Diameter range of particles in the subsurface environment (de Jonge, 2011).**

The negative surface charge of colloids and their large surface area makes them very attractive as sorbing agents for hydrophobic organic contaminants with low solubility and high sorption properties (Kretzschmar et al., 1999).

Villholth et al., (2000) concluded that both particle and pesticide leaching are associated with the initial phase of individual flow events, indicating a rapid transport through the macropores in the soil profile. Macropores are widely distributed in the soil profile (see Figure 5) and provides preferential pathways from the root zone down to the groundwater.

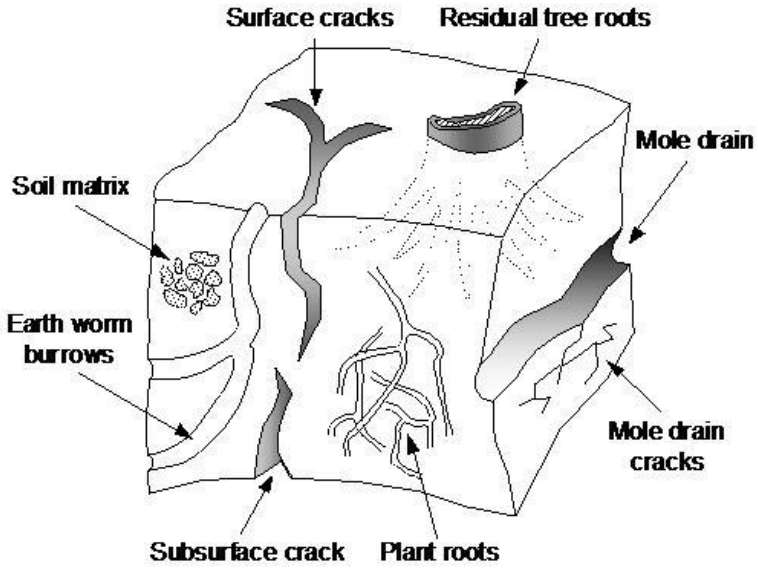


**Figure 5. A soil volume showing the heterogeneity in natural soil systems and the different kinds of macropore channels (Loll & Moldrup, 2000).**

In order for colloid-facilitated transport to take place at least three important parameters should be fulfilled:

1. The colloids should be stable and mobilised in suspension
2. The contaminants should sorb strongly to the colloids
3. A transport of colloids should take place

Mobilisation of natural occurring colloids can occur during soil tillage or strong rainfall events that change the soil solution chemistry. Particle release in most soil is favoured by high pH, high $Na^+$ saturation, and low ionic strength (Kretzschmar et al., 1999).

Pesticides can be dissolved in the percolating water or sorbed to either the soil matrix or the colloidal particles that moves with the flowing water, see Figure 6.

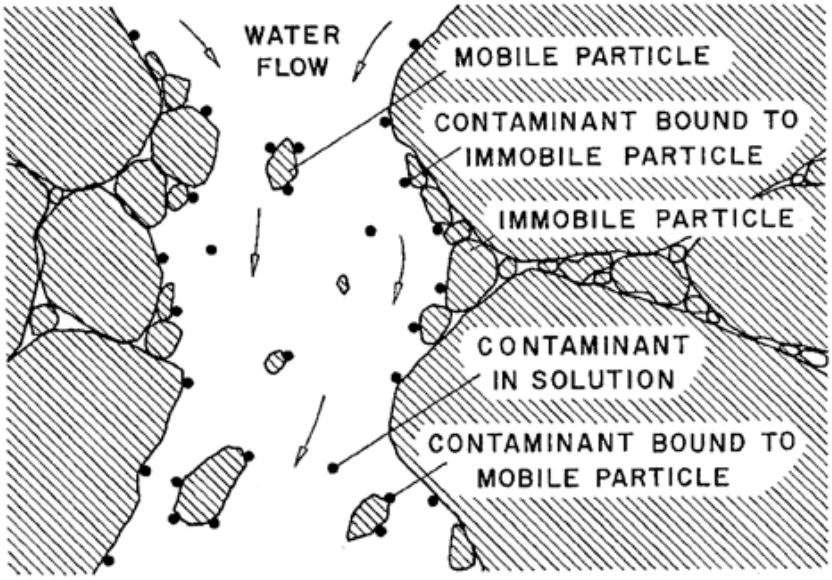


**Figure 6. Colloid-facilitated contaminant transport in the soil (de Jonge, 2011).**

The sorbing properties or the mobility of the pesticide depend on its $K_{oc}$ coefficient [L water (kg OC)$^{-1}$] (organic carbon partitioning coefficient) - the smaller the $K_{oc}$ value, the greater the concentration of the pesticide in solution. $K_{oc}$-values are estimated from the linear distribution coefficient, $K_d$ [L kg$^{-1}$], and the fraction of organic carbon in the soil, $f_{oc}$ [–] (Loll & Moldrup, 2000):

$$K_{oc} = \frac{K_d}{f_{oc}} \qquad \textbf{(Eq. 1)}$$

Pesticides with high $K_{oc}$-coefficients are expected to sorb to the immobile soil matrix thus having time for degradation. However colloid-facilitated transport limits the retention time in the upper soil matrix preventing the pesticides from being completely nor partially degraded. Pesticides are primarily degraded or broken down over time by microbial- or physiochemical reactions in the top soil, and the degradation time is increased when and if the pesticides leach to depths without any microbial activity and oxygen. The degradation is expressed by the half-time, $DT_{50}$ which is a measure of the time it takes 50 percent of the parent compound to break down. $DT_{50}$ is in practice often derived from the first order degradation rate constant, $K_1$ [h$^{-1}$] (Loll & Moldrup, 2000):

$$DT_{50} = \frac{ln\,(2)}{K_1} \qquad \textbf{(Eq. 2)}$$

As the pesticides degrade, some of them produce intermediate substances (degradation products or metabolites) whose biological activity may also have an impact on the environment, and whose toxic properties might be worse than the parent pesticide. Some degradation products are still unknown and their properties and behavior in soil is therefore unknown. Compounds with an extremely long degradation time are considered persistent in the environment. Persistent compounds disperse into the environment without being degraded.

In order to explain the transport of pesticides glyphosate and fluazifop-P-butyl are chosen as examples. The two pesticides have different properties regarding sorption and degradation, Table 1. The chosen pesticides are both systemic herbicides used in agriculture where they are absorbed through the leaves of the plants.

**Table 1. Typical values for glyphosate and fluazifop-P-butyl from the Pesticide Properties Database (UH, 2011).**

| | **Used in e.g.:** | **$K_{oc}$ [ml g$^{-1}$]** | **Typical field half-time, $DT_{50}$ [days]:** |
|---|---|---|---|
| Glyphosate | Roundup | 21699 | 12 |
| Fluazifop-P-butyl | Fusilade Max | 3394 | 1 |

Because of the high $K_{oc}$-values glyphosate sorbs tightly to soil organic matter, and the pesticide is mainly degraded by microorganisms in the top soil. It was previously assumed the ability of glyphosate to sorb made this compound stay in the upper soil matrix long enough for it to be almost degraded. Never the less new findings indicate that both glyphosat and its degradation product AMPA are leached to the groundwater (GEUS, 2009) and (GEUS, 2010a). This might be due to the fact that glyphosate is sorbed to the mobilized colloids, and thus the microorganisms don't have enough time for degradation. Fluazifop-P-butyl on the other hand is more likely to be dissolved in the percolating water instead of absorbing to the soil matrix. Fluazifop-P-butyl is mainly degraded by hydrolysis, and the half-time is only one day indicating that Fluazifop-P-butyl doesn't have to sorb for a longer period of time before it degrades.

In order to understand the pesticide transport leaching mechanisms thoroughly and being able to transfer the knowledge and results gained from laboratory and field experiments to the Danish pesticide legislation, initiatives like The Danish Pesticide Leaching Assessment Programme is established.

## 1.2 The Danish Pesticide Leaching Assessment Programme (PLAP)

The Danish Pesticide Leaching Assessment Programme (PLAP) was initiated in 1998 with the purpose to monitor the leaching of pesticides and their degradation products, and analyse whether the applied pesticides leach to the groundwater in unacceptable concentrations. The program was established after an increase in the detection of pesticides and degradation products in monitoring screens in the period from 1993-1998 reported by The Danish Groundwater Monitoring Programme (GRUMO) (GEUS, 2000). PLAP should serve as a warning system providing the authorities with scientific basis for registration of pesticides.

When established, PLAP consisted of six test sites located different places in Denmark, representing the dominant soil types and climate conditions, Figure 7. The sites are grown as conventional arable fields as part of a routine agricultural practice in accordance with current regulations. This means that the pesticides are applied to the fields in the prescribed manner in maximum permitted dose, and that the findings are evaluated according to the pesticide detection criteria on 0.1 µg/l 1 m below ground surface (b.g.s) (Lindhardt et al., 2001).

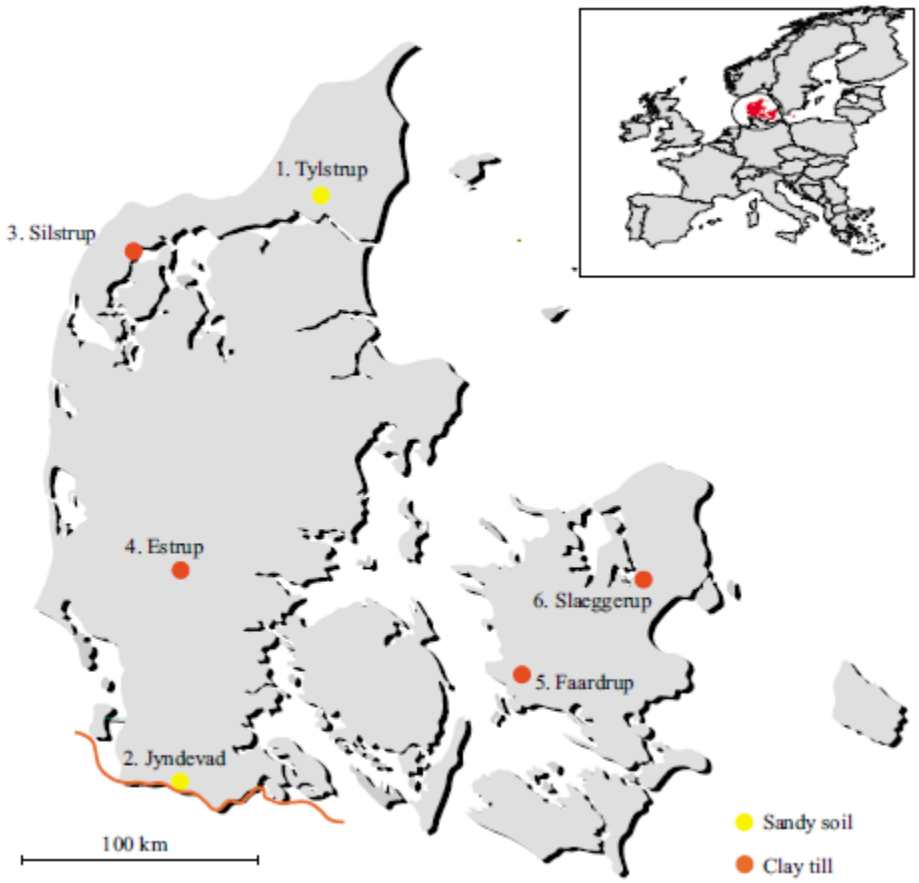


**Figure 7. Location of the six text sites in Denmark (Lindhardt et al., 2001). Monitoring at Slaggerup was terminated in 2003.**

Each test site was characterised and equipped during 1999 and monitoring was initiated at the test sites during 1999 and 2000. The characterisation included information about the site area e.g. size, history and for practical reasons site access. A short description of some of the analyses carried out and equipment installed at the six test sites is given in Appendix A.

Besides all the information that is collected automatically and continuously since 1999 information about cultivation history has been noted thoroughly – in one field since 1983. This includes e.g. which crops, nutrients and pesticides are applied, how they are applied, at which time they are applied, under which field conditions, and in which amounts they are applied.

The concentrations of pesticides and selected degradation products are measured on collected water samples from vertical monitoring wells, horizontal screens (both monthly sampling) and drains (weekly sampling).

The installations at the test sites allow for continuous monitoring and sampling and together with the cultivation history this makes an ideal base for evaluating the leaching of e.g. pesticides and nutrients. The monitoring data are supported by a hydrological model simulating water flow in the unsaturated zone at each site and an annual mass balance. Each year the newest data is collected, evaluated and published in a report by GEUS. With the latest report, Rosenbom et al.,(2010), PLAP evaluates the leaching risk of 40 pesticides and 27 metabolites, but of course the programme is restricted to evaluate the risk of know metabolites – it is not possible to monitor compounds that we do not know exists.

## 1.3 Silstrup

The field in Silstrup is one of the six test sites in PLAP. The field is located in the North-western part of Jutland and consists of clay till, Figure 8.


**Figure 8. Location of the test field in Silstrup. Modified from (Lindhardt et al., 2001).**

Management practice applied to the field in Silstrup in the period from December 2008 to September 2010 is shown in Table 2.

**Table 2. Management practive applied to the field in Silstrup from December 2008 to September 2010.**

| Date: | Management practice: |
|---|---|
| 15-12-2008 | Ploughed – depth 23 cm |
| 30-3-2009 | Harrowed two times across – depth 5 cm |
| 11-4-2009 | Rolled |
| 11-4-2009 | Sowing with spring barley and undersown with red fescue |

Thus no soil management has been applied to the field since the 30$^{th}$ of March 2009 – the field has been with Red Fescue ever since.

Information about the site area is given in Table 3 and all the installations on the field are shown in Figure 9. The installation setup represents a typical design of a PLAP field. Note the different abbreviations for the vertical monitoring wells (M) and the horizontal screens (H1 and H2). The tile-drains is noted D.

**Table 3. Site characteristics of the field in Silstrup (Lindhardt et al., 2001).**

| | |
|---|---|
| Length and width of the test field | 185 m x 91 m |
| Total area of the site, incl. buffer zone | 3.3 ha |
| Area of the test field | 1.69 ha |

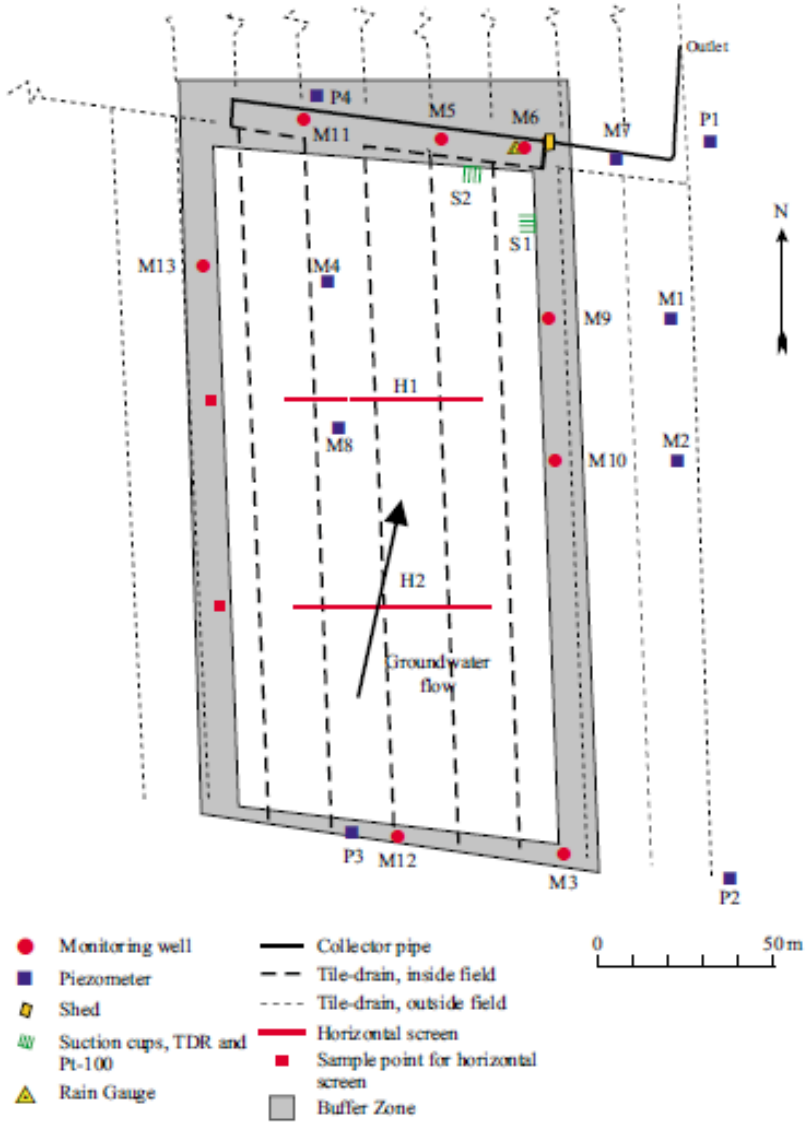


**Figure 9. Sketch showing the technical installations, buffer zone and groundwater direction at the field in Silstrup. The five parallel tile-drains that run inside the field from south to north are connected to a transverse collector pipe in the northern end of the field. The test pit, mentioned in Appendix A, in Silstrup is located outside the buffer zone in the in the north-eastern corner of the area and the two excavated soil profiles are located in the same place as the suction cups (Lindhardt et al., 2001).**

To the east there is a neighbour field grown in the exact same way as the actual field. Form this field is it possible to sample without disturbing the physical structure of the field.

The monitoring wells (M1-M13) each have screens in the four different depths shown in Table 4. The horizontal sampling wells H1 and H2 are 58 m long and each consists of three 18 m screen sections.

**Table 4. ID and depth of screens in the vertical monitoring wells (Lindhardt et al., 2001).**

| No./ID: | Depth (m b.g.s): |
|---|---|
| 1 | 1.5-2.5 |
| 2 | 2.5-3.5 |
| 3 | 3.5-4.5 |
| 4 | 4.5-5.5 |

The measured precipitation, groundwater table and drain water runoff is shown in Appendix B together with the simulated estimation of these data.

### 1.3.1 Soil physical structure

Results from the total organic carbon mapping of the topsoil (0-25 cm depth) in Silstrup indicate that the highest TOC contents are found in the southern end of the field, Figure 10. EM-38 (Figure 11) indicates that the highest clay contents are located in the northern end of the field. The two gradients run in opposite directions.

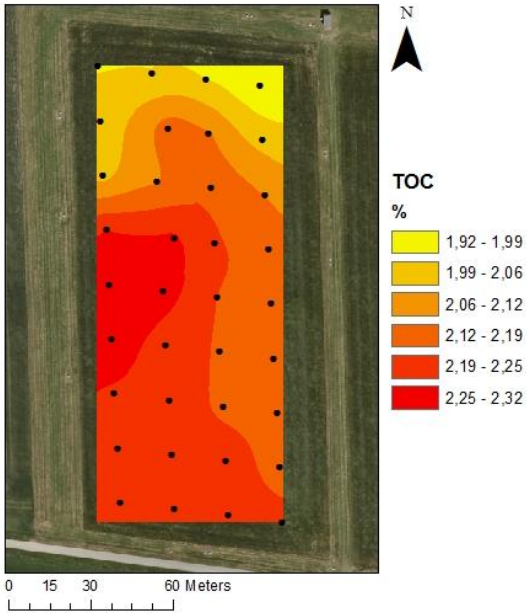


**Figure 10. Contour map showing the TOC content in the top soil (0-25 cm). The sampling points are shown with black dot. Modified from Lindhardt et al., (2001).**

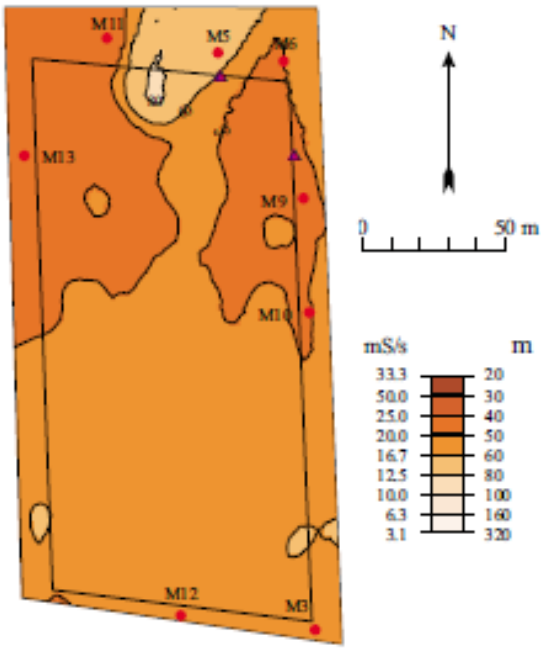


**Figure 11. Contour map showing the resistivity measured with EM-38 in one meters penetration depth as an expression for the clay content across the field (Lindhardt et al., 2001).**

The test pit in Silstrup was excavated just outside the buffer zone in the in the north-eastern corner of the site area. Grain size analyses from the test pit and from seven different wells indicate that the clay content is ranging from 28% to 36%. From the same samples points, the content of TOC was ranging from 0.14% to 2.1% (Lindhardt et al., 2001).

In the upper half of the field the clay minerals are expected to be less stable because of the limited amount of TOC present to form stable soil aggregates. Therefore it is expected, that the colloid-facilitated transport risk is largest in the upper half of the field, while the risk should be considerable lower in the southern part of the field where the aggregates are stabilised by the larger amount of TOC present.

### 1.3.2 New pesticide findings at Silstrup

The report published by GEUS in 2010 - *Monitoring results May 1999-June 2009*, reveals new pesticide findings from the field in Silstrup. A clear connection between the application of the herbicide Fusilade Max and detection of the degradation product downstream in monitoring wells, horizontal screens and drains reveals an until now unknown degradation pathway and soil behaviour for Fusilade.

Fusilade was applied to the field in Silstrup for the first time in June 2000 in the form of Fusilade X-tra. The active compound in Fusilade X-tra is fluazifop-P-butyl and the pesticide was applied in the maximum permitted dose, 1.5 l/ha (250 g fluazifop-P-butyl per litre). Due to the fact that fluazifop-P-butyl degrades relatively fast the leaching risk is associated with its degradation products fluazifop-P and 5-(trifluoromethyl)-2(1H)-pyridinone (TFMP), see Figure 12 (Mills and Simmons, 1998) and (Tu et al., 2001).

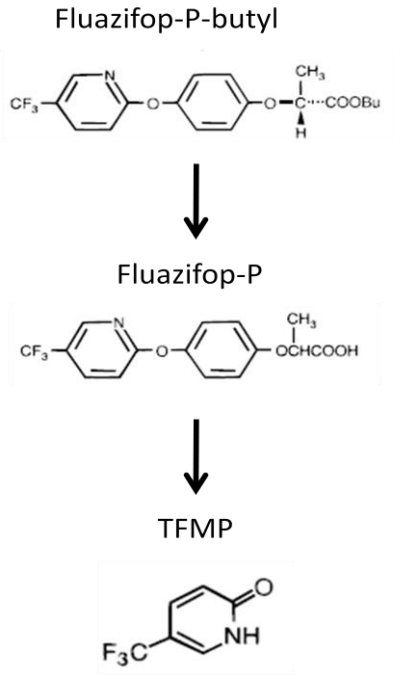


**Figure 12. Degradation pathway for Fluazifop-P-butyl. Modified after (Mills & Simmons, 1998).**

In 2000 after the first application of Fusilade, focus was mainly on the degradation product fluazifop-P because this compound was considered the main degradation product. For that reason only fluazifop-P was analysed for, but neither found in drain water nor groundwater. On July 1$^{th}$ 2008 fluazifop-P-butyl was applied to the field in Silstrup again, this time as Fusilade Max, but still in the maximum permitted dose, 3.0 l/ha (125 g fluazifop-P-butyl per litre). TFMP was now included in the analyses, and on August 7$^{th}$ TFMP

was detected for the first time in monitoring well no. 5 1.5-2.5 m b.g.s. in concentrations exceeding 0.1 µg/l - see Figure 13 and Figure 14 for TFMP concentrations detected in monitoring screens and drain water runoff respectively. Fluazifop-P was still included in the analyses but not detected, see Figure 13 and Figure 14 (Rosenbom et al., 2010).

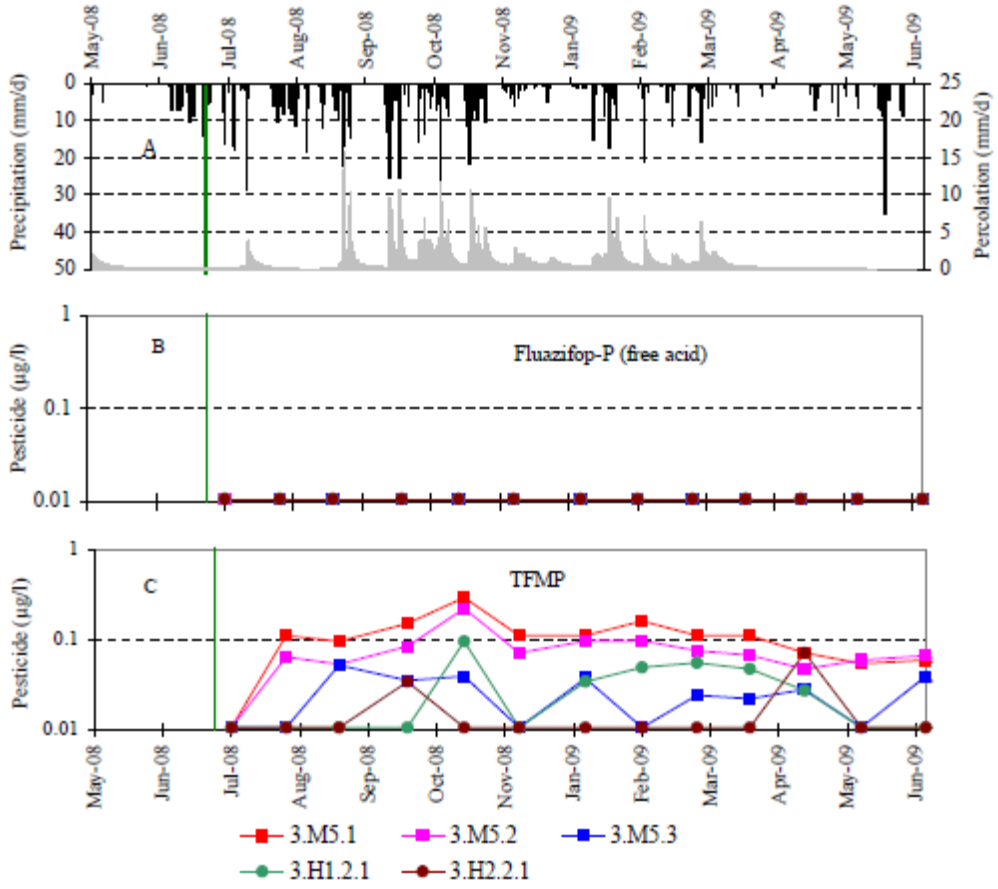


**Figure 13. Measured precipitation (black) and simulated percolation (grey) in the period May 2009 to June 2009 (A). Concentrations of fluazifop-P and TFMP in groundwater monitoring screens after application of Fusilade Max to the field in Silstrup on July 1th 2008 (green line) (B) and (C). The dotted line indicate the criterion for pesticides 1 m b.g.s. on 0.1 µg/l (Rosenbom et al., 2010).**

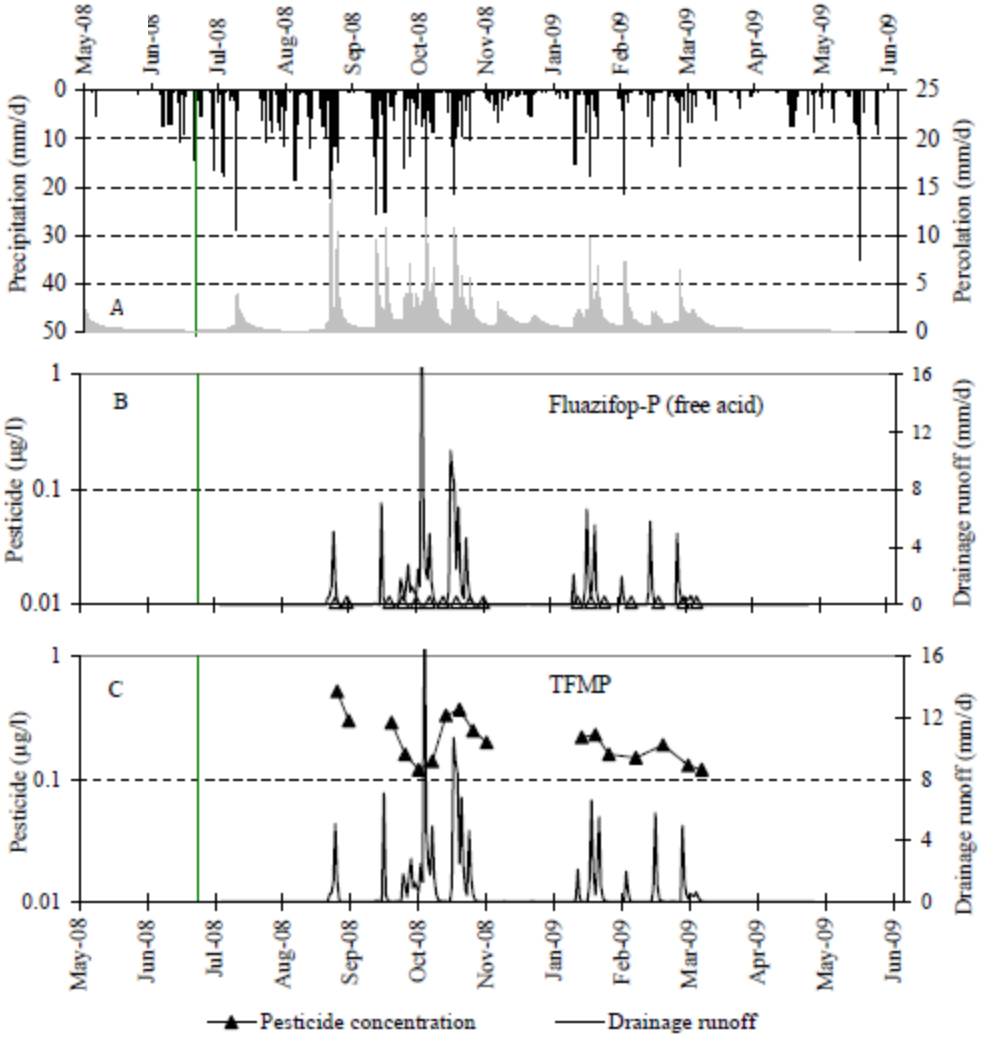


**Figure 14. Measured precipitation (black) and simulated percolation (grey) in the period May 2009 to June 2009 (A). Concentrations of fluazifop-P and TFMP in drain water runoff after application of Fusilade Max to the field in Silstrup on July 1th 2008 (green line) (B) and (C). The dotted line indicate the drinking water criterion on 0.1 µg/l and open symbols indicate pesticide concentrations below the detection limit on 0.01 µg/l (Rosenbom et al., 2010).**

Detection of TFMP after August 7th in the different screens and drain across the field is shown Appendix D.

The detection of TFMP when it was included in the analyses, confirms the statement made previously; it is not possible to monitor compounds that we do not know exists. According to the Pesticide Property Data Base fluazifop-P can form seven known metabolites. The cost and time if all metabolites, from all 40 pesticides applied in PLAP, had to be analysed, would be too big.

Fluazifop-P-butyl is mainly degraded through hydrolysis and to some extend by microbial degradation. As mentioned before, fluazifop-P-butyl is slightly mobile (UH, 2011). The degradation product fluazifop-P is also herbicidically active, is degraded through microbial degradation, and is assumed to have a high or very high mobility. Opposite to fluazifop-P-butyl, fluazifop-P is very soluble in water. According to the European Food Safety Authority (2010) the degradation product TFMP is medium to moderate persistence in soil and $DT_{50}$ is said to vary between 13 and 82 days. The large interval in $DT_{50}$ and a general lack of knowledge about the compound establishes that TFMP is relatively new on the market. Basic soil physical properties for fluazifop-P-butyl, fluazifop-P and a few for TFMP can be found in Appendix E.

From a metabolite study in a new report published by the European Food Safety Authority (EFSA) (2010) TFMP, or Compound X as it is also called, was the main metabolite from fluazifop-P-butyl in soil (European Food Safety Authority, 2010).

The general idea with PLAP is to describe and characterise the five test fields in regards to transport parameters that effects the leaching of pesticides. From PLAP knowledge about pesticide leaching risks is obtained, and implemented in risk- and vulnerability assessments.

# 2 Project objective

This thesis should be seen as a small part of The Danish Pesticide Leaching Assessment Programme. The aim of the project is to create a tool for risk- and vulnerability assessments that can be used when evaluating pesticide leaching risks on field scale. Is it possible to determine vulnerable areas within a field which in relation to the total area encompasses only 20% of the field, but is responsible for 80% of the pesticide leaching?

Focus will be on the field in Silstrup with the latest discoveries of TFMP leaching making this field particularly interesting. For convenience phosphorus will be used as a model compound instead of pesticides when evaluating the colloid-facilitated transport mechanisms.

## 2.1 Field-scale leaching experiments

Leaching experiments will be carried out on undisturbed soil columns sampled both from the A- and B-horizon. The leaching experiments will be carried out with three tracers: tritium, colloids, and phosphorus. Tritium is a conservative tracer used to explain the transport of water through the columns. The leaching of colloids will be included in order to study the colloid-facilitated transport mechanisms, and phosphorus will be used as an example of an adsorbing agent with properties similar to at least some pesticides.

## 2.2 Field-scale texture analyses

According to literature the contents of clay and organic carbon has a great impact on the soil physical structure in relation to marcopores and macropore flow. From new soil texture analyses it is examined whether the contents of clay and organic carbon can be coupled to the leaching of phosphorus. Soil texture analyses and Near Infrared spectroscopy (NIR) will be carried out on bulk soil sampled across the field, and the results will be compared with the previous measurements from 1999 given in Lindhardt et al., (2001).

The large amounts of data already available from the field in Silstrup, the three tracers studied in the leaching experiment, and a study of the soil texture will end up with a tool that should identify areas especially vulnerable to leaching, and estimate potential fingerprints with an influence on contaminant leaching.

# 3 Materials and methods

## 3.1 Leaching experiment

### 3.1.1 Sampling procedure

Sixty-five 20x20 cm soil columns were sampled from the top soil in the field in Silstrup on October 10, 2010. At that time the field was cultivated with Red Fescue. To get a representative impression of the spatial variability across the field, the columns were sampled from a rectangular grid of app. 15 x 15 m as shown in Figure 15.

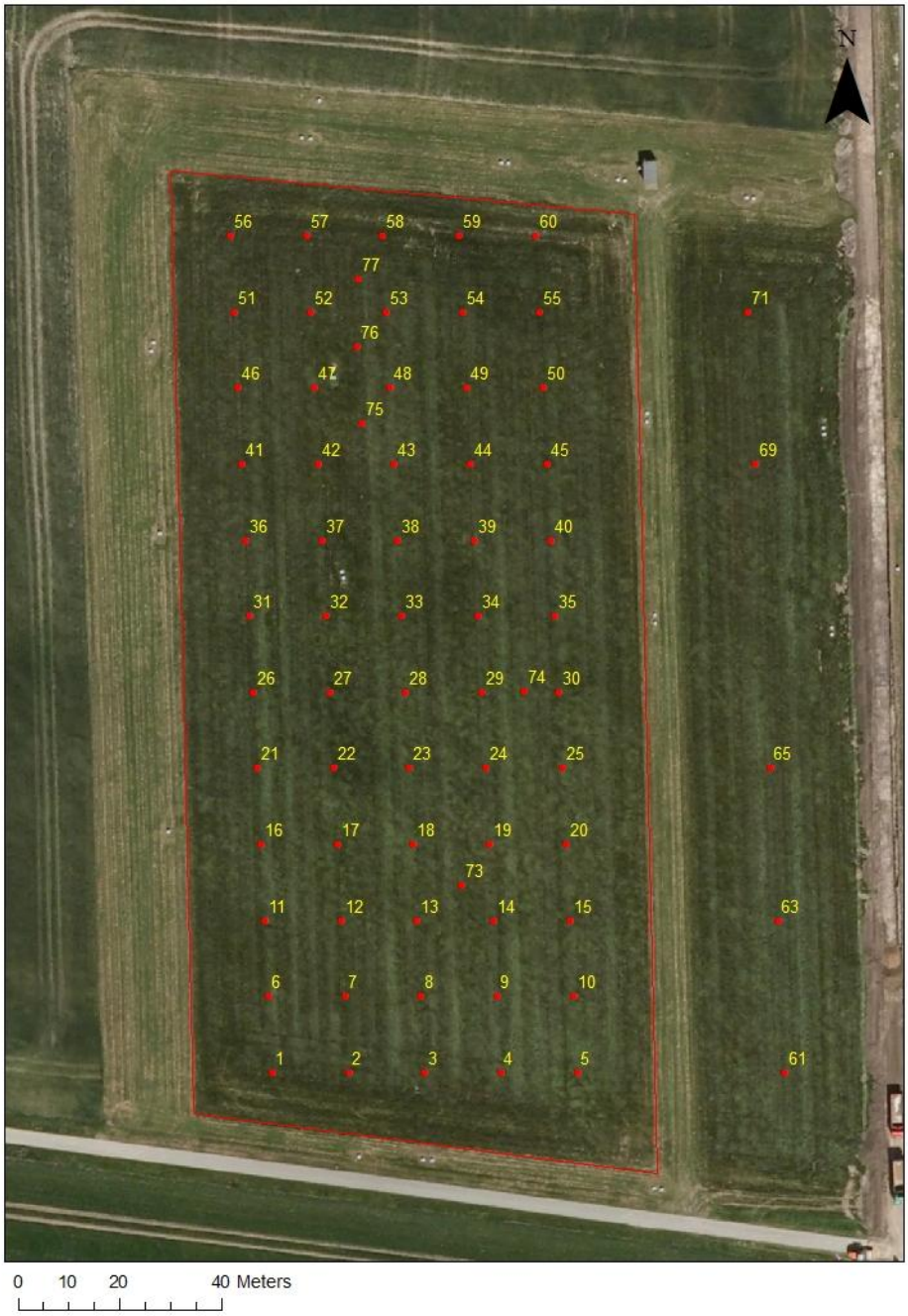


**Figure 15. Map showing the 15x15 m grid from where the columns were sampled. The assigned numbers corresponds to the column and sampling ID used further on in the thesis.**

The sampling points in the grid were placed randomly, either at the grid intersects or 1 m away from the grid intersects in random directions to avoid repeated phenomena caused by the cultivation of the field. Five of the columns were sampled from areas within the field with special interest (areas with significant differences in TOC content) according to Figure 10. The columns were pushed into the top soil with the hydraulic pressure from a tractor until the edge of the column levelled with the soil surface. The columns were carefully excavated by hand, trimmed and sealed with plastic caps.

Additionally five columns were collected from the B-horizon in the neighbouring field, see Figure 15. These columns were sampled in order to see which effect the B-horizon has on the leaching pathways. After digging down to a depth of approximately 0.5-1 meter the columns were pressed into the soil by the hydraulic press of the tractor. Once again the columns were carefully excavated, trimmed and sealed.

Further treatment of the columns when they arrived at the laboratory is shown in Figure 16 and afterwards there will be a short explanation of the leaching experiment.

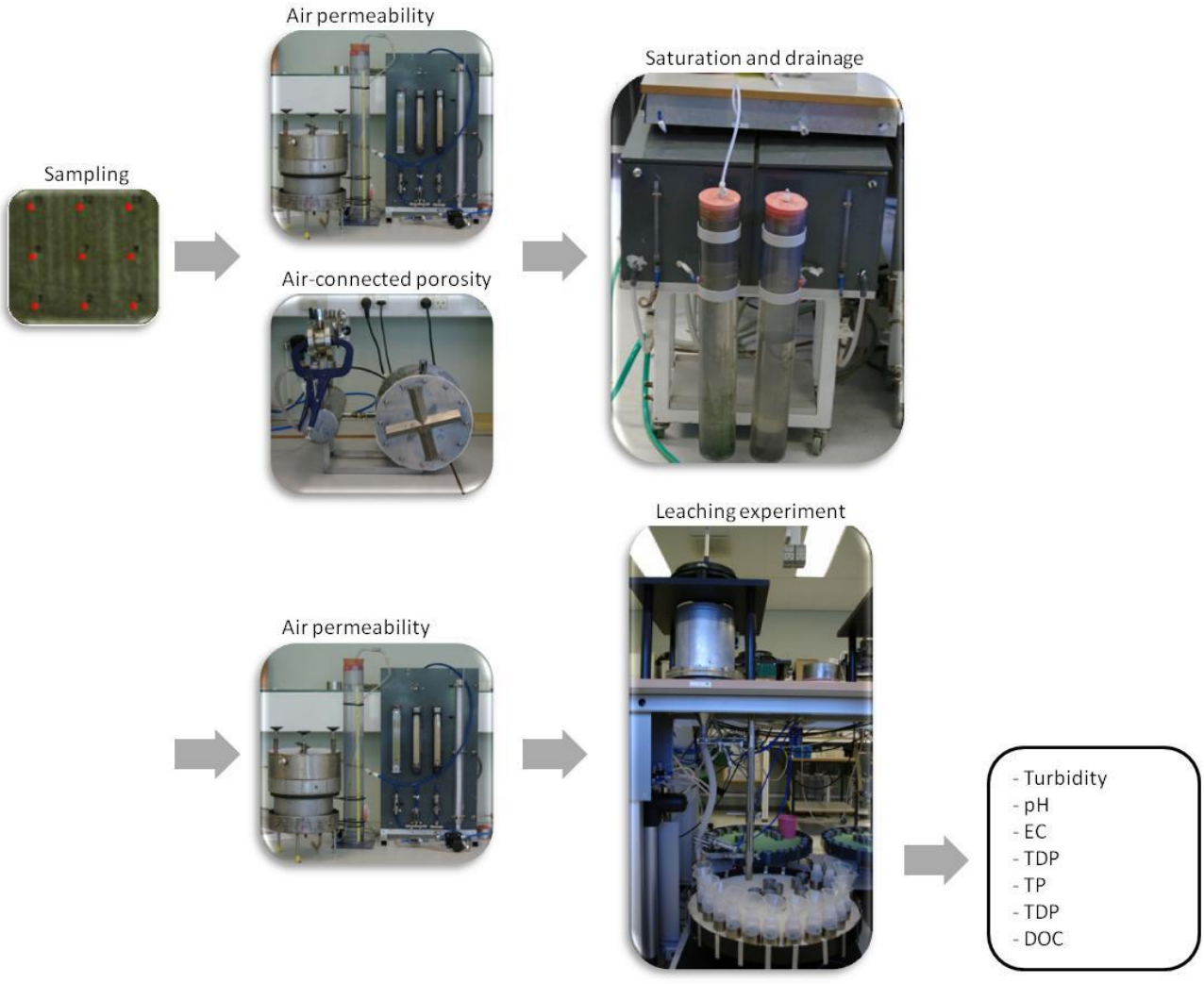


**Figure 16. Flow chart showing the treatment of the columns. The columns were weighted after sampling, after drainage and after the leaching experiment. For further insight into the leaching setup see Figure 17.**

### 3.1.2 Leaching experiment

Air permeability and air-connected porosity were measured on the columns when they arrived to the laboratory (in situ). The columns were saturated from the bottom in artificial soil water (0.652 mM NaCl, 0.025 mM KCl, 1.842 mM CaCl2 and 0.255 mM MgCl2; pH = 6.38; EC = 0.6 mmho) for approximately three days, and then drained to -20 cm matrix potential relative to the centre of the column (app. 3 days). After saturation and drainage, the columns were weighed and air permeability was measured again, $K_a$ (-20 cm).

During the leaching experiment the columns were placed on a steel grid with a mesh size of 1 mm and no lower boundary. The columns were irrigated with 10 mm artificial rain water per hour (0.012 mM $CaCl_2$, 0.015 mM $MgCl_2$ and 0.121 mM NaCl; EC = 22.5-27 µmho; pH = 5.76-7.26) from a rotating irrigation head equipped with 44 needles places randomly to ensure a homogenous application. Effluent was collected through a funnel leading down to 24 plastic bottles rotating automatically. The leaching setup is shown in Figure 17.

The breakthrough time was registered, and when the outflow from the column was steady (t=0) tritium was applied as a pulse for 10 minutes. Tritium is a radioactive conservative tracer and it was applied in the same intensity as the rain water.

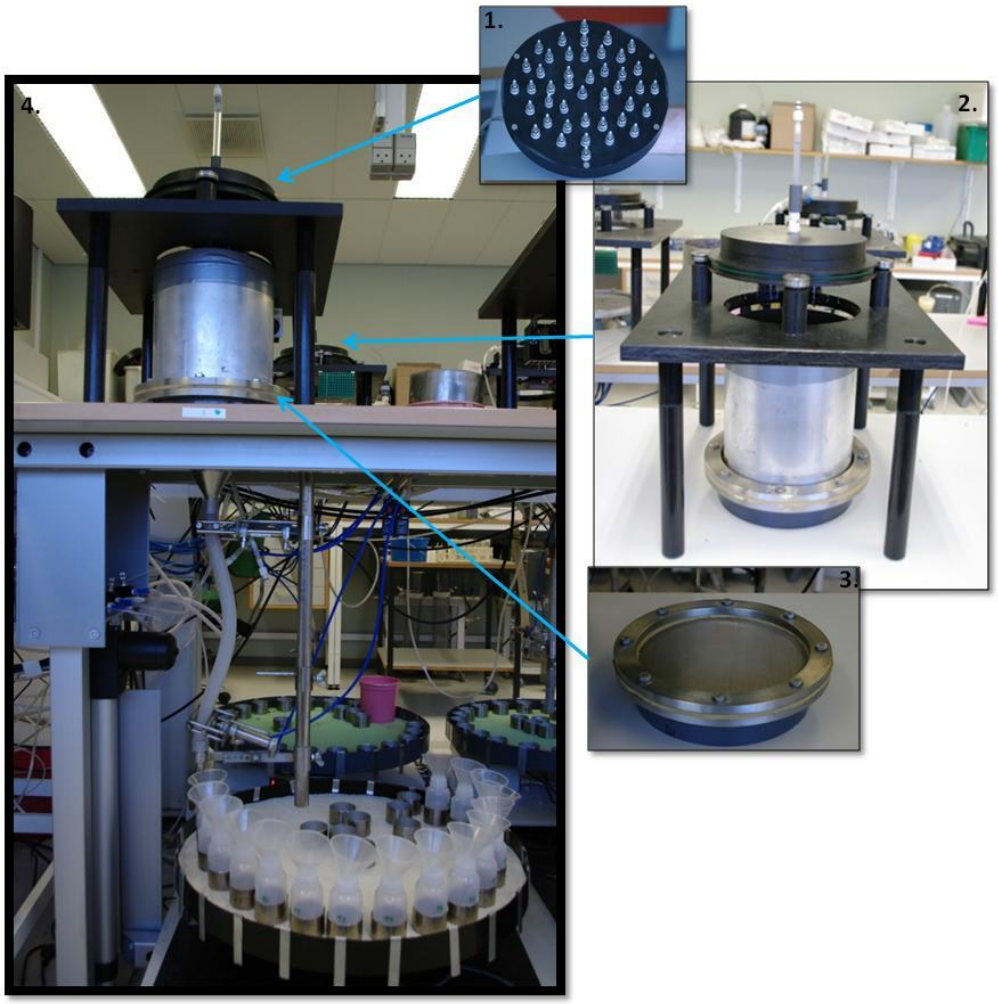


**Figure 17. Pictures showing the leaching setup. Picture 1 shows the irrigation head with the 44 needles, picture 2 shows the installation of the column in the irrigation system, picture no. 3 shows the steel grid where the columns were placed and picture no. 4 shows the roundabout with the sampling bottles and the funnel leading effluent from the bottom of the column down to the bottles.**

After water breakthrough, the columns were irrigated for 6.5 hours and the effluent was collected in the plastic bottles on the roundabout in sample intervals of 9x10 min, 12x15 min and 4x30 min. The effluent in the bottles was analysed for turbidity, pH, EC, total phosphorus (TP), total dissolved phosphorus (TDP), dissolved organic carbon (DOC) and amount of tritium. Explanation of the different analyses can be found in Appendix F. After the leaching experiment the columns were weighted.

The correlation between turbidity (in NTU), measured on the effluent, and particle concentration was found from the different suspensions shown in Appendix F. Two relationships (one power and one linear) were used to calculate the particle concentration (mg $L^{-1}$):

For NTU<1000: $C = 1.776 \cdot \mathrm{NTU}^{0.685}$ **(Eq. 3)** (Figure 18)

For NTU>1000: $C = 0.376 \cdot NTU + 272.44$ **(Eq. 4)** (Figure 19)

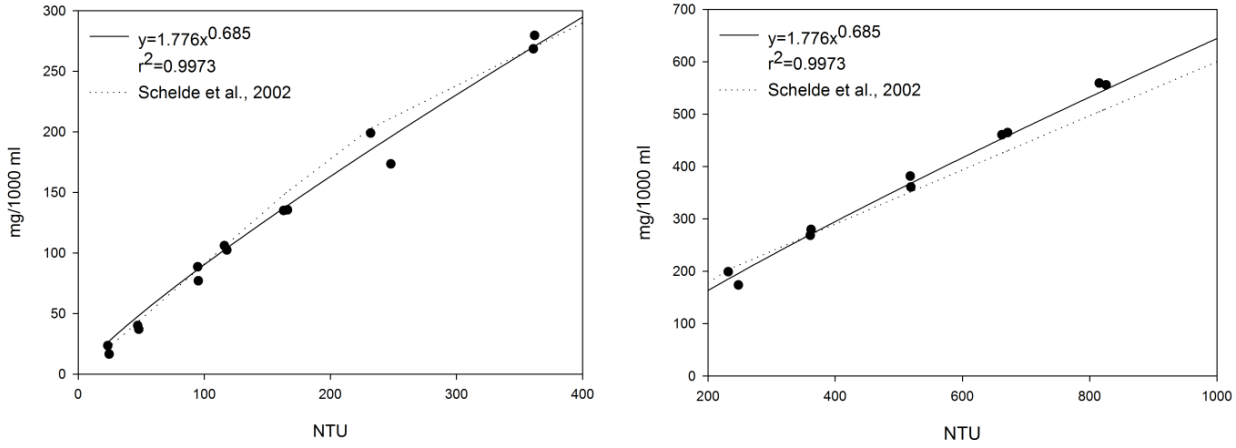


**Figure 18. The power relationship between NTU and particle concentration (mg $L^{-1}$) separated into two graphs. To the left the interval from 0-400 NTU and to the right 200-1000 NTU. The linear relationship from Schelde et al., (2002) is shown with the dotted line. Schelde et al., (2002) uses to linear relationships – one for NTU < 200 and another for NTU > 200 which explains the bump in the dotted line in the figures.**

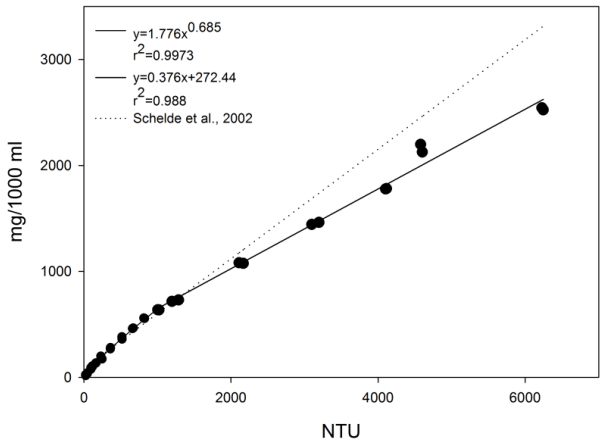


**Figure 19. The linear- and the power relationship between measured NTU and particle concentration (mg $L^{-1}$). The linear relationships from Schelde et al., (2002) are shown with the dotted line.**

## 3.2 Texture analyses

### 3.2.1 Sampling procedure

Bulk soil samples for texture analyses were collected from October 6 to October 12 2010, from the same grid points as were the columns were taken, se Figure 15 and Figure 20, except that no bulk soil was sampled from the B-horizon. The samples represent the same profiles as the columns, the profile 20 cm down.

Additionally 152 samples were taken solely for the Near Infrared spectroscopy (NIR) in order to get a statistic representative impression of the clay- and OC content. These additional samples were taken between two grid intersect both in the south-north directions and in the East-West directions and in each diagonal in the grid, see Figure 20.

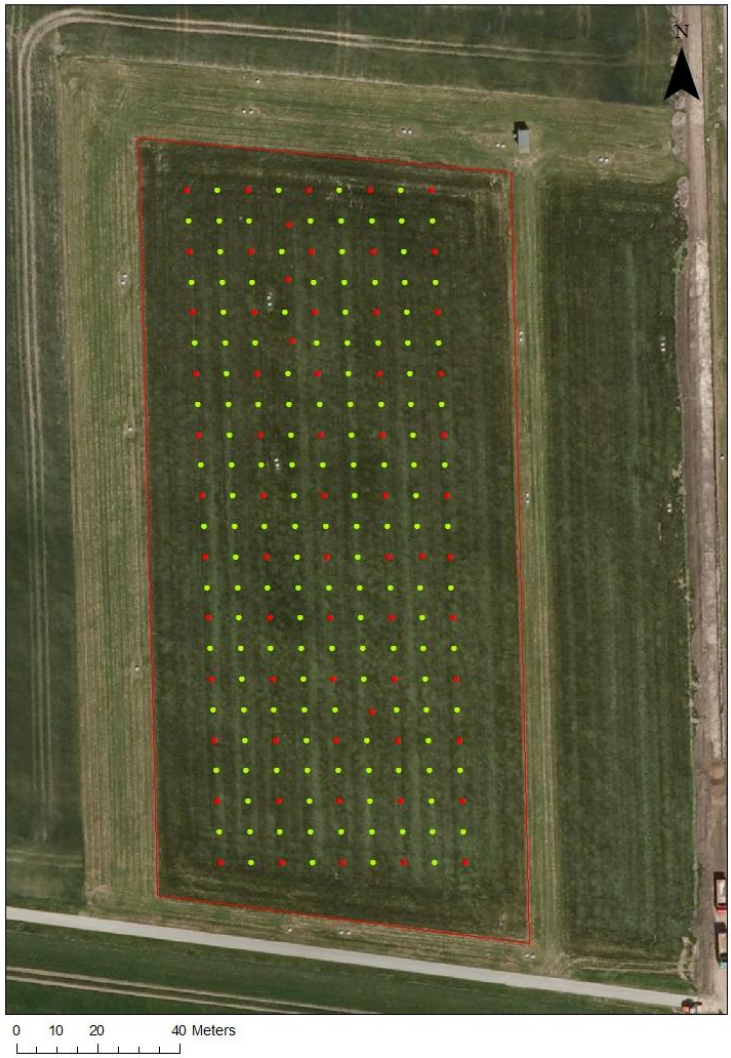


**Figure 20. Map showing the sampling points for the texture analyses (red dots) and the sampling points for NIR (green dots).**

Further treatment of the bulk soil samples in the laboratory is shown in Figure 21 along with a short explanation.


**Figure 21. Flow chart showing the treatment of bulk soil samples from Silstrup.**

### 3.2.2 Texture analyses

Each sample was dried at approximately 30 degrees and during that time regularly separated into aggregates, step two in Figure 21. The dried soil was separated and crushed by a mill to pass a 2 mm sieve. The texture analyses was carried out according to Gee and Or, (2002).

### 3.2.3 NIR

Because of time limitations it was not possible to get the NIR measurements done for the present thesis.

# 4 Results and discussion

The following results and discussions are separated into six main points;

1. Soil-air parameters: air permeability, air-connected porosity, and total air-filled porosit,

2. Soil texture

3. Water transport

4. Particle leaching

5. Tracer (tritium) breakthrough curves

6. Phosphorus leaching

Highlights from the sections are extracted at the end of each section. Statistics on some of the measured data is given in Appendix L.

## 4.1 Soil-air parameters: air permeability, air-connected porosity, and total air-filled porosity

### 4.1.1 Air permeability

Air permeability was measured on the columns just after sampling (in situ) and once again after saturation and drainage of the columns to -20 cm matrix potential, Figure 22 and Figure 23. The air permeability on column no. 1-6 was not measured at -20 cm matrix potential, so the interpolation in that area is not reliable. Results from the B-horizons are not included in the contour maps, but these results are pointed out in Figure 23.

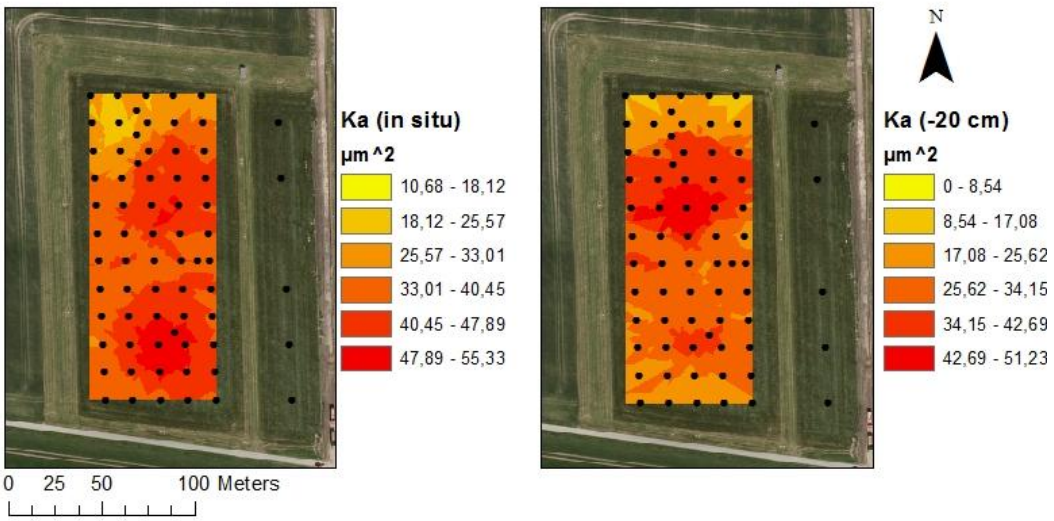


**Figure 22. Contour maps showing the air permeability measured in situ just after sampling and at -20 cm matrix potential after drainage.**

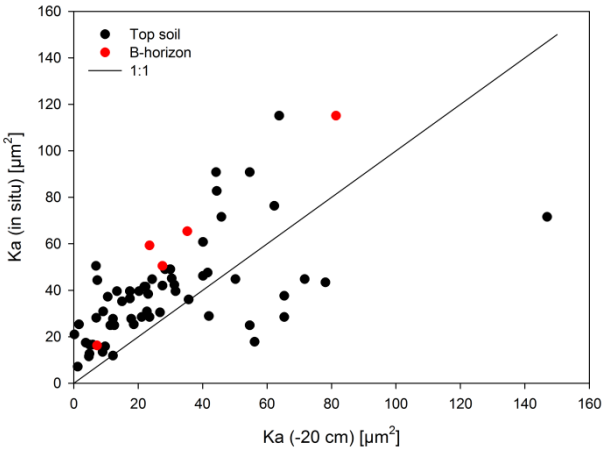


**Figure 23. Plot showing the measurements of air permeability right after sampling of the columns (in situ) and after drainage to -20 cm matrix potential. The line indicates the 1:1 relationship. Data from column no. 1-6 are not included. Columns from the B-horizon are shown with red dots.**

When sampled (in situ) the columns were at approximately -50 cm to -100 cm matrix potential. Compared to the air permeability at -20 cm matrix potential, it was expected that the air permeability in situ would be higher as can also be seen in Figure 23. It is only in the columns no. 9, 11, 16, 19, 32, 33, 43, 48, 52 and 75 where this is not the case. To see the location of the columns mentioned within the field see Figure 15.

### 4.1.2 Air-connected porosity

Air-connected porosity was measured on the pycnometer when the columns arrived at the laboratory (in situ). A pycnometer measures the volume of air-filled pores connected to the column top and bottom only. Results from the pycnometer measurements are shown in Figure 24.

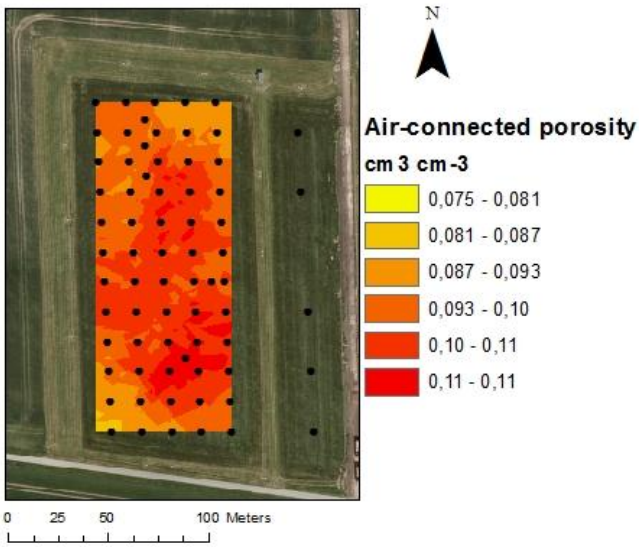


**Figure 24. Air-connected porosity measured on the columns with the pycnometer.**

### 4.1.3 Air-filled porosity

Air-filled porosity in situ and at -20 cm was calculated from bulk density, water content and dry weight of the columns, Figure 25 and Figure 26. Opposite to the pycnometer measurements this is the total porosity of the columns, and not just the connected pore volume.

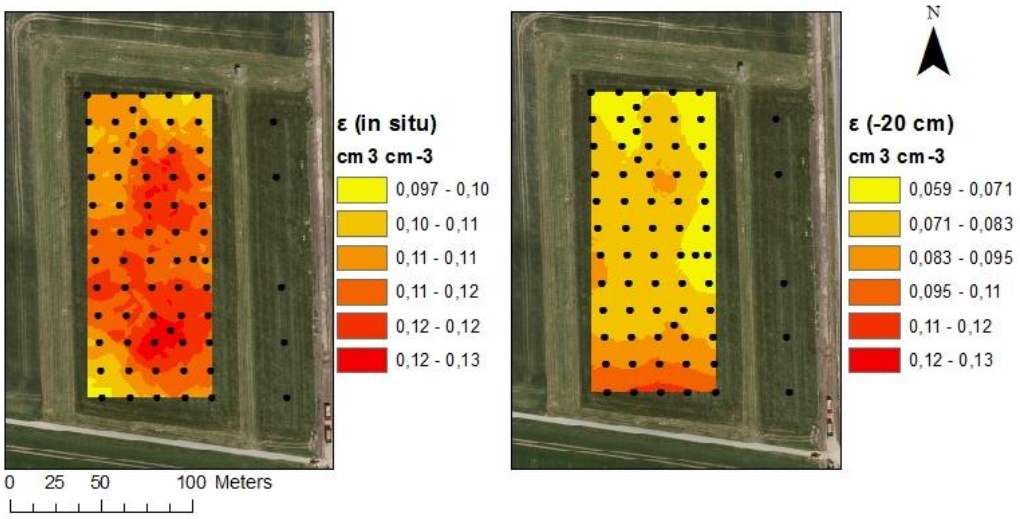


**Figure 25. Calculated air-filled porosity in situ and at -20 cm matrix potential. Results from the B-horizons are not included in the contour maps, but these results are pointed out in Figure 26.**

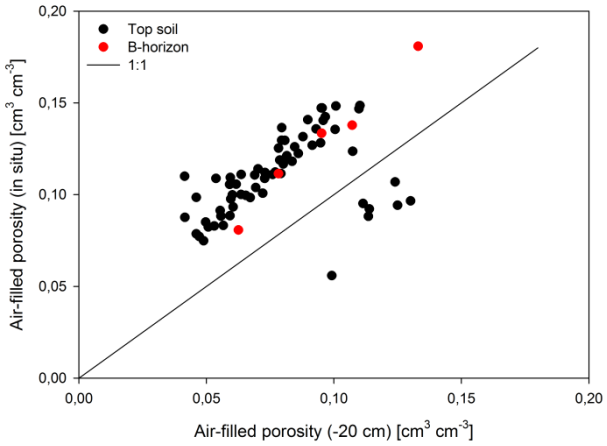


**Figure 26. Calculated air-filled porosity in situ and at -20 cm matrix potential. Columns from the B-horizon are shown with the red dots. The line indicates the 1:1 relationship.**

As with the air permeability the calculated air-filled porosity in situ is expected to be higher than the air-filled porosity at -20 cm matrix potential, just like Figure 26 indicates. It is only in the columns no. 1, 2, 3, 4, 5, 6 and 41 where this is not the case. The very high value for the air filled porosity in situ originates from column no. 71.

### 4.1.4 Soil-air parameter correlations

The measured air-connected porosity and the calculated air-filled porosity, both at in situ conditions, are plotted in Figure 27.

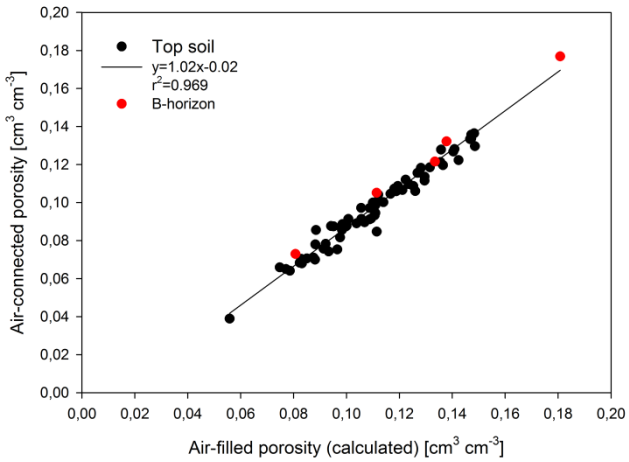


**Figure 27. Air-connected porosity measured with the pycnometer as a function of the calculated air-filled porosity in situ. Columns from the B-horizon are shown with the red dots and they are included in the linear regression.**

According to the graph above air-connected porosity is a little lower than the calculated air-filled porosity. This difference is due to the fact that the pycnometer only measures pores directly connected to the atmosphere while the calculated value is the total air-filled porosity of the columns. Besides this difference there seems to be a good correlation between the two parameters.

According to Moldrup et al., (2010) the ration of air permeability to gas diffusivity can be expressed as:

$$P = \frac{K_a \cdot D_o}{D_P} \qquad \textbf{(Eq. 5)}$$

Where P is a gas transport parameter that express the structure of the soil. According to Moldrup et al., (2010) medium structured soils has P-values around 700 µm$^2$. Buckingham (1904) states that $\varepsilon^2 = D_P/D_o$, leading to the following relationship between air permeability and air-filled porosity (ε) (noted the Kawamoto-Buckingham model):

$$K_a = P \cdot \varepsilon^2 \qquad \textbf{(Eq. 6)}$$

The Kawamoto-Buckingham model is fitted to the three plots in Figure 28 where the air permeability (in situ and at -20 cm) is shown as a function of respectively air-connected porosity (measured with the pycnometer), and calculated air-filled porosity in situ, and at -20 cm matrix potential.

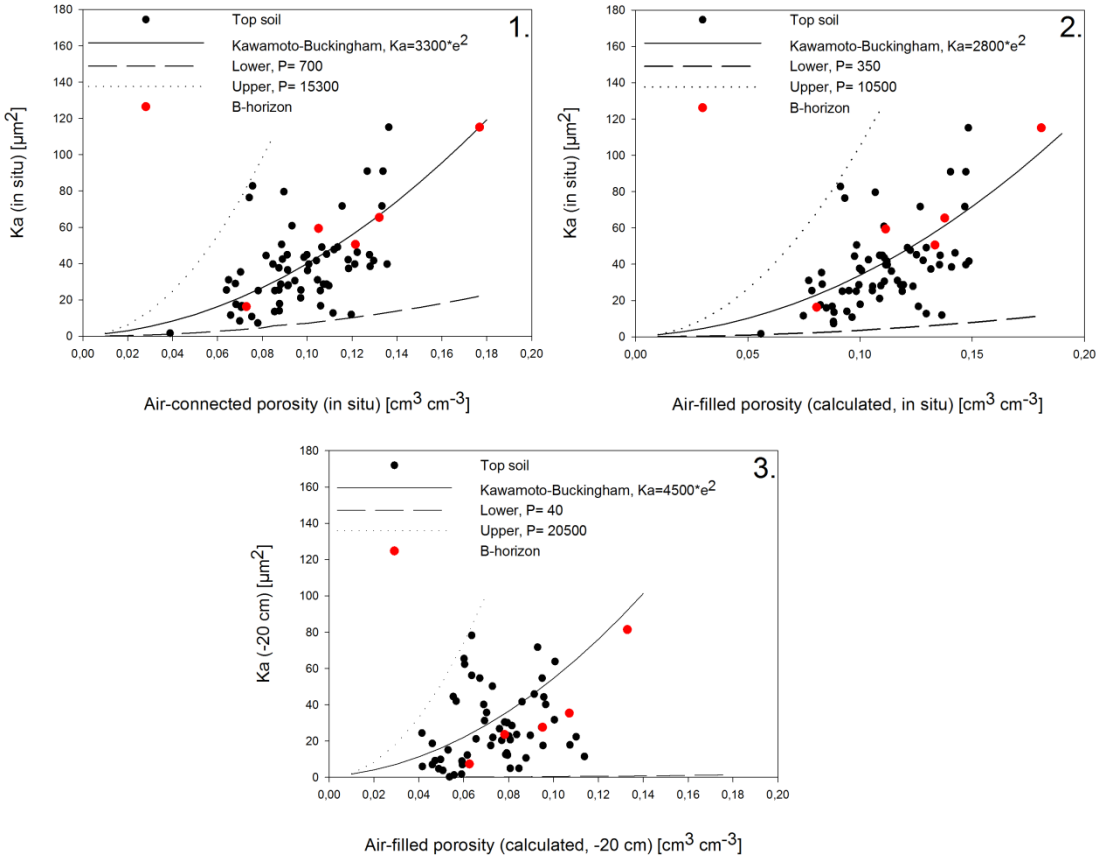


**Figure 28. Plot no. 1 shows the air permeability measured in situ as a function of air-connected porosity. Plot no. 2 shows the air permeability as a function of the calculated air-filled porosity in situ. Plot no. 3 shows the air permeability at -20 cm as a function of the calculated air-filled porosity at -20 cm. All three plots are shown together with the Kawamoto-Buckingham model, $Ka=P*\varepsilon^2$ and lower- and upper P-intervals for the model. Columns from the B-horizon are shown with red dots.**

In the figure above it is worth noticing the very large P-intervals in average indicating a very well structured soil. This is in agreement with the fact that the soil hasn't been disturbed since December 15, 2008 (or March 30, 2009). Without soil management on the field for almost two years, there has been plenty of time for the biological and physical processes to form a very well structured soil. From Figure 28 it can be concluded that the structure is very well established up there and thus conditions for pronounced macropore flow is present.

### 4.1.5 Highlights in soil-air parameters

The soil-air results show that there is a general consistency between the measured and calculated parameters. Air permeability and air-filled porosity are higher at in situ conditions because of the difference in matrix potential. Comparing air-connected porosity with calculated air-filled porosity there is a good correlation, where the smallest values are air-connected porosity since this is only pores directly connected to the columns top and bottom. When looking at the contour maps it is not possible to see any obvious tendencies across the field.

No soil management has been carried out on the field for almost two years, and during that time the biological and physical processes have had plenty of time to develop a highly structured soil confirmed by the large P-values applied to the Kawamoto-Buckingham models.

## 4.2 Soil texture

Results from the texture analyses can be found in Appendix G in table form. The contour maps in Figure 29 shows the bulk density, gravimetric clay content (<2 µm), volumetric clay content (<2 µm), and organic carbon content (OC). Contour maps for silt (3-50 µm) and sand (50-2000 µm) can be found in Appendix H. Since there were no calcium carbonate in the samples total OC from the analyses corresponds to the amount of OC shown in the map. There are no texture analyses on soil from the B-horizon.

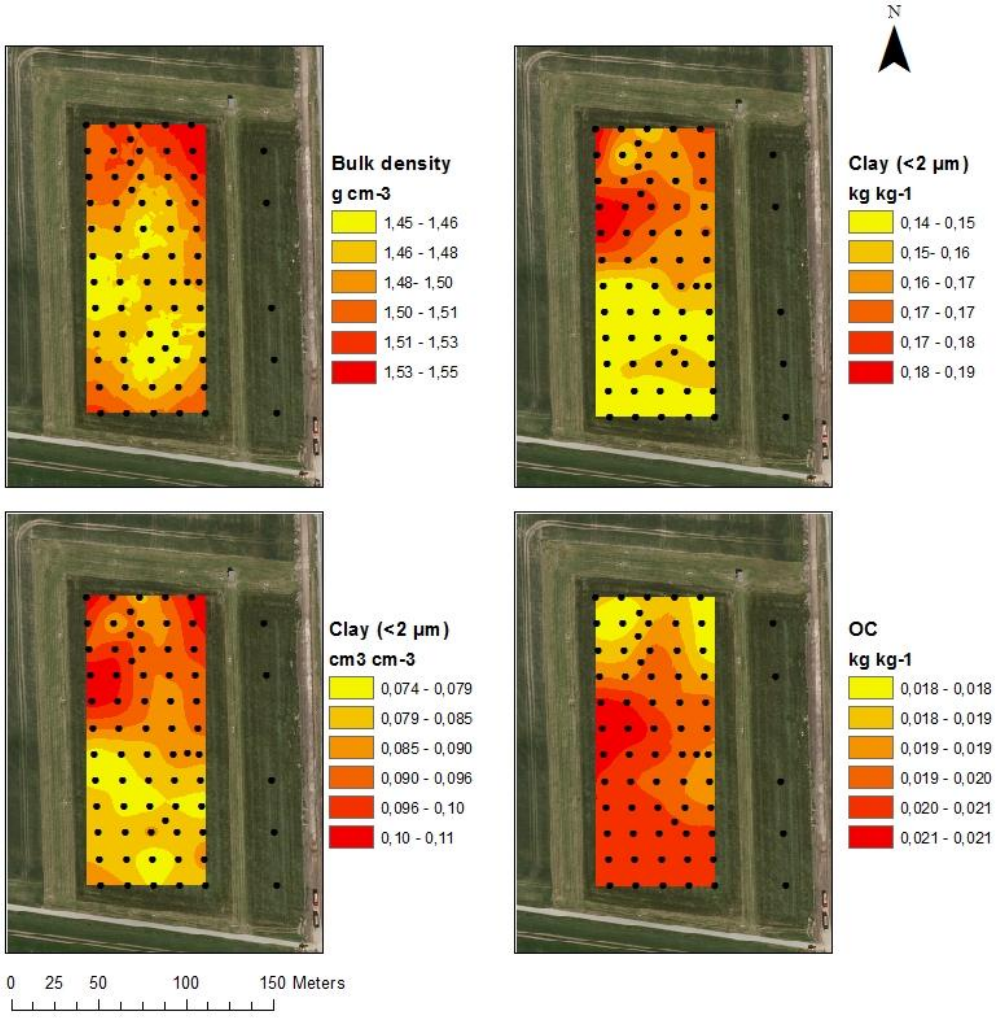


**Figure 29. Contour maps showing the bulk density (g $cm^{-3}$), gravimetric clay content (kg $kg^{-1}$), volumetric clay content ($cm^3$ $cm^{-3}$), and OC content (kg $kg^{-1}$).**

The highest bulk densities are found in the northern part of the field. The bulk densities range from 1.39-1.6 g $cm^{-3}$, with an average on 1.49 g $cm^{-3}$ throughout the field. Bulk densities in the B-horizon range between 1.5-1.6 g $cm^{-3}$, with an average of 1.58 g $cm^{-3}$, see Table 5.

**Table 5. Bulk densities from the B-horizon.**

| Column no.: | Bulk density [g $cm^{-3}$]: |
|---|---|
| 61 | 1.62 |
| 63 | 1.58 |
| 65 | 1.57 |
| 69 | 1.63 |
| 71 | 1.51 |
| **Average** | **1.58** |

The resistivity from the measurements carried out in 1999 (Figure 11) doesn't give any direct value of the clay content, but texture analyses on soil from the excavated test pit and from selected wells indicate, that the clay content was ranging between 28 and 36%. In the texture analyses carried out in this project, the clay content was ranging from 14.2 to 18.9% (15.9% in average), Figure 29. The sampling depth was lower in 1999, but still the clay contents measured in this project period seems to be considerably lower than in 1999. Comparing the contour maps in Figure 10 and Figure 29 the OC and TOC contents seems to be the same. The measurements carried out in 1999 showed that the TOC contents were ranging from 1.9 to 2.4% (2.16% in average). In the texture analyses carried out during this project the OC content is ranging from 1.7 to 2.2% (2% in average). Like in 1999 the two gradients of clay and OC still run in opposite directions with the highest contents of clay in the northern end of the field and the highest contents of OC in the southern end of the field.

During this project no texture analyses was carried out on bulk soil from the B-horizon, but from the texture analyses carried out in 1999 the clay content was 57.8% at 1.5 m depth in the excavated test pit and 21.1% in well no. 8 in 1.5 m depth (Lindhardt et al., 2001). Assuming that the clay content haven't changed that much since 1999 in the B-horizon and looking at the bulk densities in Table 5 who are all above the average bulk density for the top soil, the flow paths should be even more structured in the B-horizon than in the top soil.

From the maps in Figure 29 it seems as if there are some special conditions within the northern part of the field. In this third the highest bulk densities, the highest clay contents and the smallest OC contents are found. High bulk densities indicate that the soil is fairly compacted (Keller and Hakansson, 2010), and increasing clay contents might lead to very persistent cracks in the soil. From the P-values in the Kawamoto-Buckingham model it was obvious that the field in Silstrup it very well structured, but now it can also be hypothesized that the structure consists of persistent flow paths, at least in the upper third of the field that might contribute more to the leaching than the rest of field.

### 4.2.1 The Dexter Index, n

In de Jonge et al., (2009) it is stated that the tilth conditions and self-organization skills of soils are determined by the amount of clay complexed with OC. It is stated that soils with a pool of non-complexed clay show severe signs of structural degradation and tendencies to create aggregates that are unstable during wet conditions and hard as cement during dry conditions. This originates from a theory presented in Dexter et al., (2008) where a lower threshold of OC, for sustaining the self-organization process in soil, is presented. A clay/OC ration (n) above 10 indicates that there is a pool of non-complexed clay in the soil, and the soil is said to be "hungry". This non-complexed clay is more easily dispersed in water than complexed clay, and thus contributes to the colloid-facilitated transport of environmental pollutants like e.g. phosphorus that adsorb to the colloids. For soil to be saturated with OC, and in order for the soil to be healthy, the Dexter index, n should be around 10 or below.

The relation between clay and OC for the soil in Silstrup is shown in Figure 30 to the left together with the saturation line symbolizing 10 g of clay per g OC. The variations in Dexter n across the field are shown to the right.

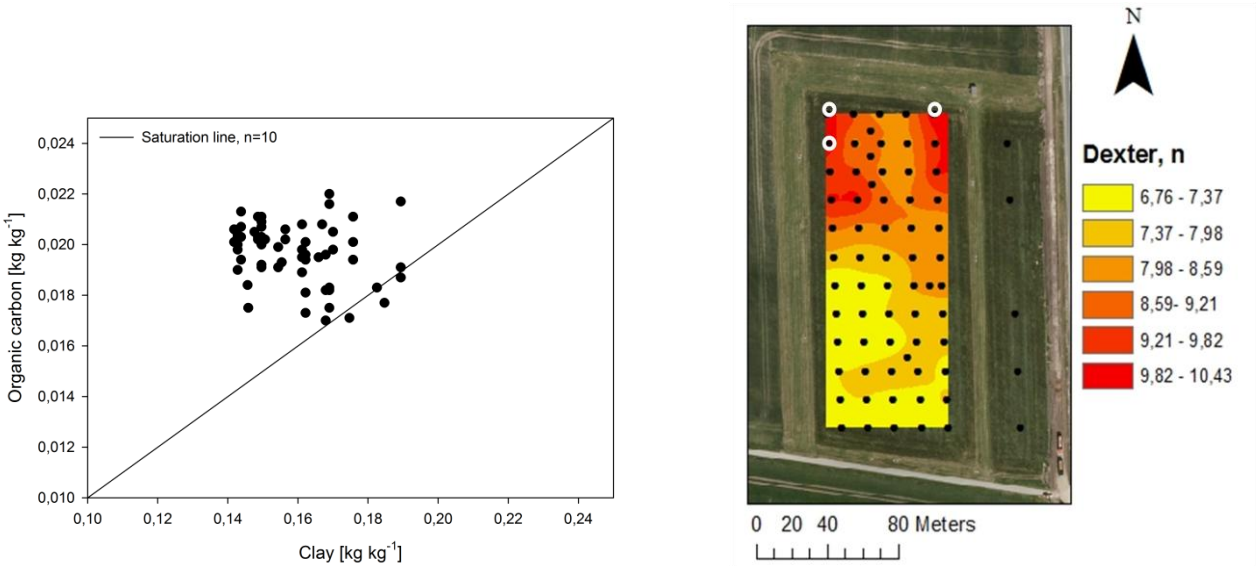


**Figure 30. To the left the relation between the content of clay and OC for the soil in Silstrup. The saturation line indicates the 10:1 relationship between clay and OC. To the right a contour map showing the distribution of Dexter n across the field. The sampling points with values of n>10 are marked with white circles.**

From the Dexter plots it can be seen that the soil is saturated with OC (n<10) in all sampling points, except for sampling point no. 51, 56 and 60 that is marked with white circles in the contour map to the right. Once again it can be confirmed that the soil in the field in Silstrup is very structured. Since Dexter is based on the contents of clay and OC, it is once again the upper third that is interesting, as was seen in Figure 29. It is also in this third the three columns with n>10 are located.

### 4.2.2 Highlights in soil texture

From the Kawamoto-Buckingham model it was assumed that the soil structure throughout the field was very structured. This assumption is confirmed when looking at the soil texture where the Dexter n is smaller than 10 in almost all sampling points - all sampling points (with the exception of three) were above the Dexter saturation line.

From the soil-air parameters is was not possible to see any tendencies across the field on the contour maps, but now looking at the bulk density, clay- and OC content, it seems as if there is something special with the upper third of the field. High bulk densities and high clay contents indicate that the soil might be highly compacted in this part of the field leading to very persistent macropores. Even though soil texture analysis was not carried out on soil from the B-horizon the high bulk densities, and previous estimates of the clay contents states that the same is the case with the B-horizon.

As mentioned in the introduction page 5, especially three conditions should be present in order for colloid-facilitated transport to take place. One of the points listed was that a transport of colloids should take place. With the structured soil leading to highly persistent macropores, it can be established that the transport ways for colloid-facilitated transport to take place are present.

## 4.3 Water transport

Some of the basic results from the leaching experiment are shown in this section. Six columns are selected to point out the general tendencies. For location of the selected columns see Figure 15.

### 4.3.1 Outflow

The outflow as a function of time is shown in Figure 31.

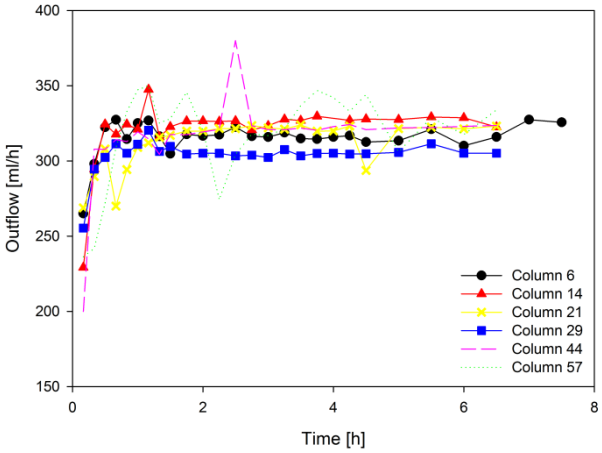


**Figure 31. Outflow examples during the leaching experiment.**

Breakthrough time, defined as the time from when irrigation was applied until the first effluent exited the column, was registered after 12 and 40 minutes, and the outflow from the columns were generally stable after 20 minutes with a few exceptions (column no. 60 and 61 ponded). When steady state was reached tritium was applied – in the breakthrough curves this time is t=0 min.

### 4.3.2 pH

pH measured in the collected effluent is plotted in Figure 32 as a function of the outflow volume.

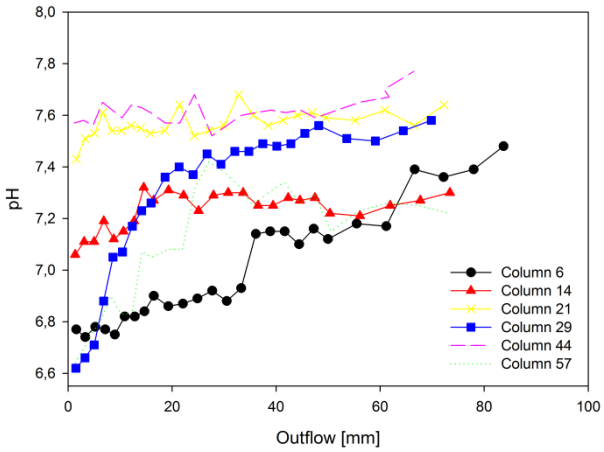


**Figure 32. Variations in pH during the leaching experiment.**

pH in the first bottle with effluent collected during the first 10 minutes varied between 5.81-8.36 among the columns, but at the end of the leaching experiments pH was at a constant level between 7 and 8 for all columns, except for no. 61 and 71 where pH was above 8.

### 4.3.3 Electrical conductivity

EC as a function of the outflow volume is shown in Figure 33.

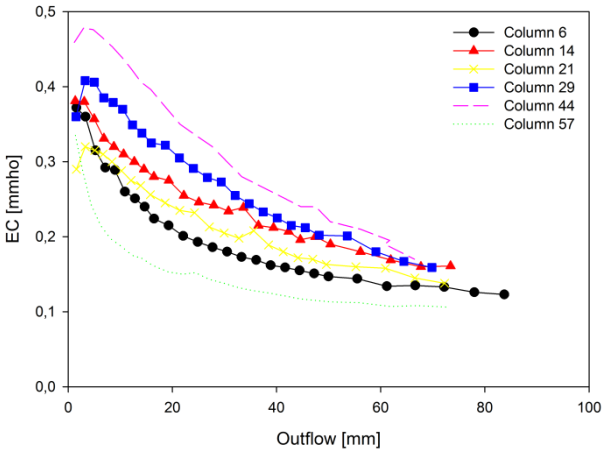


**Figure 33. Variations in electrical conductivity during the leaching experiment.**

The electrical conductivities were in the range of 0.52-0.195 mmho in the beginning of the leaching experiment, but like the pH it reached a constant level between 0.1 and 0.2 mmho at the end of the experiment, except column no. 1 and 61 where EC≈0.06 mmho.

EC in the used soil water was ≈0.6 mmho, and in the artificial rain water is was ≈ 22-27 µmho. Thus, when the leaching starts it is soil water from inside the column that that is collected first, but as the rain water is applied as a function of time the water inside the column is replaced, and EC in the effluent decreases because of the lower EC in the rainwater. Within the 6.5 hours of leaching EC in the effluent never decreases all the way down to the level of the rain water. This indicate that there is still some exchange of solute between the macropores and the soil matrix.

### 4.3.4 Highlights in water transport

The apparent decrease in EC, the rise in pH and the more or less constant level both pH and EC reaches, indicates a pronounced macropore flow through the columns - the faster the decrease, the more macropore flow, though it seems as if there is also a little exchange of solutes with the soil matrix.

## 4.4 Particle leaching

### 4.4.1 Leached particle concentrations

From the relationship found in Materials and methods between turbidity and particle concentration, the particle concentration in the collected effluent was calculated, and plotted as a function of the outflow, Figure 34. The columns are arranged according to the Dexter index, n. The particle concentrations, as a function of the outflow from the columns sampled in the B-horizon are shown in Figure 35. Texture analyses were not carried out on soil from the B-horizon so the Dexter index is not known for these columns.

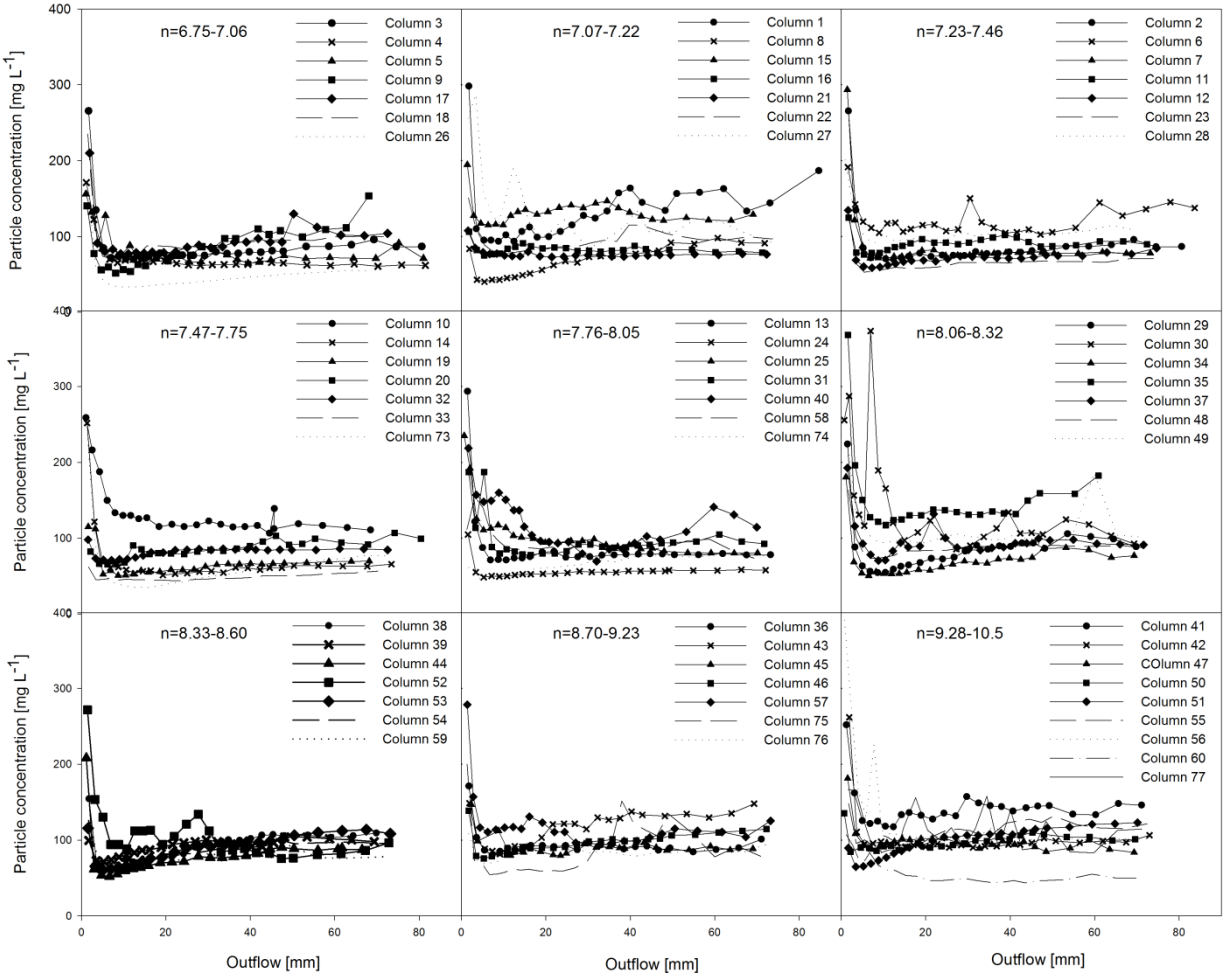


**Figure 34. Particle concentrations (mg $L^{-1}$) in the effluent as a function of the outflow arranged according to the Dexter index, n. Columns from the B-horizon are not included in the figure.**

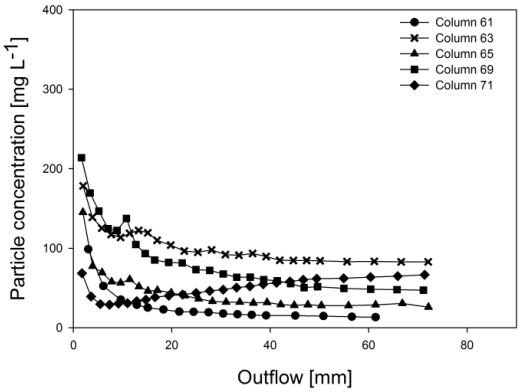


**Figure 35. Particle concentrations (mg $L^{-1}$) in the effluent collected during the leaching experiment from columns sampled in the B-horizon.**

As experienced in literature by e.g. Schelde et al., (2002), Laubel et al.,(1999) and de Jonge et el., (2004b), there was a considerable leaching of particles in the beginning of the experiment (first flush) followed by a decrease in particle concentration to a lower and more constant level after approximately 8 mm outflow. This first flush consists of loose, immediately assessable particles that is brought into suspension and transported

with the irrigation water to the bottom of the column (de Jonge et al., 2004b) and (Laubel et al., 1999). During the leaching experiments some of the columns (or the bottom of the columns) got unstable, and the particle concentrations increased a little toward the end. This increase in particle concentrations might be the effect of high intensity irrigation for a long period of time, and therefore the structure of the soil collapses. First flush particle concentrations from the columns are shown in Table 6 together with several literature values.

**Table 6. Literature values for particle concentrations leached with first flush.**

| Literature | Min. value – Max. value<br>Average value<br>[mg $L^{-1}$] | Conditions |
|---|---|---|
| Silstrup, 2010 | 62 – 390<br>177 | Irrigation on undisturbed soil columns with 10 mm $h^{-1}$ for 6.5 hours.<br>Clay content: 14.2 - 18.9% |
| (de Jonge et al., 2004b) | 188 – 1849<br>448 | Irrigation on undisturbed soil columns with 10 mm $h^{-1}$ for 3.5 hours.<br>Clay content: 10.7 – 16.1% |
| (Vendelboe et al., 2011) | 123.51 – 368.96<br>235.33 | Irrigation on undisturbed soil columns with 10 mm $h^{-1}$ for 4 hours.<br>Clay content: 11 – 23% |
| (Schelde et al., 2002) | 80 – 4100<br>- | Irrigation on undisturbed soil columns with irrigation rates ranging from 11 to 30 mm $h^{-1}$.<br>Average clay content: 15.7% |
| (Laubel et al., 1999) | 63 – 334<br>- | Irrigation on experimental plots (25 $m^2$) sampling from the drain pipe outlet.<br>Irrigation rates: 15.3-37 mm.<br>Clay content: 15.5 – 22% |
| (Kjaergaard et al., 2004a) | 6 – 167<br>- | Irrigation on undisturbed soil columns with 1 mm $h^{-1}$ for 6 hours.<br>Clay content: 12 – 43% |

Comparing the values in Table 6 the first flush particle concentration from the columns in Silstrup is comparatively small. As mentioned in relation to the Kawamoto-Buckingham plots no tillage has been carried out on the field for almost two years resulting in a very stable and structured soil. The dispersibility of colloids will depend on whether they have been mobilised by tillage (Etana et al., 2009). Thus the amount of easily dispersed colloids is also expected to be smaller compared to at least some of the literature values in Table 6. Kjaergaard et al., (2004a) found smaller first flush values, but the applied irrigation rate was also considerably lower than the one used in this project. The first flush effect may to some extend be a laboratory phenomenon were the magnitude depends on the irrigation rate applied.

From Figure 34 it is possible to see the same tendencies as in the contour map in Figure 30 with the highest n-values found in the northern part of the field. Besides that, there doesn't seem to be any connection between the leached particle concentrations and the Dexter index. The same plot was tested in respect to the clay content, but it wasn't possible to see any tendencies there either. It makes sense that there is no correlation between particle leaching and Dexter n as the soil was saturated with OC in all points – other parameters than the clay and OC contents control the leaching of particles.

The same tendencies with considerable particle leaching in the beginning of the experiment, followed by a decrease to a more constant level, were also experienced with the columns from the B-horizon. The peak concentrations from these columns varied between 68 and 214 mg $L^{-1}$, with an average on 141 mg $L^{-1}$. The

peak particle concentrations from the B-horizon are thus a little lower than the particle concentrations leached from the top soil columns, but still within the same interval. Opposite to the top soil columns the bottom of the columns sampled from the B-horizon seemed to be more stable and the particle concentrations did not increase toward the end of the experiment in the same pronounced manner. The similarities with the shape of the particle leaching curves from the top soil indicate that the B-horizon might have the same pronounced structure as the top soil. Also the bulk densities from the B-horizon were larger than the average bulk densities for all columns which might support the assumptions that the B-horizon is indeed well structured.

### 4.4.2 Accumulated particle leaching

The accumulated amount of particle leached from the columns during the leaching experiment is shown as a function of the outflow in Figure 36 and Figure 37 (B-horizon). Just like with the particle concentrations, the plots are arranged according to the Dexter index, n.

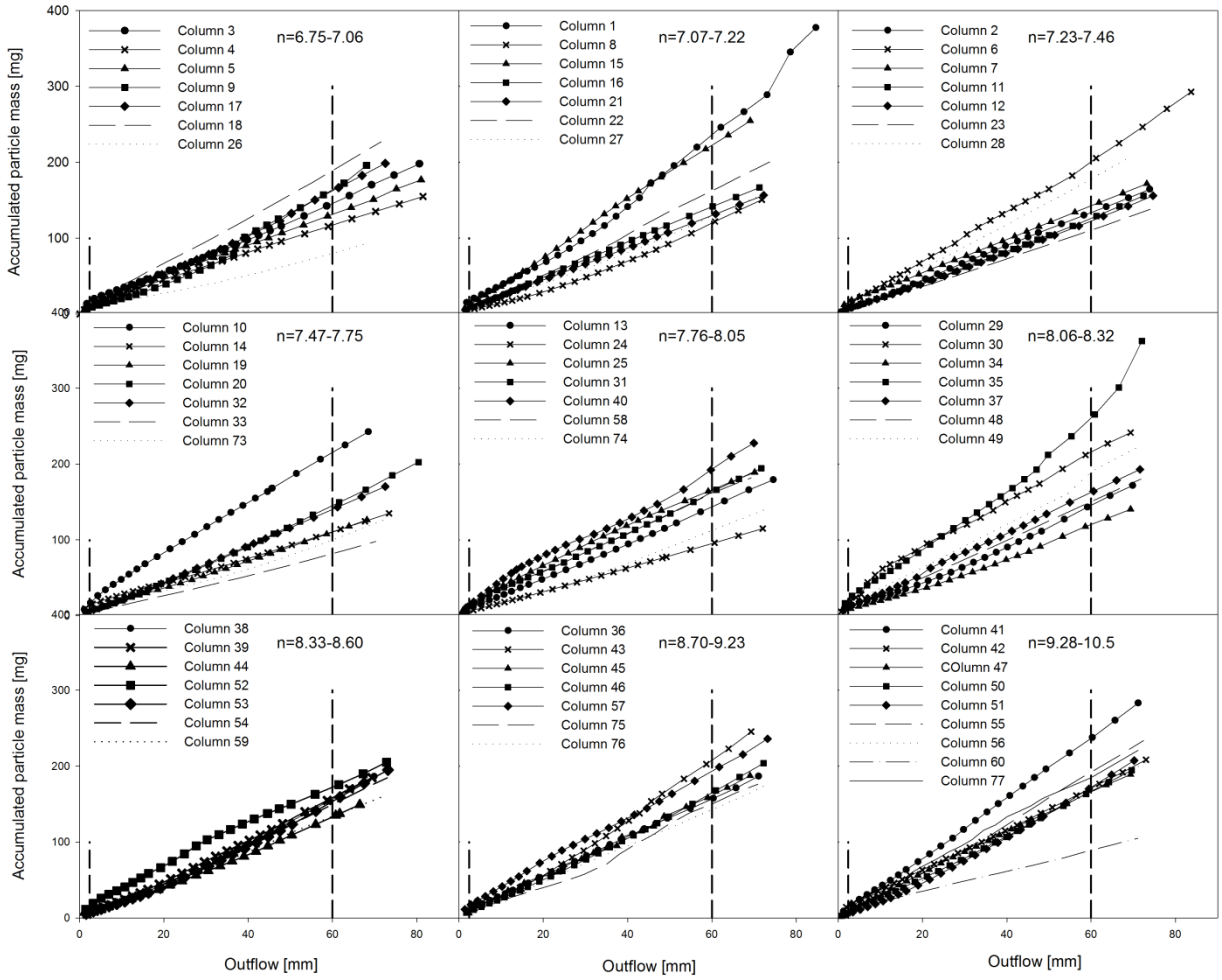


**Figure 36. Accumulated mass of particles (mg) as a function of the accumulated outflow (mm) arranged according to the Dexter index, n. The dashed lines indicate the 2.4 and 60 mm outflow (explanation follows). Columns from the B-horizon are not included in the plots.**

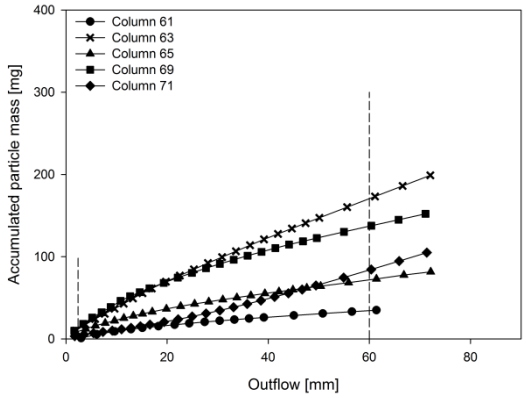


**Figure 37. Accumulated mass of particles (mg) as a function of the accumulated outflow (mm) for the columns sampled in the B-horizon. The dashed lines indicate the 2.4 and 60 mm outflow (explanation follows).**

The accumulated mass of leached particles from the columns sampled in the top soil ranged between 91 and 377 mg, with an average on 185 mg during the 6.5 hours of irrigation. From the B-horizon the accumulated mass ranged between 35 and 199 mg, with an average on 115 mg. In de Jonge et al., (2004b) the accumu-

lated mass of leached particles ranged between 8.8 and 598 mg, with an average of 157 mg during 3.5 hours of irrigation. Keeping in mind that the average leached particle concentrations were more than twice as large in de Jonge et al., (2004b) the smaller amount of accumulated particles leached is due to the shorter irrigation period that was only 3.5 hours compared to this experiment where the irrigation lasted for 6.5 hours. Once again there doesn't seem to be any connection between the Dexter index nor the content of clay, and the amount of particles leached. Vendelboe et al., (2011) conducted irrigation experiment on undisturbed soil columns with clay contents ranging from 11 to 23% and irrigation rates on 10 mm $h^{-1}$ for ~4 hours. It was found that the particle release was depending on the clay content when the clay content was above 15%. Once again it can be concluded that the clay- and OC contents doesn't play any role in the leaching of particles from the field in Silstrup, or perhaps the clay range is to narrow compared to Vendelboe et al., (2011). The average clay content on 15.9% found in this project is only a little higher than the threshold value on 15% found by Vendelboe et al., (2011).

In order to compare the columns, a 2.4 mm outflow was chosen to represent the concentration of colloids leached in the first flush, and likewise a 60 mm outflow was chosen to represent the outflow at the end of the experiment. The point was to capture the colloid concentration at first flush, but in order to compare the columns, 2.4 mm was chosen as the value where all columns had reached breakthrough (except for column no. 61). The two threshold values are shown with the vertical dashed lines in Figure 36 and Figure 37. To evaluate the graduate release of particle after first flush, these masses have been subtracted the total mass of leached particles at 60 mm outflow. These three threshold values are presented in the contour maps in Figure 38.

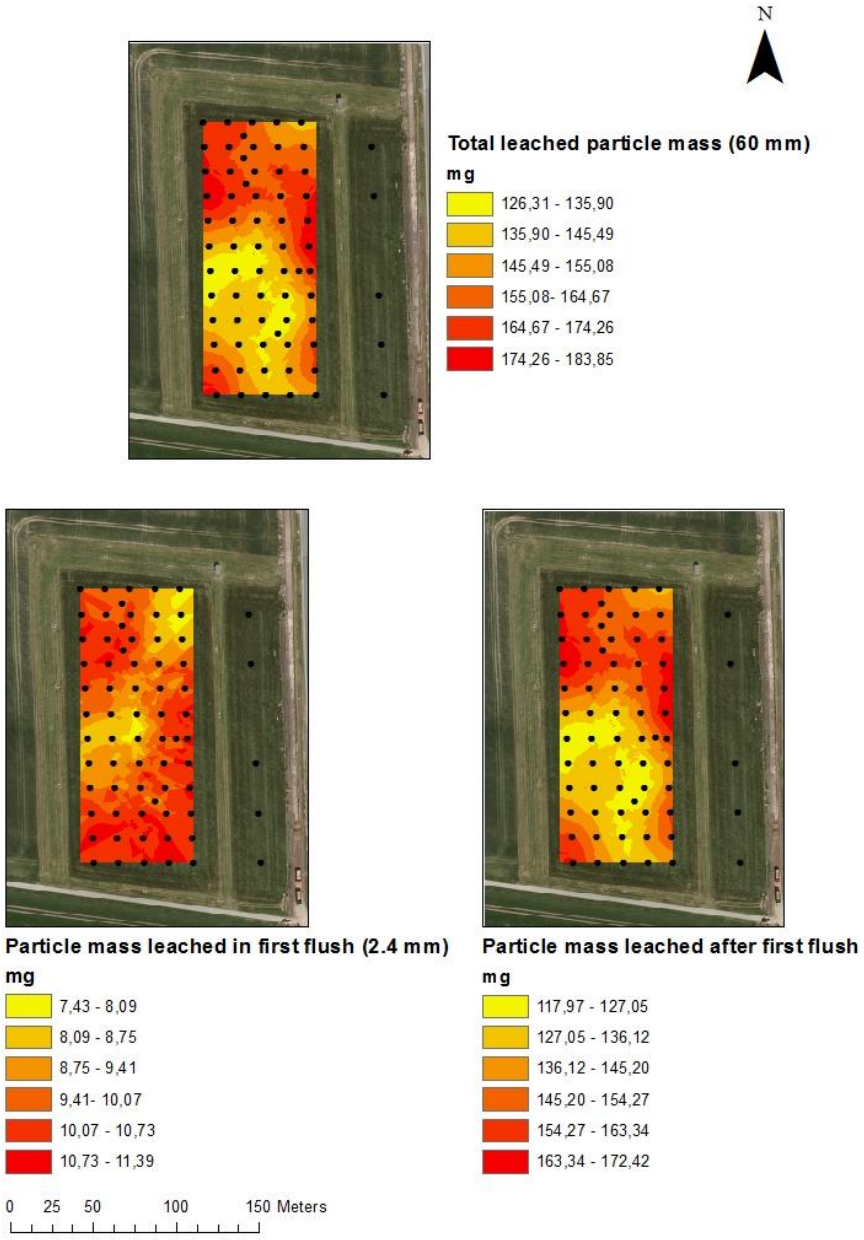


**Figure 38. Contour maps showing the total mass of particles leached after 60 mm outflow, the mass of particles leached in first flush (after 2.4 mm outflow), and the amount of particles leached between 2.4 and 60 mm outflow. Values from the B-horizon are not included in the interpolated plots.**

The magnitude of particles leached in the first flush is within 4 to 21 mg (with values from the B-horizon included), with an average on 10 mg. At 60 mm the amount of leached particles lies between 34 and 260 mg, with an average on 151 mg. In Vendelboe et al., (2011) the values at 4 mm ranged between 14 and 33 mg, with an average on 24 mg and at 32 mm, which was the threshold expressing the end of the experiment, the leached particle mass ranged between 26 and 104 mg, with an average on 51 mg. For comparison with Vendelboe et al., (2011) the accumulated mass of particles at 32 mm outflow was found to be 80 mg in average. The higher amount of particles at 32 mm outflow compared to Vendelboe et al., (2011), might be due to the fact that the columns in this experiment were getting unstable towards the end of the experiment as was seen in Figure 34.

From the contour map in Figure 38, showing the total mass of leached particles at 60 mm, it can be seen that the highest amount of particles is leached from the northern third of the field. The same is the case for the map showing the continuous release of particles after first flush. It was also in this third the highest bulk densities and the highest clay contents were observed. To summarise; the largest amount of particles is released from the upper third of the field where the transport pathways are particular dominant. The contour map showing the amount of particles leached during first flush doesn't really show any tendencies, and is more scattered across the field.

It is worth remembering that the interpolation tool and the contour maps are only ways to visualise the results, but what can be seen are only tendencies, not facts. In order to se past the interpolation in Figure 38, the 12 biggest values for the total amount of particles leached at 60 mm is shown in Figure 39.

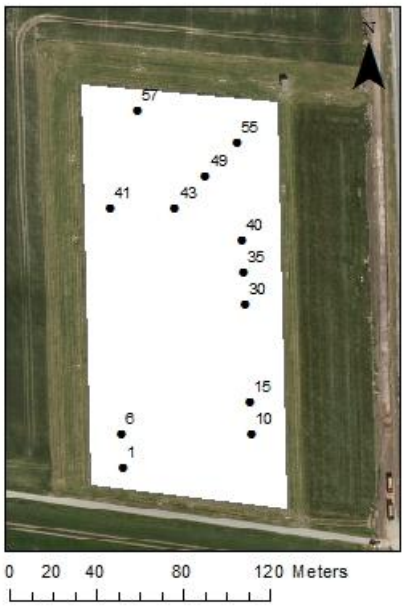


**Figure 39. The 12 biggest values for the amount of particles leached at 60 mm.**

Comparing Figure 38 and Figure 39 it is only the sampling points no. 41 and 57 that results in the very dark red area in the north-western part of the field in Figure 38, but still the majority of high values are located in the upper half. The same map was made for the continuous release of particles without the first flush effect, and that map looked the same – it would be the same 12 points.

### 4.4.3 Particle leaching and parameter correlations

The best correlation obtained with the three threshold values for accumulated particle leaching is shown in Figure 40.

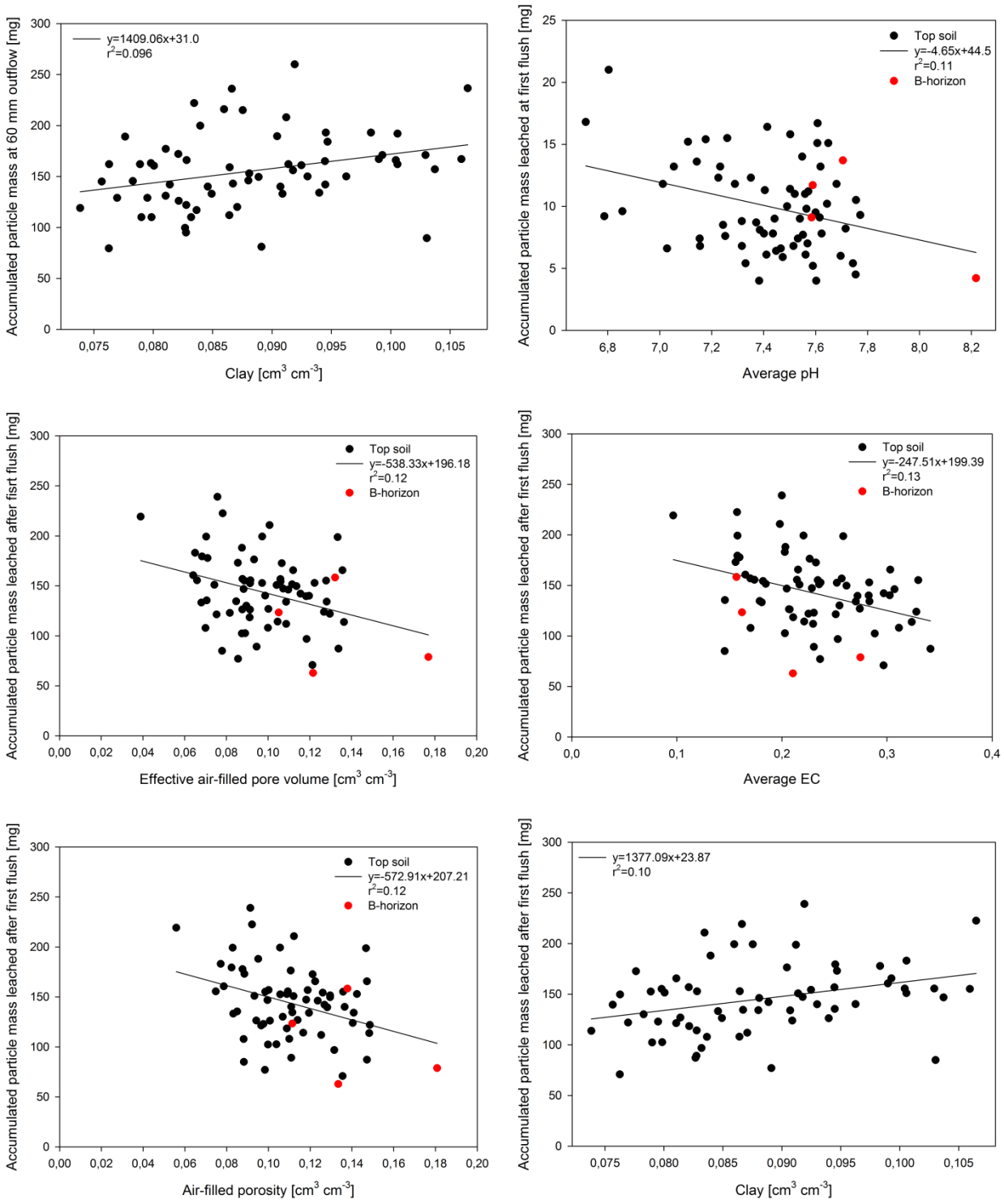


**Figure 40. In the first row the best correlations between the total accumulated amount of particles leach after 60 mm and volumetric clay content, and the amount of particles leached in the first flush and average pH. The last four plots is the best correlations gained from the accumulated amount of particles leached after first flush as a function of the air-connected porosity measured with the pycnometer, average pH, calculated air-filled porosity and the volumetric clay content.**

Even though these plots give the best correlations when evaluating the three particle threshold values with other parameters, the correlations obtained are not good. This might indicate that not just one parameter, but several parameters effect the leaching of particles.

### 4.4.4 Highlights in particle leaching

The shape of the particle concentration curves as a function of the outflow is similar to what is found in other literature studies. The first flush average value is a little lower than what is seen in similar leaching setups with similar irrigation rates, but once again no soil management has been carried out for almost two years, and only a small amount of particles are mobilised for particle leaching. Opposite Vendelboe et al., (2011) other parameters than the clay- and OC content play a role in the leaching of particles. This might be due to the fact that Dexter n is smaller than 10 in all sampling points and thus there is no excess clay that contribute to the particle load. In this thesis it hasn't been possible to establish just one parameter with a determining effect on particle leaching, and instead it must be assumed that several parameters play a role in the leaching of particles.

From the contour maps with the accumulated amount of particles leached at 60 mm outflow it can once again be confirmed that there is something special with the upper third of the field. The same tendencies were seen in the contour map where the first flush mass was subtracted from the total accumulated particle mass. As indicated before in the soil texture section, it is in this part of the field where the right structure is present for colloid-facilitated transport to take place. This has been supported since the largest amount of particles leaches from this area.

The particle concentrations leached from the B-horizon are a little lower than the particle concentrations leached from the top soil, the particles here might be even less mobilised than in the top soil.

## 4.5 Tracer (tritium) breakthrough curves

Breakthrough curves for each column are shown in Figure 41 and Figure 42 (B-horizon). The curves from the top soil are arranged according to the Dexter index to see if there were any trends. The time t=0 is the time where tritium was applied.

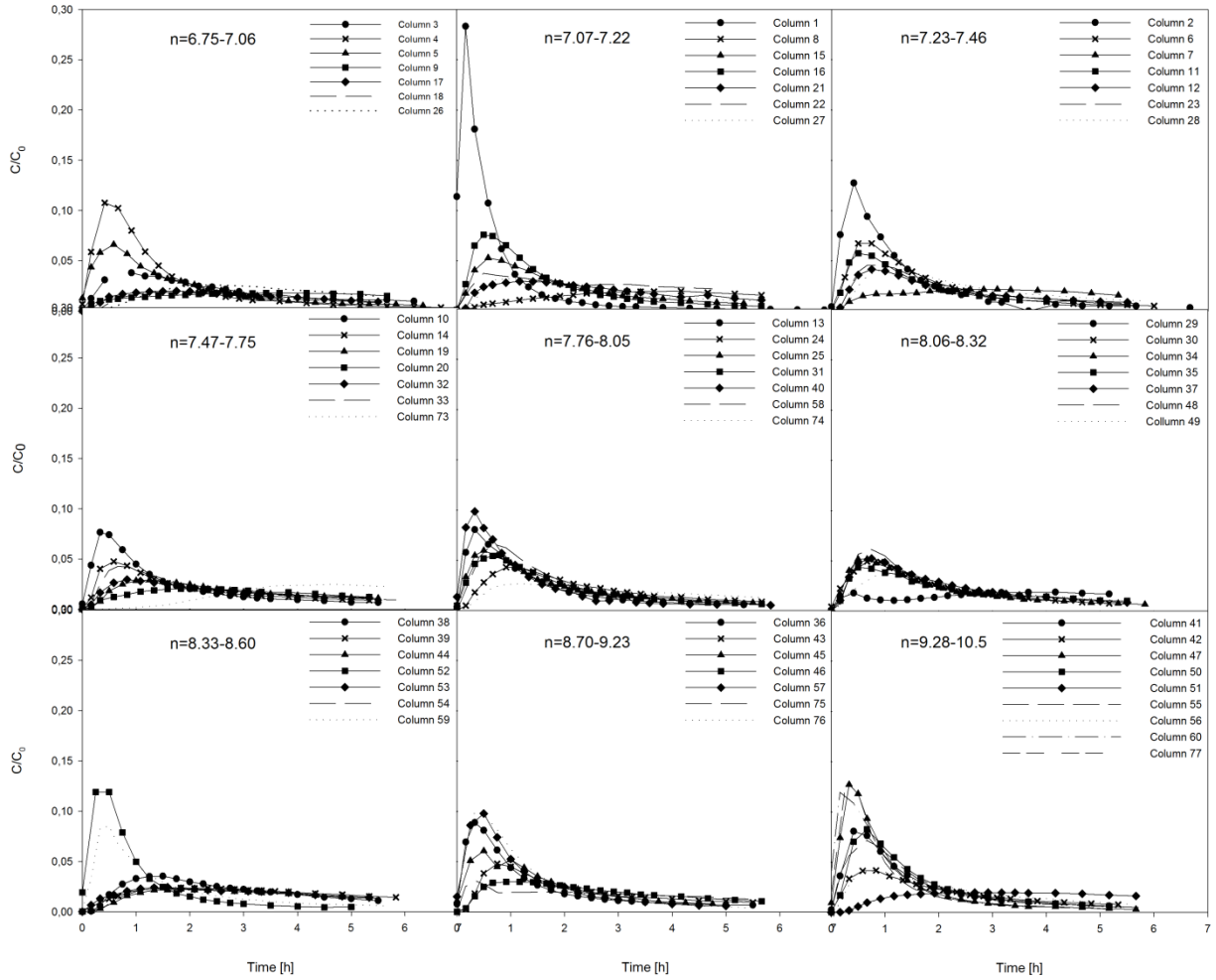


**Figure 41. Breakthrough curves from the leaching experiment arranged according to Dexter index, n. Columns from the B-horizon are not included in the plots.**

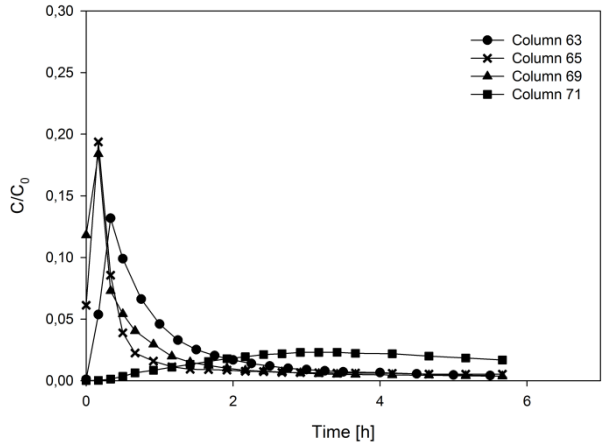


**Figure 42. Breakthrough curves from the B-horizon (except for no. 61 that ponded). There were no texture analyses carried out on bulk soil from the B-horizon and the Dexter index is not shown.**

The shapes of the breakthrough curves are very different from each other; a few of them show a very high peak, some, an almost unclear peak in the scale applied in the plot. Common for several of the columns are

that they peak very fast after $t_0$ and then tails of more slowly. Kjaergaard et al., (2004b) saw the same asymmetric breakthrough curves at clay contents above 18% and Glæsner et al., (2011) also experienced earlier breakthrough for loamy soils compared to sandy loams. The early breakthrough times and asymmetric curves emphasis the pronounced macropore flow, but also there it a small fraction of the solute that is limited by diffusion, between the mobile and immobile water phase, indicated by the tailing of the curves (Kjaergaard et al., 2004b). There is no clear connection between the looks of the breakthrough curves and Dexter n across the field.

The shape of the breakthrough curves from the B-horizon doesn't vary significantly from the breakthrough curves obtained from the top soil columns, but with the exception of column no. 1, the highest initial concentrations of tritium was found in the effluent from column no. 65 and 69 in the B-horizon. These results indicate that there might be very large preferential flow paths in these two columns from the B-horizon and support the assumptions about a structured B-horizon with a high bulk density and persistent cracks with pronounced macropore flow.

### 4.5.1 5% arrival time and tritium recovery

5% arrival time was found from mass accumulated tritium curves and the results are plotted in Figure 43 together with the percentages of tritium rediscovered in the effluent compared to the amount that was applied.

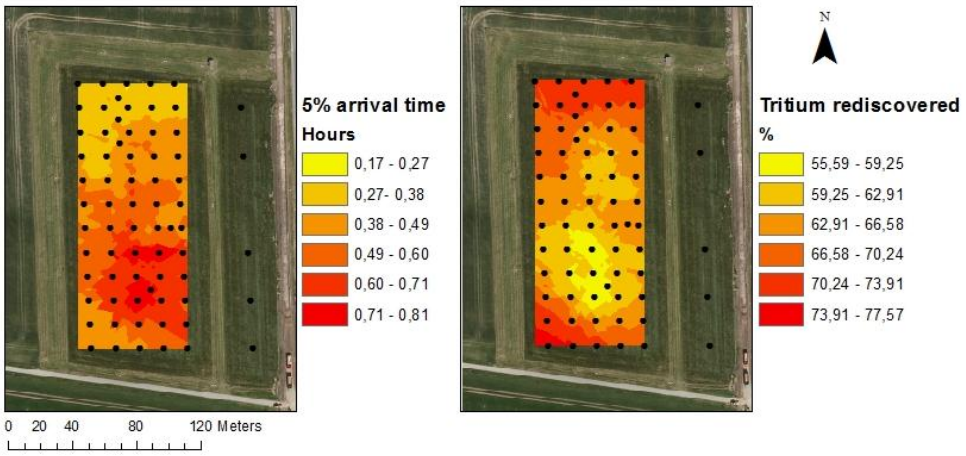


**Figure 43. 5% arrival and the percentages of tritium rediscovered in the effluent. Results from the B-horizon can be seen in Table 7.**

The fastest arrival times are found in the northern third of the field, and also from the columns sampled in this area, most tritium was recovered in the collected effluent compared to how much was applied. The high tritium recovery found in this part of the field indicate that the exchange of solute with the soil matrix is very limited compared to the rest of the field. This supports the assumption about a very compact soil with high clay contents leading to very persistent cracks. The fast arrival times once again supports the hypothesis about pronounced macropore flows in that part of the field.

Mass recovery of tritium was in average 67% for all the columns including the ones sampled from the B-horizon. In Glaesner et al., (2011) column effluent was collected for ~10 hours with a suction of -50 cm applied at the bottom of the columns and they obtained an average mass recovery on 94%. The higher amount of tritium found in Glaesner et al., (2011) is probably due to the higher sampling time compared to the 6.5 hours of sampling in these experiments.

The columns from the B-horizon are not included in Figure 43 and instead they are given Table 7. Column no. 61 ponded and thus no tritium were added to this column. Column no. 65 and 69 gave very high concentrations of tritium during the first 10 minutes of sampling, and therefore it was not possible to derive the 5% arrival time from the accumulated tritium curves. Still the very high concentrations during the first 10 minutes from column no. 65 and 69 indicate that there was macropore flow in these columns as well.

**Table 7. % tritium rediscovered and 5% arrival time for the columns sampled in the B-horizon.**

| Column no.: | % tritium rediscovered: | 5% arrival time [h]: |
|---|---|---|
| 61 | - | - |
| 63 | 74,25 | 0,16 |
| 65 | 61,70 | - |
| 69 | 72,88 | - |
| 71 | 56,67 | 1,28 |

### 4.5.2 Tritium breakthrough curves and parameter correlations

5% arrival time is plotted as a function of the gravimetric, and the volumetric clay content in Figure 44.

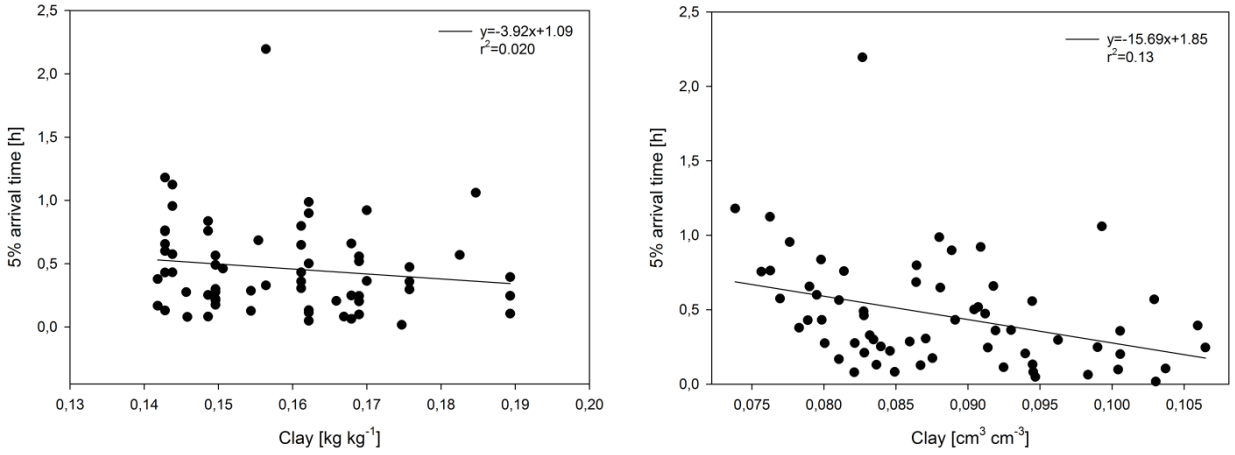


**Figure 44. 5% arrival time as a function of the gravimetric (kg kg$^{-1}$), and the volumetric clay content (cm$^3$ cm$^{-3}$).**

As it can be seen from Figure 44 the volumetric clay content has the greatest impact on the 5% arrival time, but none of the two correlations are particularly good.

In Figure 45, 5% arrival time is plotted as a function of bulk density, P-values (calculated from the air permeability and air-filled porosity in situ), air permeability in situ and the specific air permeability in situ (calculated from the air permeability and the air-connected porosity in situ). In Appendix I the 5% arrival time is plotted as a function of the air-connected porosities.

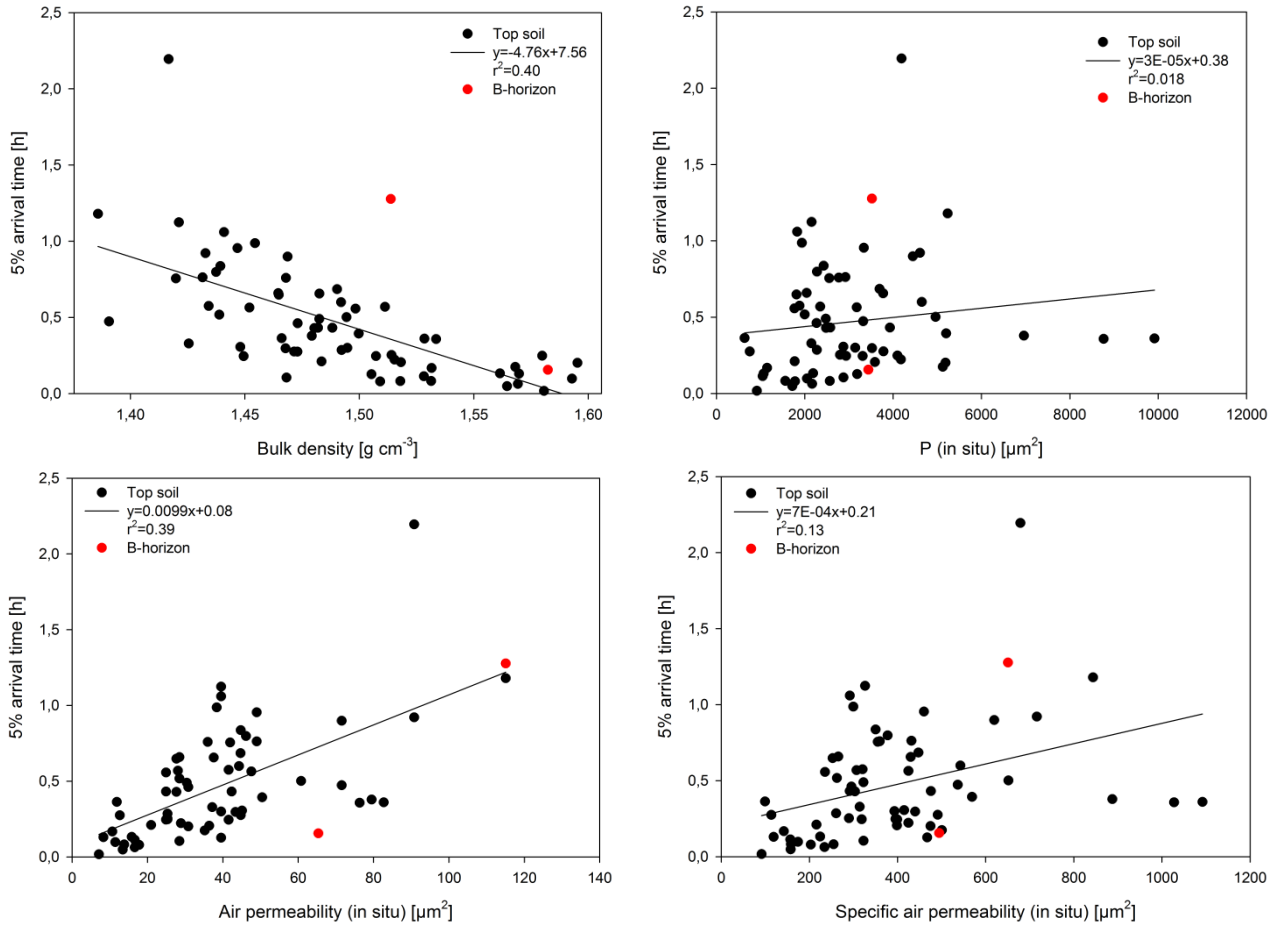


**Figure 45. 5% arrival time as a function of bulk density, P-values, air permeability in situ and, the specific air permeability ($K_a$ in situ divided by air-connected porosity). The two columns from the B-horizon from where it was possible to estimate the 5% arrival time are shown with red dots and these points are included in the regressions.**

The outlier with a breakthrough time on ~2.2 is column no. 73. The best correlation with 5% arrival time is achieved from the bulk density - the higher the bulk density, the smaller the arrival time. The negative correlation between these two parameters confirms the compact structure with preferential flow paths leading to fast arrival times through the columns. The correlation between the 5% arrival times, and the calculated P-values is not as good as expected from the Kawamoto-Buckingham models. The positive correlations between the 5% arrival time, the air permeability, and the specific air permeability is not what was expected either – at high arrival times it was expected that the two air-parameters would be low, but this is not the case. At in situ conditions the columns might have been drained to a point where it is no longer only the large flow controlling macropores who determine the air permeability. Though, when plotting the 5% arrival time as a function of the air permeability at -20 cm matrix potential, the same positive correlation can be seen, and here it should be the large macropores who mainly determine the air permeability. From these data it seems as if air parameters like air permeability and air-connected porosity not are the most certain parameters when predicting the transport of tritium, and thus water – at least they should be used with thoughtfulness.

In Figure 46 the percent of tritium rediscovered in the effluent is plotted as a function of bulk density, 5% arrival time, air permeability in situ and specific air permeability in situ ($K_a$ in situ divided by air-connected

porosity). In Appendix I the percentage of tritium rediscovered in the effluent is plotted as a function of the air-connected porosity measured with the pycnometer.

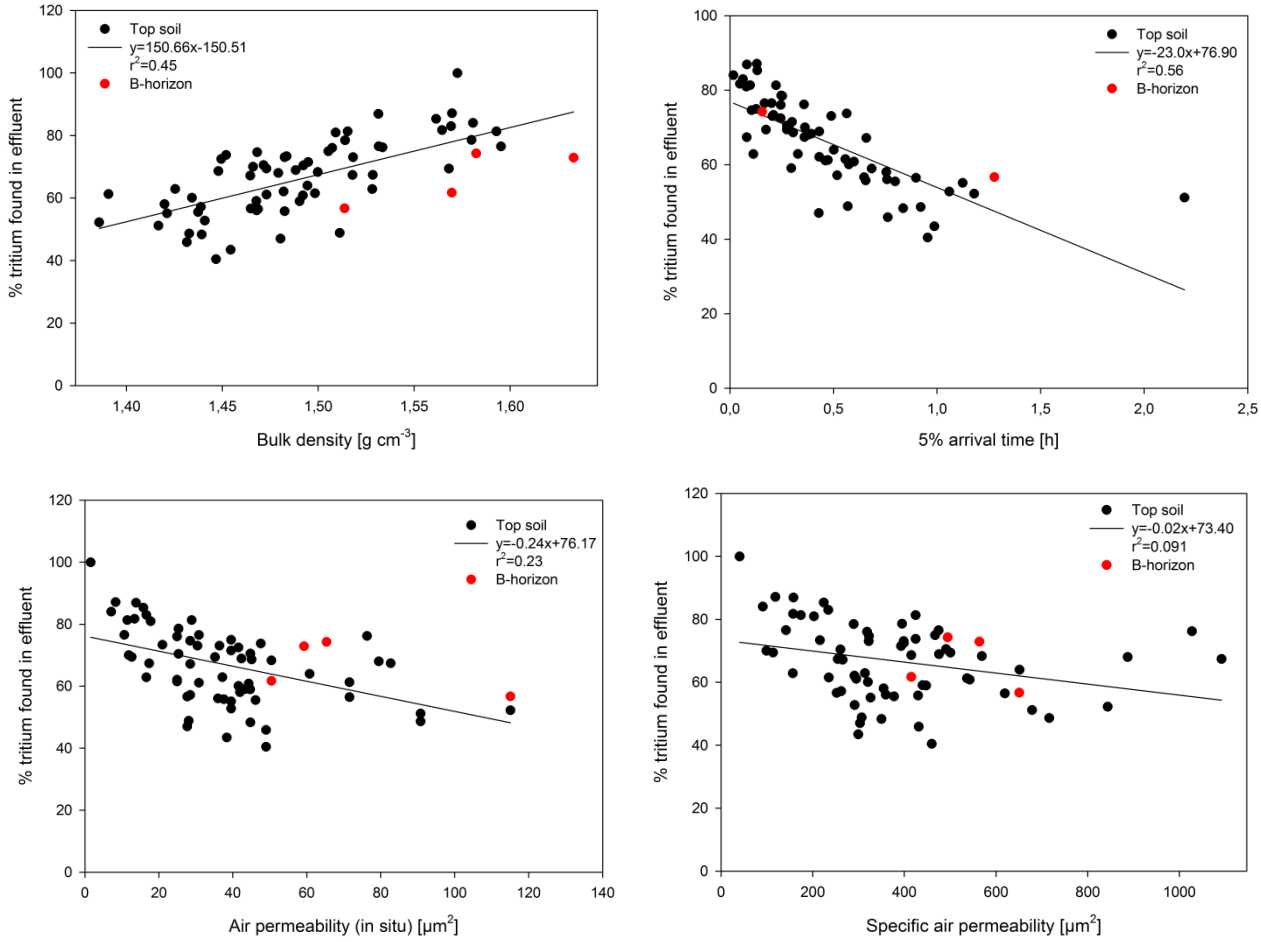


**Figure 46. Tritium recovery in the effluent as a function of bulk density, 5% rrival time, air permeability in situ and specific air permeability. Columns from the B-horizon are shown with red dots and they are included in the regressions.**

Once again there is a god correlation with the bulk density which confirms the compressed structure - at higher bulk densities, and also higher clay contents, more tritium is leached directly through the columns because of the persistent macropores. The correlation with the 5% arrival time confirms that the small retention times derived from the compact columns with pronounced macropore flow, results in higher recoveries of tritium in the effluent because the exchange of solute between the macropores and the soil matrix is limited.

Because of the connection seen with bulk density in Figure 45 and Figure 46 this parameter was linked with the total mass of particles leached at 60 mm, the mass of particles leach during first flush, and the mass of particles leached after first flush. These plots are shown in Figure 47.

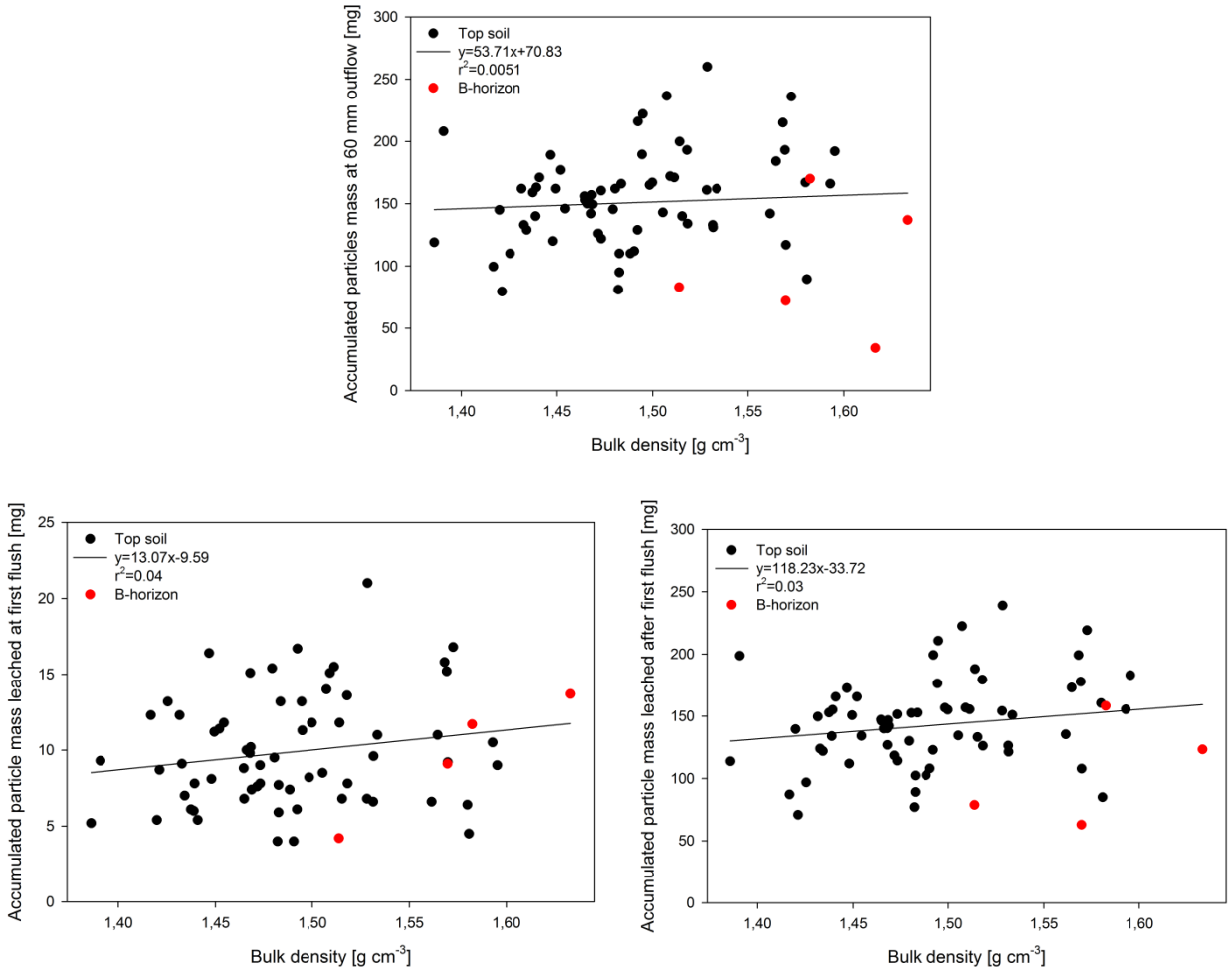


**Figure 47. Particles leached in total, in the first flush, and after the first flush as a function of bulk density.**

The same plots were made with 5% arrival time instead of bulk density in Figure 48.

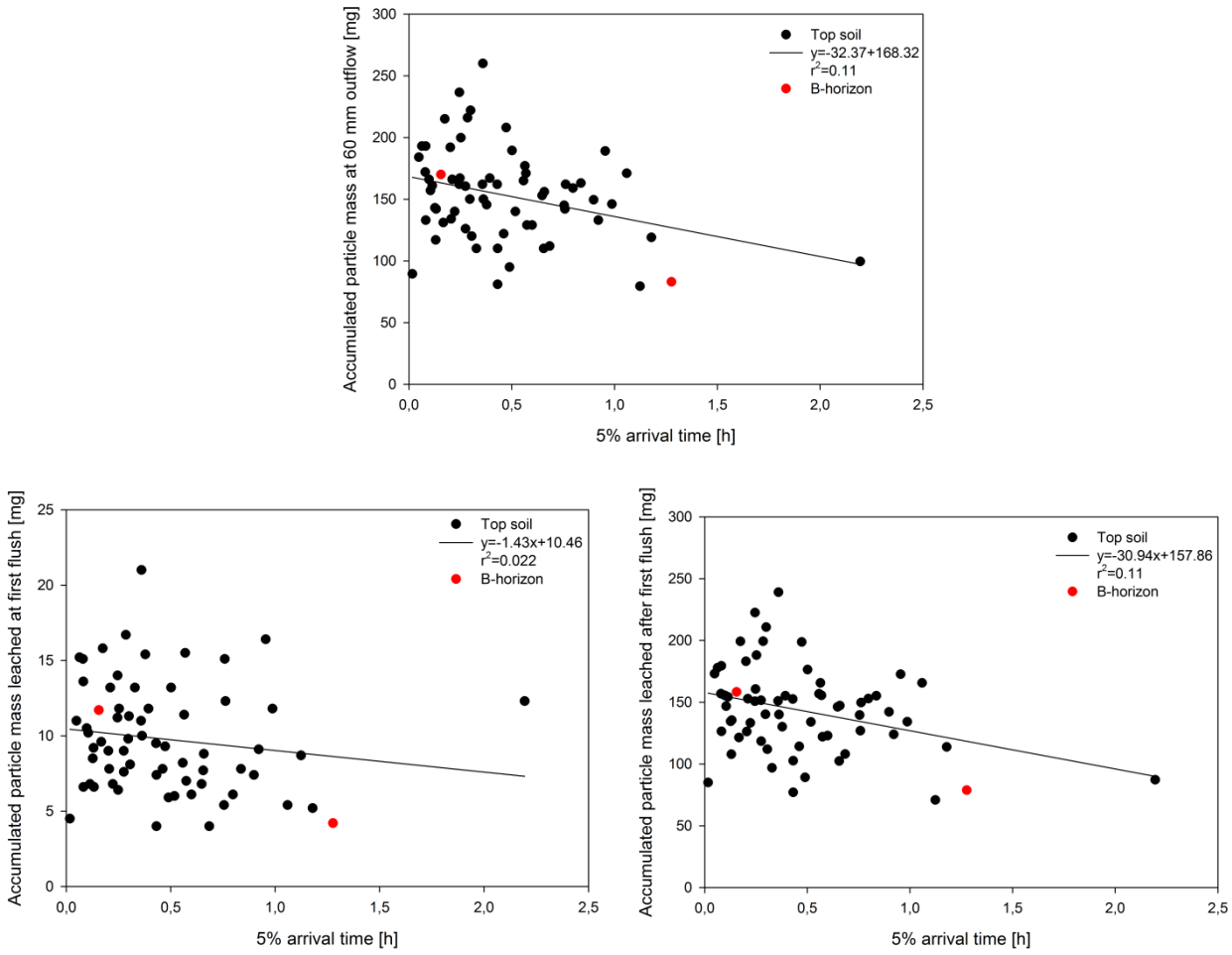


**Figure 48. Particles leached in total, in the first flush, and after the first flush as a function of 5% arrival time.**

Even though bulk density and the 5% arrival time could be used to explain the behaviour of tritium and thus the movement of water through the columns, the leaching of particles cannot be connected to these two parameters. 5% arrival time seem to give the best correlations compared to bulk density.

### 4.5.3 Highlights in tritium breakthrough curves

From the different shapes of the breakthrough curves, it is assumed that soil is very heterogeneous. In this thesis still no connection was established with Dexter n. The fastest 5% arrival times was obtained from the upper third of the field. 5% arrival times were tested against all other parameters, and the best correlation was obtained with bulk density. The high bulk density soil in the upper third of the field creates preferential transport pathways with high saturated hydraulic conductivity in the persistent macropores, while the saturated hydraulic conductivity is much smaller in normal-compacted soils where both soil matrix and macropores contribute to the transport intensity, see Figure 49. Also the highest tritium recoveries were detected in the upper third of the field confirming the limited amount of solute exchange with soil matrix in highly-compacted soils.

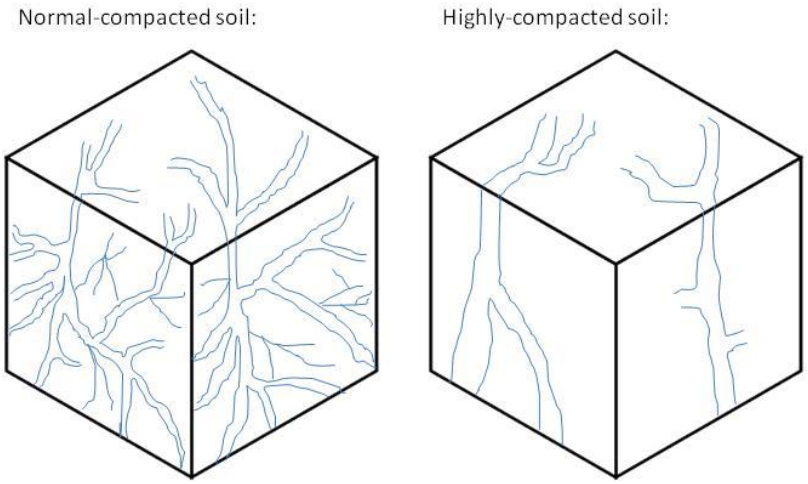


**Figure 49. To the left a simple illustration showing a normal-compacted soil with low bulk densities where there is both water transport within the soil matrix and in the macropores. To the right a highly-compacted soil where the transport is limited to the persistent macropores increasing the saturated hydraulic conductivity and the decreasing 5% arrival time.**

It was not possible to connect 5% arrival time nor tritium recovery to the amount of particles leached.

## 4.6 Phosphorus leaching

### 4.6.1 Total phosphorus and total dissolved phosphorus

The concentrations of TP and TDP in the collected effluent were determined from standard curves like the one shown in Appendix J. The concentrations of TP and TDP are shown in Figure 50 as a function of the outflow from the columns.

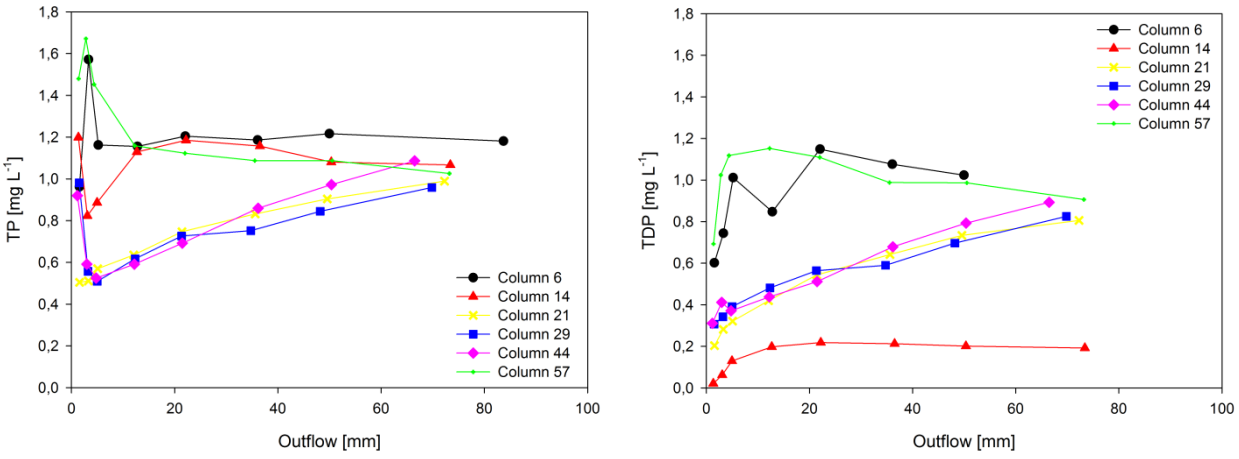


**Figure 50. TP and TDP as a function of the outflow during the leaching experiment. The location of the six selected columns can be seen in Figure 15.**

It is different whether the total phosphorus concentrations starts at a low concentration, and then stabilises at a higher level, or starts at a higher concentration level and then stabilises to a lower level, but the stable level is almost the same. The TP concentrations in first flush vary between 0.1 and 3 mg $L^{-1}$ and stabilises at a level around 0.05 and 2.06 mg $L^{-1}$. TDP concentrations in first flush were not as pronounced as it was for the TP concentrations. TDP concentrations were in general more constant during the experiment ranging from 0.03 to 1.83 mg $L^{-1}$. In Vendelboe et al., (2011) TP concentrations in first flush ranged between 0.6 and 1.8

mg $L^{-1}$ and was stabilised at a level from 0.1 to 0.4 mg L-1. The TDP concentrations varied between 0.02 and 0.2 mg $L^{-1}$. In general phosphorus concentrations found by Vendelboe et al., (2011) are smaller and more constant. The higher concentration of phosphorus found in this project compared to Vendelboe et al., (2011) might be due to higher concentrations of phosphorus in the soil, but these concentrations was not measured in this project.

### 4.6.2 Particular phosphorus

It is only the particular phosphorus (PP) concentrations that are in interest when considering colloid-facilitated transport of phosphorus and these concentrations was estimated as the difference between TP and TDP. PP concentrations as a function of the outflow are shown in Figure 51. Since TDP can't be connected to the leaching of particles it will only be the PP concentrations that will be treated further in the thesis.

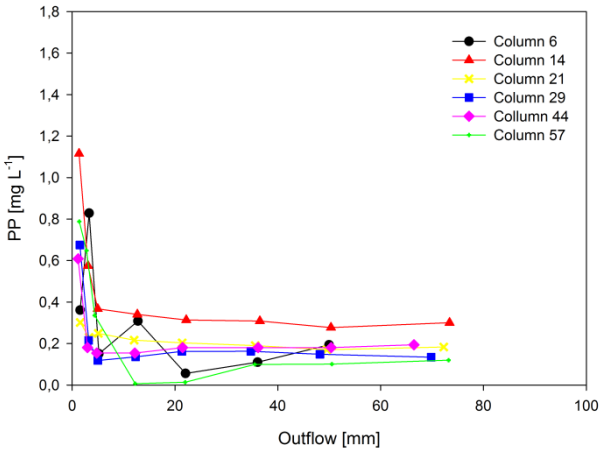


**Figure 51. Particular phosphorus concentrations in the collected effluent during the leaching experiment.**

Like with the particle concentrations PP concentrations are high during first flush and after approximately 8 mm outflow the concentrations stabilises at a lower level. The particular phosphorus peak concentrations in the first flush ranged between 0.07 and 1.73 mg $L^{-1}$, and stabilised around 0.1 and 0.35 mg $L^{-1}$.

PP concentrations as a function of particle concentrations are shown in Figure 52 together with literature regressions. For this plot matching values was needed, so the only points used are those not pooled for the determination of TP and TDP (bottle 1, 2 and 3, see Table 13 in Appendix F). The same plot with all columns shown can be seen in Appendix K.

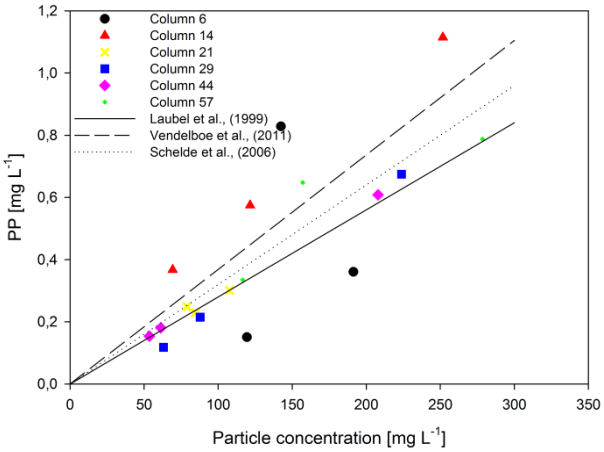


**Figure 52. PP concentrations as a function of the particle concentrations for six selected columns. Regressions from Laubel et al., (1999), Vendelboe et el., (2011) and Schelde et al., (2006) are included in the plot.**

The obtained correlation between the PP concentrations and the particle concentrations is consistent with correlations in literature, and the same can be seen when all the columns are included.

The accumulated mass of PP leached from each column is shown on the contour map in Figure 53.

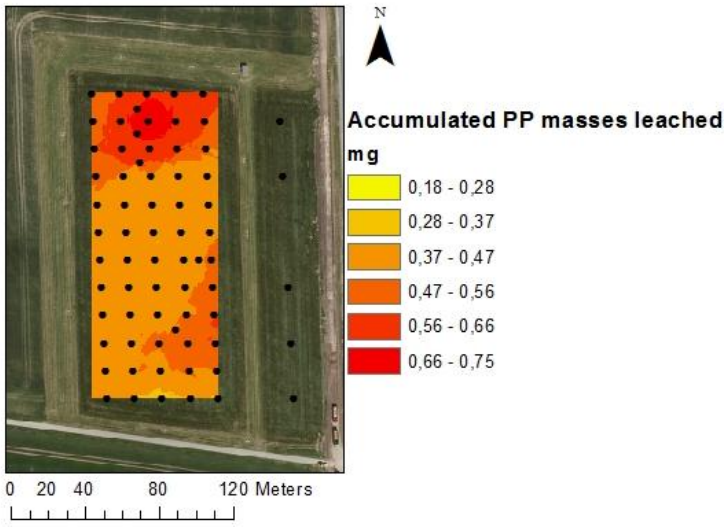


**Figure 53. Accumulated PP mass leached from the columns.**

Figure 53 once again confirms that it is in the upper third of the field where the structure is right for pronounced leaching to take place. From here the highest accumulated PP masses are leached and it was also here the largest accumulated particle masses were found.

The amount of particular phosphorus leached accounted for 3 to 62% of the total leached phosphorus masses, while total dissolved phosphorus accounted for 12 to 43% of the total leached phosphorus masses. Vendelboe et al., (2011) found that particle bound phosphorus accounted for 70-86% of the total phosphorus leached, and Schelde et al., (2006) found that 80% of the leached phosphorus was particle bound. Once again this might have something to do with the amount of phosphorus present in the soil.

### 4.6.3 Particular phosphorus and parameter correlations

The mass of accumulated PP is plotted in Figure 54 as a function of the accumulated particles mass for six selected columns.

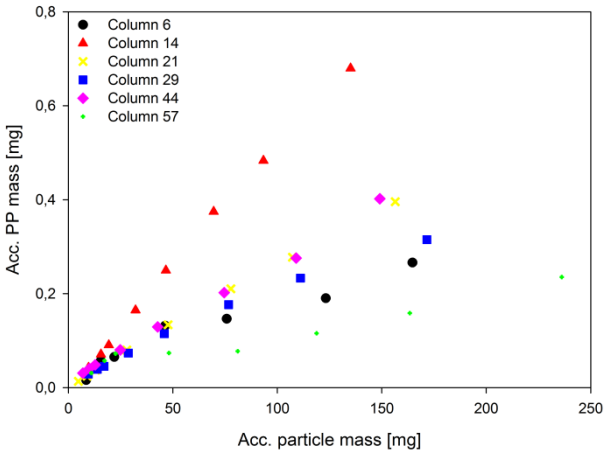


**Figure 54. Accumulated mass of PP as a function of the accumulated mass of particles from six selected columns.**

As in other literature studies (Vendelboe et al., (2011), Schelde et al., (2006) and de Jonge et al., (2004b)) there is a positive correlation between the accumulated particular phosphorus mass and the accumulated particle mass. Once again it should be pointed out that the same will not apply for TDP.

The slopes are mainly within 0.18 and 5.8 mg PP $g^{-1}$, with an average slope on 2.5 mg PP $g^{-1}$ particles. Schelde et al., (2006) found that the particular phosphorus concentrations was linearly related to the concentration of particles, with slopes varying between 3.2 and 5.8 mg P $g^{-1}$. Laubel et al., (1999) observed the phosphorus content of particular matter to be constant in the order of 2.8 mg P $g^{-1}$. Thus the amount of particular phosphorus per gram particle corresponds very well to the values also found in literature.

The slope of the plots in Figure 54 is mapped in Figure 55 as a function of the gravimetric clay content.

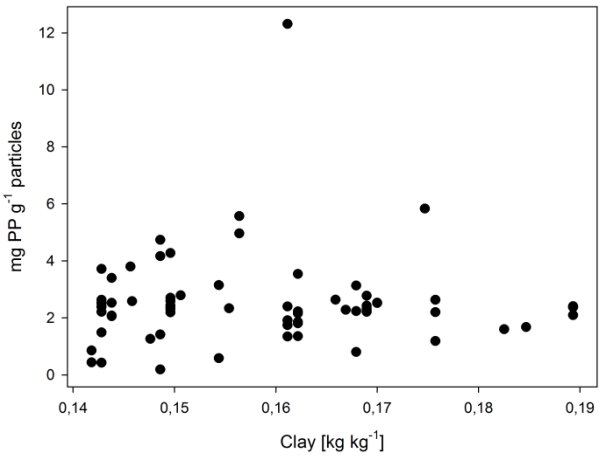


**Figure 55. The accumulated mass of phosphorus per g particle as a function of clay content. The columns from the B-horizon are not included.**

Figure 55 doesn't really show any tendencies that can be correlated to the amount of clay, but it gives an idea about the range. The outlier with ~12 mg PP g-1 particle is column no. 53. This column was sampled from the upper third of the field. The 12 biggest values are shown in Figure 56.

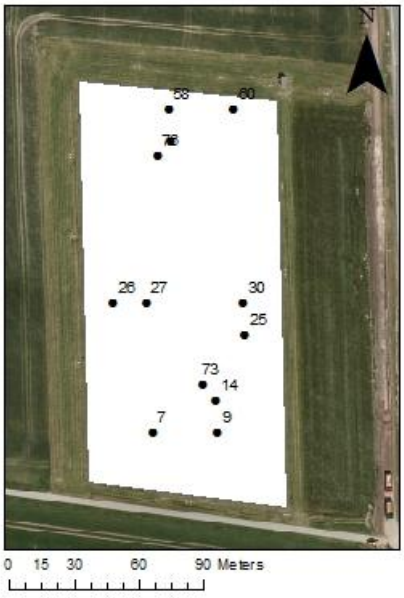


**Figure 56. The 12 biggest values of mg PP per g particle mass. The points 53 and 76 lay on top of each other in the upper part of the field.**

The largest amount of PP $g^{-1}$ particle was thus found in the southern part of the field. Even though the majority of the highest PP $g^{-1}$ particles were found here, the amount of particles leach from this part of the field was relatively small compared to the amount of particles leached from the upper third. As long as the particles doesn't leach there shouldn't be any worries regarding how much phosphorus is attached.

### 4.6.4 Highlights in phosphorus leaching

A positive correlation was obtained between the amount of particular phosphorus leached and the amount of particles leached. This is consistent with what is found by e.g. Schelde et a., (2006) and Vendelboe et al., (2011). In average 2.8 mg particular phosphorus was attached per gram particle. The largest amount of particular phosphorus was leached from the northern third of the field, and it was also from this area where the largest amount of particles was leached from. 3 to 63% of the total phosphorus mass was particle bound, and compared to other literature studies this is relatively low. However, it is hard to conclude anything from these percentages without knowing the concentration of phosphorus in the soil.

# 5 Vision analyses: towards a mapping-based risk and decision tool

When looking at colloid-facilitated transport of contaminants several factors or switches, so to speak, has to be turned on throughout the soil profile. Imagine that each switch represents a soil physical property with a certain effect on the colloid-facilitated transport pathways - the switch is either turned on or off. First step is to determine which factors play a role, and need to be present within the soil profile for leaching to take place. Secondly we must understand how to derive these from basic soil parameters, or fingerprints. Four "switches" are relevant for the soil matrix in Figure 57. The four switches and their mutual interaction are all known to have an effect on the colloid-facilitated leaching of contaminants. Additionally, a number of fingerprints are given in Figure 57 to the right. Fingerprints determined and mapped in this project period, are shown in boxes with continuous lines. Fingerprints not measured, but still important for the matching switch are shown in the dashed boxes.

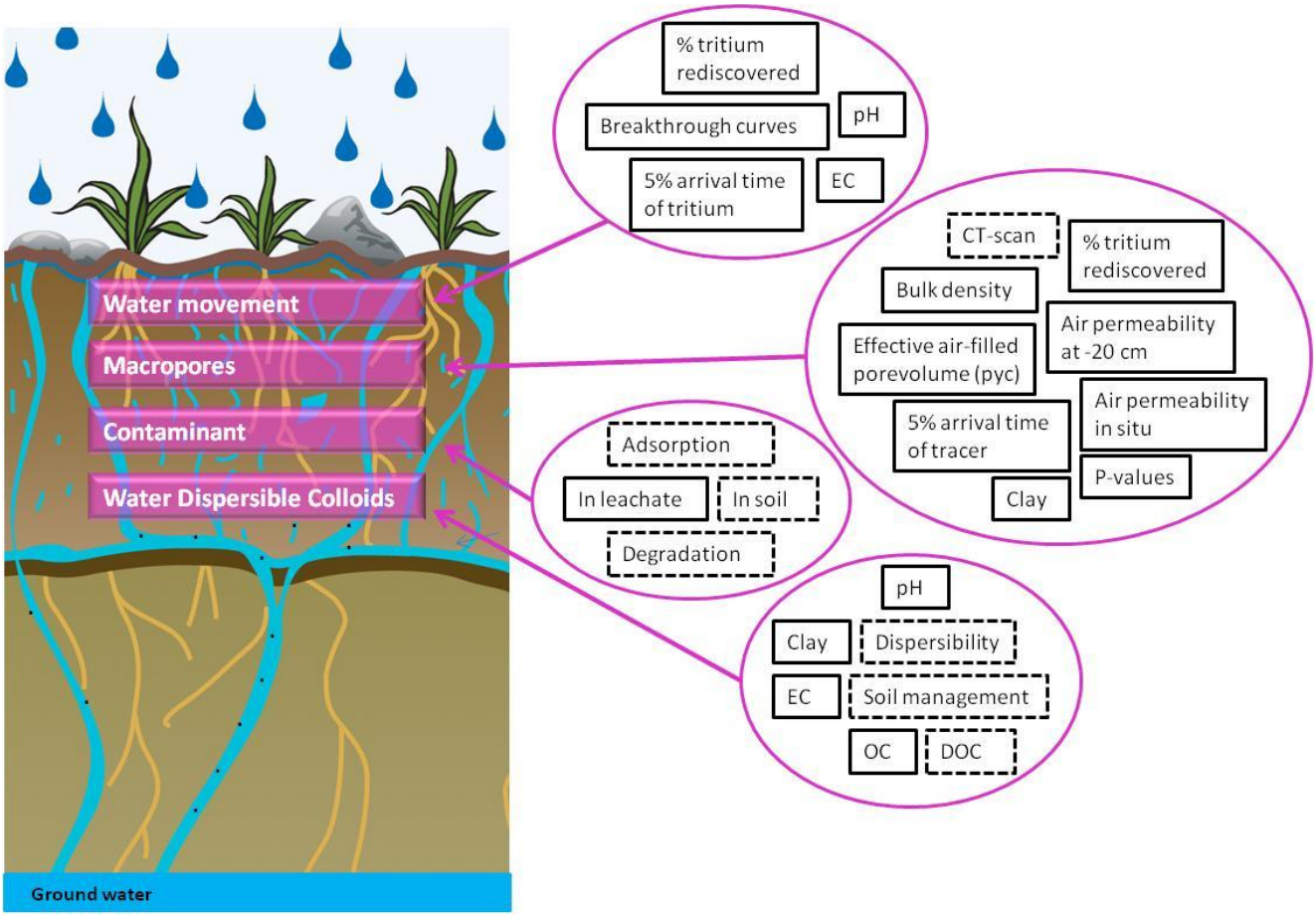


**Figure 57. Visualisation showing the switches that have to be turned on in the soil matrix in order for contaminant leaching to take place (to the left) and the fingerprints that might tell something about the switches (to the right). The boxes with the dashed lines are drawn around fingerprints that is not estimated or measured in this project, but still it is know that they play a role for the switch whereto it is connected.**

In order for colloid-facilitated transport to take place there needs to be a transport of water through the profile. It should be established whether water flows within the matrix thereby facilitating the exchange of solutes with the soil, or if the main transport of water takes place in macropores, leaving little time for solute exchange with the soil matrix and little time for sorption and degradation. An estimate of the risk related to water transport is gained from information about water transport, and the possibility for solute exchange can

be obtained from EC and to some extend the pH measurements, but also from the shape of the breakthrough curves, the 5% arrival time and the recovery of tritium in the effluent.

The amount of macropore pathways available for colloid-facilitated transport can be determined from several parameters. Bulk density and clay content were particularly related to the degree of macropore flow in the soil from Silstrup, but e.g. CT-scans can also be used to quantify the existence and size of macropores. Keller and Hakansson (2010) studied the effect of soil texture on bulk density, and found that the bulk density could be estimated from the particle size distribution parameters, and the organic matter content. This could be the next step in a multi-parameter analysis. In most cases it is necessary also to determine transport pathways within the underlying soil layers. The more compact structure in these layers might either facilitate or limit transport pathways from the soil surface.

Contaminants are transported either dissolved or sorbed to the colloids. For colloid-facilitated transport of contaminants to take place, the contaminant should sorb to the colloids. In these leaching experiments phosphorus concentrations were measured in the collected effluent, but sorbtion and degradation properties should also be considered when evaluating the colloid-facilitated transport of contaminants. In addition the concentrations of contaminants present in the soil should be determined in order to understand the leaching concentrations.

The amount of water dispersible colloids (WDC) depends on several factors like e.g. clay content, soil-water content, pH, EC, and OC content which are determined in this project. Furthermore the amount of WDC will depend on e.g. soil management conducted on the field, the dispersibility, and the amount of dissolved organic carbon (DOC). DOC was measured during the project, but only on 21 columns (therefore the dashed box). The results are not included in this thesis, but because it is particles <0.1 µm the DOC concentrations contribute to the colloid-concentrations. Pesticides like glyphosate with high $k_{oc}$-coefficients will sorb to the dissolved organic carbon and participate in the colloid-facilitated transport of contaminants down to the groundwater.

When evaluating the risk of colloid-facilitated transport of contaminants on field scale a time perspective should be included. Interactions the parameters in-between in some periods of the year contribute to an increased leaching risk of contaminants. In the autumn the downward water movement might be especially high and for some soils the macropores will be especially pronounced because of the dry summer period. In periods like these soil management and the application of e.g. pesticides should be planned carefully in order to prevent increased loads of contaminant leaching to the groundwater.

# 6 Conclusions

- Texture analyses in this project showed that the OC content is in the same range as the TOC measurements made in 1999. The clay contents on the other hand are in average approximately 50% smaller than the clay measurements carried out in 1999, and the clay range is rather narrow. This finding is rather interesting since clay content often is assumed to be constant over short time periods. It is therefore advisable to stay updated on knowledge about texture in order not to base estimations on old and erogenous data.

- The soil in the field in Silstrup is a highly -structured soil and in some periods of the year this might lead to the formation of very pronounced macropores.

- The best correlations were obtained between bulk density and 5% arrival time and tritium recovery in the effluent. The negative correlation between bulk density and 5% arrival time, and the positive correlation between bulk density and tritium recovery in the effluent both indicate that the soil is highly-compacted. Highly -compacted soils with persistent macropores dominate the leaching path ways which lead to small residence times, limited exchange of solute with the soil matrix, and limited time for sorption and degradation of contaminants.

- A reliable conversion of the turbidity (in NTU) to particle concentrations was obtained from several soil suspensions. Using the turbidity provided us with a fast method of estimating particle concentrations.

- Like in the literature there was a considerable leaching of particles in the beginning of the leaching experiment (first flush). A considerable amount of contaminants might therefore be leached during this first flush phenomenon due to the colloid-facilitated transport. Soil management and pesticide application should be coordinated in order to minimise the amount of contaminants leached together with the large amounts of readily dispersible colloids during first flush.

- The study has shown that there is a risk for pronounced leaching to take place from the northern third of the field due to the highly-compacted structure, and the amount of particles and phosphorus leached from this area.

- Contrary to other studies it was not possible to establish any connections between the leaching of particles and the content of clay and OC. This deviation from other studies might be due to the fact that the Dexter Index n was smaller than 10 in all sampling points and the soil should therefore be saturated with OC.

- A positive correlation was found between particle leaching and particular phosphorus leaching indicating that colloid-facilitated transport plays an important role in the leaching of phosphorus and other strong sorbing compounds. The largest risk for colloid-facilitated leaching is when there are many macropores and readily mobilised colloids in the soil.

- The quality of a mapping-based tool for risk assessments depends on the parameters included in the mapping, and how the included parameters are correlated. Few extreme points expressing the heterogeneous soil system might result in interpolations that show the wrong tendencies on field scale.

- It was possible to make a 1st draft concept for risk assessments from basic soil mapping pointing out fingerprints and parameters with an influence on general colloid-facilitated leaching. The concept is not yet complete and still many interactions has to be clarified, but it highlights some of the parameters that has to be taken into consideration when evaluating colloid-facilitated leaching risks on field scale.

# 7 Perspectives for continued research

This project will be carried on in a PhD project starting the 1th of August this year. The PhD project will keep its focus on the field in Silstrup, but the field in Estrup will also be included. With the PhD it will be possible to look further into the data already obtained during this project period, but it will also be possible to finish all the measurements there was no time to do in this project e.g. finishing the measurements of DOC and doing the NIR. As explained in Materials and methods, additionally 152 bulk soil samples was collected for NIR determination of clay and organic matter contents in a very fine sampling grid. Because of time limitations is was not possible to measure NIR on these samples, but it could be an interesting perspective to include those data in the contour map already made showing the clay content derived from the texture analyses. It would be easier to detect small changes in clay content, perhaps influencing the leaching of phosphorus, with this fine grid. Additional estimates of clay content have been carried out on the field in Silstrup with new EM-38 measurements. The results were not completely ready to be presented as a part of this thesis.

Measurements of dispersibility should have been carried out on the bulk soil samples from Silstrup. Like with NIR there was no time during this project period. In regard to the clay content and the leaching of phosphorus dispersibility however, could have been an interesting parameter to include.

Knowledge about the phosphorus content in the basic soil material would have been helpful when comparing the leached particular phosphorus concentrations with literature, and when trying to explain the low percentages of particular phosphorus out of the total amount of phosphorus.

In the autumn Fusilade Max will be applied to the field in Silstrup once again to see if it is possible to detect the same pronounced concentrations of TFMP as in 2008. Sorbicell detections will be monitored and another part of the PhD project will be to compare the Sorbicell detections with the measurements made by the elder grab sampling method installed up there.

During the PhD project there will also be an intensive study of the degradation product TFMP and its chemical properties. The degradation product will be examined in the laboratory with sorption- and degradation experiments and thus is shouldn't be necessary to use model compounds like phosphorus when assessing the leaching risks of particularly this pesticide.

CT-scan it a new thing in predicting and visualising soil structure but it is also very expensive, and in this project only 14 out of the 70 columns were scanned. The scans have not yet been treated for visualisation and therefore no pictures are shown in this thesis. The macro porosity could have been confirmed from these visualisations, but it will have to wait.

# 8 Reference list


Buckingham, E., 1904. Contributions to Our Knowledge of the Aeration Status of Soils. *Bulletin 25*.

de Jonge, L. W. Heterogen transport af vand, og miljøpåvirkende stoffer. 2011. Handouts.

de Jonge, L.W., Kjaergaard, C., & Moldrup, P., 2004a. Colloids and colloid-facilitated transport of contaminants in soils: An introduction. *Vadose Zone Journal;* 3(2). p. 321-325. ISI:000227468800001.

de Jonge, L.W., Moldrup, P., Rubaek, G.H., Schelde, K., & Djurhuus, J., 2004b. Particle Leaching and Particle-Facilitated Transport of Phosphorus at Field Scale. *Vadose Zone Journal;* 3(2). p. 462-470. ISI:000227468800014.

de Jonge, L.W., Moldrup, P., & Schjonning, P., 2009. Soil Infrastructure, Interfaces & Translocation Processes in Inner Space ('Soil-it-is'): towards a road map for the constraints and crossroads of soil architecture and biophysical processes. *Hydrology and Earth System Sciences;* 13(8). p. 1485-1502. ISI:000269440900007.

Dexter, A.R., Richard, G., Arrouays, D., Czyz, E.A., Jolivet, C., & Duval, O., 2008. Complexed organic matter controls soil physical properties. *Geoderma;* 144(3-4). p. 620-627. DOI 10.1016/j.geoderma.2008.01.022. ISI:000255343800020.

Etana, A., Rydberg, T., & Arvidsson, J., 2009. Readily dispersible clay and particle transport in five Swedish soils under long-term shallow tillage and mouldboard ploughing. *Soil & Tillage Research;* 106(1). p. 79-84. DOI 10.1016/j.still.2009.09.016. ISI:000273067300011.

European Food Safety Authority, 2010. Conclusion on the peer review of the pesticide risk assessment of the active substance fluazifop-P. *EFSA Journal 2010;* 8(11), [76 pp.]. doi: 10.2903/j.efsa.2010.1905. www.efsa.europa.eu/efsajournal.htm.

Gee, G.W. & Or, D., 2002. *Methods of Soil Analysis Part 4 - Physical Methods.* Book series No. 5. Edt. by Dane, J. H. and Topp, G. C. Madison, Wisconsin, USA. Soil Science Society of America.

GEUS, 2000. *Grundvandsovervågning 2000*. København, Danmark.

GEUS, 2009. *Grundvandsovervågningen 2009 - Grundvand. Status og udvikling 1989-2008*. De Nationale og Geologiske Undersøgelser for Danmark og Grønland, Klima- og Energiministeriet. København, Danmark.

GEUS, 2010a. *Grundvandsovervågningen 2010 - Grundvand. Status og udvikling 1989-2009*. De Nationale og Geologiske Undersøgelser for Danmark og Grønland, Klima- og Energiministeriet. København, Danmark.

GEUS, 27-7-2010b. Vi påvirker grundvandet - VIDEN OM GRUNDVAND, De Nationale Geologiske Undersøgelser for Danmark og Grønland - GEUS.

Glaesner, N., Kjaergaard, C., Rubaek, G.H., & Magid, J., 2011. Interactions between Soil Texture and Placement of Dairy Slurry Application: I. Flow Characteristics and Leaching of Nonreactive Components. *Journal of Environmental Quality;* 40(2). p. 337-343. DOI 10.2134/jeq2010.0317. ISI:000287574000007.

Hedemand, T. & Strandberg, M., 2009. *Pesticider - påvirkninger i naturen.* Hovedland.

Keller, T. & Hakansson, I., 2010. Estimation of reference bulk density from soil particle size distribution and soil organic matter content. *Geoderma;* 154(3-4). p. 398-406. DOI 10.1016/j.geoderma.2009.11.013. ISI:000275009400030.

Kjaergaard, C., Moldrup, P., de Jonge, L.W., & Jacobsen, O.H., 2004a. Colloid mobilization and transport in undisturbed soil columns. II. The role of colloid dispersibility and preferential flow. *Vadose Zone Journal;* 3(2). p. 424-433. ISI:000227468800010.

Kjaergaard, C., Poulsen, T.G., Moldrup, P., & de Jonge, L.W., 2004b. Colloid mobilization and transport in undisturbed soil columns. I. Pore structure characterization and tritium transport. *Vadose Zone Journal;* 3(2). p. 413-423. ISI:000227468800009.

Koroleff, F., 2011. *Simultaneous Oxidation of Nitrogen and Phosphorus Compounds by Persulfate. in: Methods of Seawater Analysis.* Edt. by Grasshoff, K., Eberhardt, M., and Kremling, K. Verlag Chemie.

Kretzschmar, R., Borkovec, M., Grolimund, D., & Elimelech, M., 1999. Mobile subsurface colloids and their role in contaminant transport. *Advances in Agronomy;* 66. p. 121-193. ISI:000080328600003.

Laubel, A., Jacobsen, O.H., Kronvang, B., Grant, R., & Andersen, H.E., 1999. Subsurface drainage loss of particles and phosphorus from field plot experiments and a tile-drained catchment. *Journal of Environmental Quality;* 28(2). p. 576-584. ISI:000079116500023.

Lindhardt, B., Abildtrup, C., Vosgerau, H., Olsen, P., Torp, S., Iversen, B. V., Jørgensen, J. O., Plauborg, F., Rasmussen, P., & Gravesen, P., 2001. *The Danish Pesticide Leaching Assessment Programme - Site Characterization and Monitoring design*. Geological Survey of Denmark and Greenland. ISBN 978-87-7871-279-0.

Loll, P. & Moldrup, P., 2000. *Soil Characterization and Polluted Soil Assessment.* Aalborg University.

Miljø- og Energiministeriet, 2000. *Pesticidhandlingsplan II*. Miljø- og Energiministeriet, Ministeriet for fødevarer, landbrug og fiskeri.

Mills, M.S. & Simmons, N.D., 1998. Assessing the ground-water contamination potential of agricultural chemicals: a flexible approach to mobility and degradation studies. *Pesticide Science;* 54(4). p. 418-434. ISI:000077642000013.

Moldrup, P., Hamamoto, S., Kawamoto, K., Komatsu, T., Yoshikawa, S., de Jonge, L. W., Schjønning, P., Jacobsen, O. H., & Rolston, D. E. 2010, Taking Soil-Air Measurements Towards Soil-Architectural Fingerprints, *In CESAR*, 1st International Conference and Exploratory Workshop on Soil Architecture and Physico-Chemical Functions "CESAR", pp. 229-234.

mst, 15-7-2010. Bichel-udvalget, http://www.mst.dk/Virksomhed_og_myndighed/Bekaempelsesmidler/Pesticider/Pesticidindsatsen_i_groen_vaekst/Bichel_udvalget.htm

Murphy, J. & Riley, J.P., 1962. A Modified Single Solution Method for Determination of Phosphate in Natural Waters. *Analytica Chimica Acta;* 27(1). p. 31-36. ISI:A19624070A00018.

NIRAS, 2005. *Vurdering af afværgepumpning som afværgemetode, En sammenfatning af metodens virkemåde, fordele og begrænsninger*. Amternes Videnscenter for Jordforurening.

Rosenbom, A. E., Brüsch, W., Juhler, R. K., Ernstsen, V., Gudmundsson, L., Kjær, J., Plauborg, F., Grant, R., Nyegaard, P., & Olsen, P., 2010. *The Danish Pesticide Leaching Assessment Programme - Monitoring results May 1999 - June 2009*. ISBN 978-87-7871-279-0.

Schelde, K., de Jonge, L.W., Kjaergaard, C., Laegdsmand, M., & Rubaek, G.H., 2006. Effects of manure application and plowing on transport of colloids and phosphorus to tile drains. *Vadose Zone Journal;* 5(1). p. 445-458. DOI 10.2136/vzj2005.0051. ISI:000237124500038.

Schelde, K., Moldrup, P., Jacobsen, O.H., de Jonge, H., de Jonge, L.W., & Komatsu, T., 2002. Diffusion-Limited Mobilization and Transport of Natural Colloids in Macroporous Soil. *Vadose Zone Journal;* 1(1). p. 125-136. ISI:000207557500009.

Tu, M., Hurd, C., & Randall, J.M., 2001. *Weed Control Methods Handbook: Tools & Techniques for Use in Natural Areas.* The Nature Conservancy, Wildland Invasive Species Team.

UH, 18-4-2011. PPDB: Pesticide Properties DataBase, University of Hertfordshire. http://sitem.herts.ac.uk/aeru/footprint/en/index.htm

Vendelboe, A.L., Moldrup, P., Heckrath, G., Jin, Y., & de Jonge, L.W., 2011. Colloid and Phosphorus Leaching from Undisturbed Soil Cores Sampled along a Natural Clay Gradient. *Soil Science*.

Villholth, K.G., Jarvis, N.J., Jacobsen, O.H., & de Jonge, H., 2000. Field investigations and modeling of particle-facilitated pesticide transport in macroporous soil. *Journal of Environmental Quality;* 29(4). p. 1298-1309. ISI:000089412600035.

# Appendix A

Below follows a short description of some of the analyses carried out and equipment installed at the six test sites.

The six test sites in PLAP represent the dominant soil types in Denmark; sandy soils and clay till. The geological composition of the test fields is characterized from geological maps, well data and test pit excavation at each test site.

Two to three soil profiles was excavated at each site in the buffer zone to describe the soil horizons down to 1.6 m. Soil samples were collected from each horizon for determination of e.g. soil texture, total organic carbon (TOC), pH, Fe and Al, total phosphorus, total nitrogen, exchangeable cations and cation exchange capacity. Five 6,280 $cm^3$ and nine 100 $cm^3$ soil cores were sampled from the A-, B- and C-horizon in the soil profiles. Air permeability (at -50 cm), near-saturated hydraulic conductivity and saturated hydraulic conductivity were measured on the large soil cores and air permeability (at -50 cm), saturated hydraulic conductivity and soil water characteristic were determined on the small soil cores.

Besides the TOC determined in the soil profiles, TOC mapping was carried out at each site in a 20 m grid with samples from the topsoil (0-25 cm). Geophysical mapping at the sites were carried out with EM-38 sensors down to 1 meter and the measurements at 2.5-3 m b.g.s. and 5-6 m b.g.s. were carried out using a CM-031 ground conductivity meter (Lindhardt et al., 2001).

Knowledge about the climate and its effect on pesticide leaching is retained from continuous monitoring of the precipitation, and each test site is not more than 8 km away from an automatic climate station. The annual precipitation at the five locations is shown in Table 8.

**Table 8. Annual precipitation at the five test sites based on time series for the period 1961-1990 (Rosenbom et al., 2010).**

| | Tylstrup | Jyndevad | Silstrup | Estrup | Faardrup |
|---|---|---|---|---|---|
| Annual precipitation (mm $y^{-1}$) | 668 | 858 | 866 | 862 | 558 |

There is a comparatively large difference between the annual precipitation at the five locations from Jyndevad, Estrup and Silstrup to the west, Tylstrup in the north and Faardrup in the eastern part of Denmark. The higher precipitation in the western part of Denmark allows for application of larger amounts of pesticides (or e.g. nitrate) because of the more pronounced dilution factor in these areas compared to the eastern part of Denmark.

Besides precipitation, soil temperature and soil water content is measured continuously at each site. Hydrogeological information considered when selecting and characterizing the fields were: groundwater table and groundwater flow, topographic slope and installations of tile drain systems (Lindhardt et al., 2001).

Bromide tracer was applied to each field in the beginning of the monitoring period in order to describe the water transport, and bromide concentrations has been measured continuously each month in both the saturated and the unsaturated zone, and weekly in the drain water (Rosenbom et al., 2010).

For continuous monitoring the fields were each equipped with the instruments shown in

Table 9 and a typical design of a PLAP field is shown in Figure 9 in the introduction.

**Table 9. Equipment installed in each of the six test sites (Lindhardt et al., 2001).**

| **Equipment:** | **Monitors:** |
|---|---|
| Piezometers | Potentiometric pressure of the groundwater |
| Vertical and horizontal monitoring wells | Sampling of groundwater |
| Suction cups | Water samples from the unsaturated zone |
| Automatic ISCO samplers | Sampling of drain water |
| Weather stations | Precipitation |
| TDR-probes | Soil water content |
| Pt-100 sensors | Soil temperature |
| Pressure sensors | Barometric pressure |

# Appendix B

**Monitoring results from Silstrup**

As mentioned in the introduction to PLAP a report is published each year with the latest monitoring results combined with results from previous years, hydrological modelling and measurements of the latest bromide leaching concentrations. Figure 58 gives a short presentation of monitoring data compared with modelling results from the latest report published by GEUS in 2010 - *Monitoring results May 1999–June 2009*. The hydrological model is calibrated with data from the period May 1999 to June 2004 and validated against data from July 2004 to June 2009. Each year a new validation period is added to the model. The hydrological model is validated by measurements of the groundwater level, drain flow, and measurements of soil water content measured with TDR-probes at three different depths from the two soil profiles S1 and S2 (Figure 9) (Rosenbom et al., 2010).

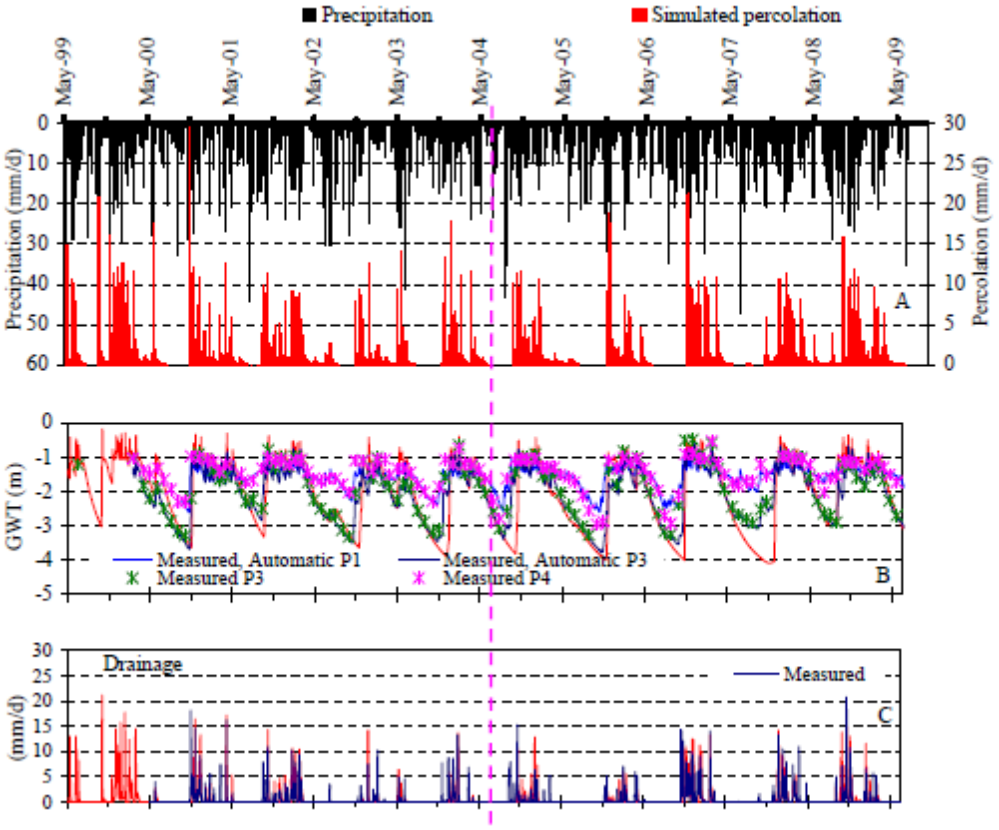


**Figure 58. (A) shows the precipitation and simulated percolation at Silstrup. (B) shows the position of the groundwater table measured manually with a "water lever indicator" in P3 and P4 and automatically with a transducer-logger systems in P1 and P3 (see Figure 9) - simulation results are shown with a red line. (C) shows the amount of drainage water measured and simulated. The pink dotted line indicated the shift between calibration and validation of the model (Rosenbom et al., 2010).**

The large amount of continuous data from the sites supported by hydrological modelling as shown in Figure 58 gives a good impression of why PLAP is useful when evaluating leaching risks of pesticides. Except for a few differences there seems to be a good agreement between the simulations and the measurements in Figure 58. Precipitation in each month for the period July 2000 –June 2009 is shown in Appendix C together with the annual water balance.

# Appendix C

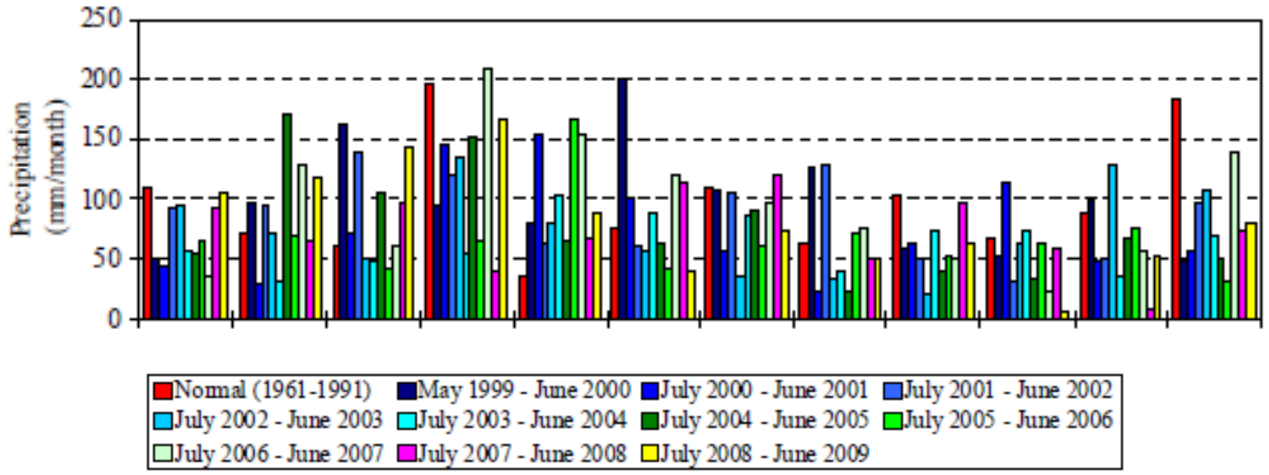


**Figure 59. Monthly precipitation from the period July 2000 –June 2009 at Silstrup. The values from 1961 to 1991 are included for comparison (Rosenbom et al., 2010).**

**Table 10. Water balance for Silstrup (mm year$^{-1}$) (Rosenbom et al., 2010).**

| | Normal Precipitation[2)] | Precipitation | Actual evapotranspiration | Measured drainage | Simulated drainage | Groundwater recharge[3)] |
|---|---|---|---|---|---|---|
| 1.7.99–30.6.00[1)] | 976 | 1175 | 457 | - | 443 | 275[4)] |
| 1.7.00–30.6.01 | 976 | 909 | 413 | 217 | 232 | 279 |
| 1.7.01–30.6.02 | 976 | 1034 | 470 | 227 | 279 | 338 |
| 1.7.02–30.6.03 | 976 | 879 | 537 | 81 | 74 | 261 |
| 1.7.03–30.6.04 | 976 | 760 | 517 | 148 | 97 | 94 |
| 1.7.04–30.6.05 | 976 | 913 | 491 | 155 | 158 | 267 |
| 1.7.05–30.6.06 | 976 | 808 | 506 | 101 | 95 | 201 |
| 1.7.06–30.6.07 | 976 | 1150 | 539 | 361 | 307 | 249 |
| 1.7.07–30.6.08 | 976 | 877 | 434 | 200 | 184 | 242 |
| 1.7.08–30.6.09 | 976 | 985 | 527 | 161 | 260 | 296 |

[1)] Monitoring started in April 2000.

[2)] Normal precipitation is based on times series from 1961-1990.

[3)] Groundwater recharge is calculated as: Precipitation – actual evapotranspiration – measured drainage.

[4)] Because of lack of measurements of drainage water, simulated drainage flow of drain was used to calculate groundwater recharge.

# Appendix D

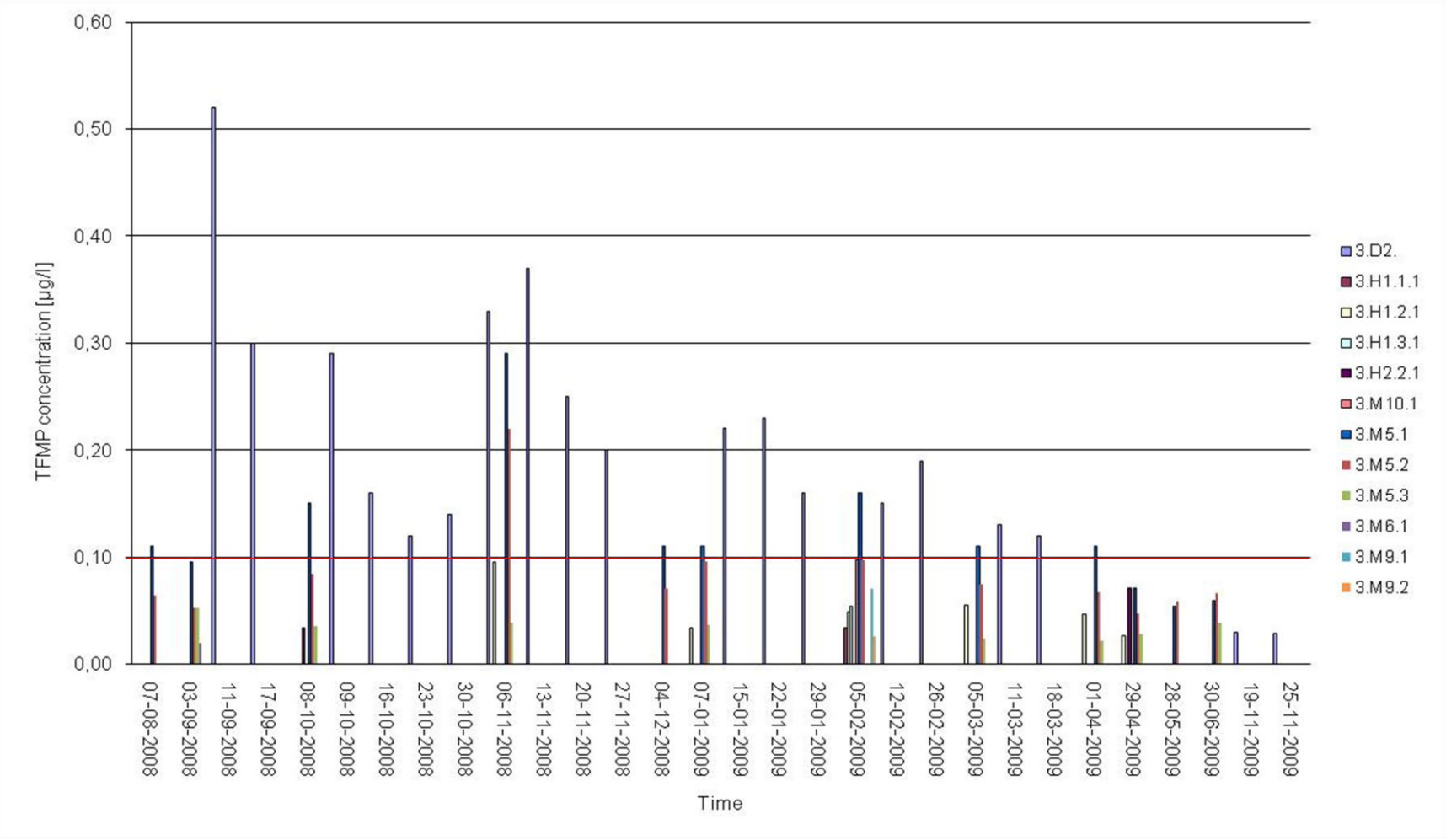


**Figure 60. Concentrations of TFMP detected at Silstrup since the application of Fusilade Max on July 1th 2008. The red line indicates the pesticide criterion for pesticides 1 m b.g.s on 0.1 µg/l. In the legend the number three means that it is in Silstrup. D, H and M respectively is drain, horizontal screens and vertical monitoring screens and the number right after the capital letter corresponds to the well number in Figure 9. The last number indicate the depth of the screen in the vertical monitoring wells (Table 4) or the number of the screen section in the horizontal screens (Rosenbom et al., 2010).**

# Appendix E

**Table 11. General information about fluazifop-P-butyl, fluazifop-P and TFMP.**

| | **Fluazifop-P-butyl:** | **Fluazifop-P:** | **TFMP:** |
|---|---|---|---|
| Chemical formula | $C_{19}H_20F_3NO_4$[1)] | $C_{15}H_{12}F_3NO_4$[1)] | $C_6H_4F_3NO$ |
| Solubility in water [mg $L^{-1}$] | 1.1[3)] | 780[3)] | 6000[3)] |
| $DT_{50}$ (soil) (days) | 1[3)] | 2.3-38.4[3)] | 13-82<br>Moderate to medium persistence in soil[3)] |
| $K_{oc}$ [m $g^{-1}$] | 3394[1) 3)]<br>Slightly mobile | -<br>Very high to high mobility[3)] | -<br>Very high mobility in soil[3)] |
| Herbicidal effect | Active[2)] | Active[2)] | Inactive[2) 3)] |
| Degraded by | Hydrolysis or microbial activity[1)] | Microbial activity[2)] | |
| Health issues | Carcinogen<br>Mutagen<br>Endocrine disrupter<br>Neurotoxicant<br>Skin irritant<br>Eye irritant[1)] | - | Toxicological relevant, but the risk for aquatic organisms was assessed as low[3)] |
| Risk classification | Reproduction risk category<br>Dangerous for the enviroment[1)] | - | - |

[1)] (UH, 2011)

[2)] (Tu et al., 2001)

[3)] (European Food Safety Authority, 2010).

# Appendix F

**Turbidity**

From the effluent collected in the plastic bottles on the rotating roundabout, 30 ml was collected for turbidity measurements on a Hach 2100AN turbidimeter (Hach, Loveland, USA) equipped with an EPA filter, measuring at wavelengths 400 to 600 nm.

The turbidity was given in nephelometric turbidity (NTU) which is assumed proportional to the particle concentration. The correlation between NTU and particle concentration (mg $L^{-1}$) was obtained from turbidity measurements on different soil suspension, see Figure 61 and Table 12. The suspensions was made from a main suspension obtained by dispersing bulk soil from Silstrup in deionized water and isolating particles >2 µm by gravitational sedimentation.

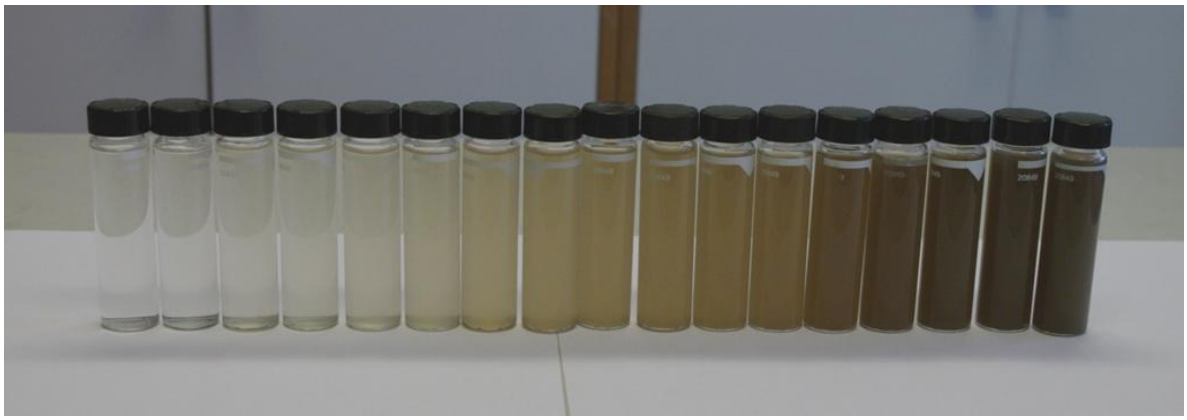

**Figure 61. Suspensions with bulk soil from Silstrup.**

**Table 12. The different suspensions used for correlating NTU with particle concentration.**

| Main suspension (ml): | Deionized water (ml): | Turbidity (NTU): | mg/1000 ml: |
|---|---|---|---|
| 0.05 | 29.95 | 24.6 | 16.5 |
| 0.05 | 29.95 | 23.6 | 23.5 |
| 0.1 | 29.9 | 48.1 | 37 |
| 0.1 | 29.9 | 47.3 | 40 |
| 0.2 | 29.8 | 94.9 | 88.5 |
| 0.2 | 29.8 | 95.4 | 77 |
| 0.25 | 29.75 | 116 | 106 |
| 0.25 | 29.75 | 118 | 102.5 |
| 0.35 | 29.65 | 166 | 135.5 |
| 0.35 | 29.65 | 163 | 135 |
| 0.5 | 29.5 | 232 | 199 |
| 0.5 | 29.5 | 248 | 173.5 |
| 0.75 | 29.25 | 361 | 268.5 |
| 0.75 | 29.25 | 362 | 279.5 |
| 1 | 29 | 519 | 360.5 |
| 1 | 29 | 518 | 381.5 |
| 1.25 | 28.75 | 671 | 464.5 |
| 1.25 | 28.75 | 662 | 460.5 |
| 1.5 | 28.5 | 826 | 555.5 |
| 1.5 | 28.5 | 815 | 559 |
| 1.75 | 28.25 | 1005 | 637 |
| 1.75 | 28.25 | 1022 | 635,5 |
| 2 | 28 | 1198 | 716 |
| 2 | 28 | 1288 | 730.5 |
| 3 | 27 | 2169 | 1075 |
| 3 | 27 | 2111 | 1081 |
| 4 | 26 | 3100 | 1442 |
| 4 | 26 | 3198 | 1462 |
| 5 | 25 | 4103 | 1777.5 |
| 5 | 25 | 4115 | 1781 |
| 6 | 24 | 4603 | 2125 |
| 6 | 24 | 4579 | 2198 |
| 7 | 23 | 6247 | 2523.5 |
| 7 | 23 | 6229 | 2543.5 |

**pH**

pH was measured on each effluent bottle with an HQ11d pH-meter (electrode type: pH C2051-8, France).

**Electrical Conductivity**
EC was measured on each effluent bottle with a radiometer (type CDM 2e No. 133606, Copenhagen, Denmark).

**Tracer analyses**
1 ml of effluent from each bottle from time t=0 minutes was mixed 2 ml elga water and 17 ml scintilations fluids (ULTIMA GOLD, High flash-point LSC cocktail, PerkinElmer, Inc, Waltham, USA) and decay per minute was counted on a liquid scintillation analyser (TRI-CARB 2250 CA).

**Total Phosphorus**
For TP, TDP and DOC the effluent bottles were pooled as shown in Table 13.

**Table 13. Pooling of the bottles for TP, TDP and DOC.**

| ID: | Pooled bottles: |
|---|---|
| 1 | 1 |
| 2 | 2 |
| 3 | 3 |
| 4 | 4, 5, 6, 7 |
| 8 | 8, 9, 10, 11 |
| 12 | 12, 13, 14, 15, 16 |
| 17 | 17, 18, 19, 20, 21 |
| 22 | 22, 23, 24, 25 |

1.25 ml effluent was mixed together with 3.75 ml deionized water and total phosphorus concentration was determined using acid persulphate digestion in an autoclave (120$^{o}$C, 200 kPa, 30 min) (Koroleff, 2011) followed by colorimetric technique (Murphy and Riley, 1962).

**Total Dissolved Phosphorus**
Dissolved phosphorus was defined as the phosphour present in the supernatant after centrifuging for 60 min at 5000 g (lower cut-off particle diameter of 0.1 μm). TDP was sampled as in Table 13, and after centrifugation 1.25 ml supernatant was mixed with 3.75 ml deionized water The total phosphorus concentrations in the supernatant were determined using acid persulphate digestion in an autoclave (120$^{o}$C, 200 kPa, 30 min) (Koroleff, 2011) followed by colorimetric technique (Murphy & Riley, 1962).

**Dissolved Organic Carbon**
DOC samples were pooled as in Table 13 and the concentrations were determined as the amount of total organic carbon (TOC) in the supernatant after centrifugation of 20 ml effluent for 60 min at 5000 g (lower cut-off particle diameter of 0.1 μm). TOC was determined on a TOC-V CPH total organic carbon analyser (SHIMADZU, Deutschland).

# Appendix G

**Table 14. Results from texture analyses.**

| Column no. | Clay (<2 µm) | Silt (2-20 µm) | Coarse silt (20-50 µm) | Fine sand (50-63 µm) | Fine sand (63-125 µm) | Fine sand (125-200 µm) | Coarse sand (200-500 µm) | Coarse sand (500-2000 µm) | Humus | JB | Total C |
|---|---|---|---|---|---|---|---|---|---|---|---|
| | kg kg$^{-1}$ | kg kg$^{-1}$ | kg kg$^{-1}$ | kg kg$^{-1}$ | kg kg$^{-1}$ | kg kg$^{-1}$ | kg kg$^{-1}$ | kg kg$^{-1}$ | kg kg$^{-1}$ | N/A | kg kg$^{-1}$ |
| 1 | 0.148 | 0.159 | 0.145 | 0.046 | 0.145 | 0.094 | 0.158 | 0.071 | 0.035 | 6.0 | 0.021 |
| 2 | 0.149 | 0.158 | 0.139 | 0.055 | 0.149 | 0.088 | 0.164 | 0.064 | 0.034 | 6.0 | 0.020 |
| 3 | 0.142 | 0.165 | 0.138 | 0.049 | 0.156 | 0.090 | 0.164 | 0.062 | 0.035 | 6.0 | 0.021 |
| 4 | 0.143 | 0.171 | 0.138 | 0.047 | 0.154 | 0.089 | 0.159 | 0.065 | 0.035 | 6.0 | 0.020 |
| 5 | 0.142 | 0.172 | 0.132 | 0.042 | 0.149 | 0.096 | 0.168 | 0.065 | 0.034 | 6.0 | 0.020 |
| 6 | 0.149 | 0.165 | 0.144 | 0.053 | 0.144 | 0.081 | 0.159 | 0.071 | 0.035 | 6.0 | 0.020 |
| 7 | 0.149 | 0.165 | 0.145 | 0.048 | 0.149 | 0.090 | 0.158 | 0.061 | 0.034 | 6.0 | 0.020 |
| 8 | 0.143 | 0.171 | 0.141 | 0.052 | 0.149 | 0.089 | 0.160 | 0.061 | 0.034 | 6.0 | 0.020 |
| 9 | 0.149 | 0.165 | 0.123 | 0.071 | 0.148 | 0.095 | 0.160 | 0.055 | 0.036 | 6.0 | 0.021 |
| 10 | 0.150 | 0.164 | 0.140 | 0.048 | 0.143 | 0.090 | 0.167 | 0.066 | 0.034 | 6.0 | 0.020 |
| 11 | 0.150 | 0.157 | 0.158 | 0.042 | 0.150 | 0.097 | 0.159 | 0.053 | 0.035 | 6.0 | 0.020 |
| 12 | 0.151 | 0.163 | 0.131 | 0.065 | 0.147 | 0.081 | 0.158 | 0.070 | 0.034 | 7.0 | 0.020 |
| 13 | 0.154 | 0.159 | 0.147 | 0.051 | 0.153 | 0.088 | 0.156 | 0.057 | 0.034 | 7.0 | 0.020 |
| 14 | 0.156 | 0.164 | 0.146 | 0.049 | 0.142 | 0.079 | 0.161 | 0.069 | 0.034 | 7.0 | 0.020 |
| 15 | 0.150 | 0.157 | 0.123 | 0.072 | 0.150 | 0.092 | 0.159 | 0.062 | 0.036 | 6.0 | 0.021 |
| 16 | 0.150 | 0.164 | 0.151 | 0.047 | 0.138 | 0.079 | 0.170 | 0.066 | 0.036 | 6.0 | 0.021 |
| 17 | 0.143 | 0.171 | 0.163 | 0.057 | 0.137 | 0.088 | 0.155 | 0.053 | 0.035 | 6.0 | 0.020 |
| 18 | 0.144 | 0.163 | 0.128 | 0.072 | 0.151 | 0.088 | 0.161 | 0.058 | 0.035 | 6.0 | 0.021 |
| 19 | 0.143 | 0.164 | 0.158 | 0.048 | 0.159 | 0.088 | 0.151 | 0.058 | 0.032 | 6.0 | 0.019 |
| 20 | 0.143 | 0.164 | 0.129 | 0.067 | 0.146 | 0.090 | 0.158 | 0.070 | 0.032 | 6.0 | 0.019 |
| 21 | 0.144 | 0.170 | 0.146 | 0.049 | 0.151 | 0.086 | 0.165 | 0.055 | 0.035 | 6.0 | 0.020 |
| 22 | 0.143 | 0.164 | 0.129 | 0.074 | 0.140 | 0.095 | 0.154 | 0.067 | 0.034 | 6.0 | 0.020 |
| 23 | 0.144 | 0.176 | 0.146 | 0.048 | 0.154 | 0.087 | 0.157 | 0.055 | 0.033 | 6.0 | 0.019 |
| 24 | 0.150 | 0.170 | 0.118 | 0.075 | 0.151 | 0.090 | 0.156 | 0.058 | 0.033 | 6.0 | 0.019 |
| 25 | 0.150 | 0.170 | 0.148 | 0.049 | 0.146 | 0.084 | 0.153 | 0.068 | 0.033 | 6.0 | 0.019 |
| 26 | 0.144 | 0.170 | 0.127 | 0.071 | 0.149 | 0.090 | 0.159 | 0.055 | 0.036 | 6.0 | 0.021 |
| 27 | 0.143 | 0.171 | 0.145 | 0.054 | 0.149 | 0.093 | 0.157 | 0.055 | 0.034 | 6.0 | 0.020 |
| 28 | 0.150 | 0.164 | 0.144 | 0.060 | 0.143 | 0.091 | 0.162 | 0.052 | 0.035 | 6.0 | 0.021 |

| Column no. | Clay (<2 µm) | Silt (2-20 µm) | Coarse silt (20-50 µm) | Fine sand (50-63 µm) | Fine sand (63-125 µm) | Fine sand (125-200 µm) | Coarse sand (200-500 µm) | Coarse sand (500-2000 µm) | Humus | JB | Total C |
|---|---|---|---|---|---|---|---|---|---|---|---|
| | kg kg$^{-1}$ | kg kg$^{-1}$ | kg kg$^{-1}$ | kg kg$^{-1}$ | kg kg$^{-1}$ | kg kg$^{-1}$ | kg kg$^{-1}$ | kg kg$^{-1}$ | kg kg$^{-1}$ | N/A | kg kg$^{-1}$ |
| 29 | 0.162 | 0.158 | 0.133 | 0.060 | 0.151 | 0.084 | 0.158 | 0.060 | 0.034 | 7.0 | 0.020 |
| 30 | 0.154 | 0.152 | 0.157 | 0.042 | 0.153 | 0.087 | 0.165 | 0.057 | 0.033 | 7.0 | 0.019 |
| 31 | 0.169 | 0.151 | 0.139 | 0.069 | 0.144 | 0.088 | 0.150 | 0.053 | 0.037 | 7.0 | 0.022 |
| 32 | 0.169 | 0.171 | 0.144 | 0.046 | 0.161 | 0.085 | 0.144 | 0.044 | 0.037 | 7.0 | 0.022 |
| 33 | 0.161 | 0.166 | 0.116 | 0.075 | 0.146 | 0.092 | 0.153 | 0.057 | 0.035 | 7.0 | 0.021 |
| 34 | 0.161 | 0.166 | 0.134 | 0.053 | 0.146 | 0.090 | 0.156 | 0.060 | 0.034 | 7.0 | 0.020 |
| 35 | 0.161 | 0.166 | 0.132 | 0.069 | 0.147 | 0.087 | 0.149 | 0.056 | 0.033 | 7.0 | 0.020 |
| 36 | 0.189 | 0.177 | 0.147 | 0.048 | 0.141 | 0.075 | 0.134 | 0.052 | 0.037 | 7.0 | 0.022 |
| 37 | 0.176 | 0.178 | 0.125 | 0.067 | 0.136 | 0.082 | 0.139 | 0.061 | 0.036 | 7.0 | 0.021 |
| 38 | 0.168 | 0.172 | 0.147 | 0.041 | 0.147 | 0.077 | 0.159 | 0.056 | 0.033 | 7.0 | 0.020 |
| 39 | 0.161 | 0.166 | 0.133 | 0.069 | 0.149 | 0.088 | 0.146 | 0.056 | 0.032 | 7.0 | 0.019 |
| 40 | 0.167 | 0.160 | 0.140 | 0.046 | 0.163 | 0.082 | 0.146 | 0.061 | 0.035 | 7.0 | 0.021 |
| 41 | 0.189 | 0.177 | 0.148 | 0.041 | 0.134 | 0.082 | 0.131 | 0.066 | 0.033 | 7.0 | 0.019 |
| 42 | 0.183 | 0.164 | 0.126 | 0.069 | 0.135 | 0.084 | 0.142 | 0.067 | 0.031 | 7.0 | 0.018 |
| 43 | 0.176 | 0.171 | 0.148 | 0.048 | 0.143 | 0.077 | 0.137 | 0.066 | 0.034 | 7.0 | 0.020 |
| 44 | 0.170 | 0.163 | 0.126 | 0.077 | 0.146 | 0.087 | 0.144 | 0.054 | 0.034 | 7.0 | 0.020 |
| 45 | 0.162 | 0.164 | 0.135 | 0.062 | 0.149 | 0.082 | 0.144 | 0.071 | 0.031 | 7.0 | 0.018 |
| 46 | 0.169 | 0.164 | 0.151 | 0.050 | 0.142 | 0.081 | 0.143 | 0.068 | 0.031 | 7.0 | 0.018 |
| 47 | 0.169 | 0.164 | 0.124 | 0.062 | 0.139 | 0.098 | 0.152 | 0.060 | 0.031 | 7.0 | 0.018 |
| 48 | 0.170 | 0.177 | 0.142 | 0.053 | 0.145 | 0.081 | 0.140 | 0.058 | 0.035 | 7.0 | 0.021 |
| 49 | 0.162 | 0.164 | 0.126 | 0.071 | 0.146 | 0.087 | 0.144 | 0.066 | 0.033 | 7.0 | 0.020 |
| 50 | 0.168 | 0.159 | 0.138 | 0.047 | 0.152 | 0.086 | 0.148 | 0.074 | 0.029 | 7.0 | 0.017 |
| 51 | 0.185 | 0.182 | 0.122 | 0.072 | 0.136 | 0.081 | 0.134 | 0.059 | 0.030 | 7.0 | 0.018 |
| 52 | 0.146 | 0.208 | 0.113 | 0.047 | 0.148 | 0.088 | 0.147 | 0.074 | 0.030 | 5.0 | 0.018 |
| 53 | 0.161 | 0.152 | 0.135 | 0.062 | 0.142 | 0.083 | 0.145 | 0.088 | 0.032 | 7.0 | 0.019 |
| 54 | 0.162 | 0.164 | 0.114 | 0.068 | 0.142 | 0.092 | 0.153 | 0.072 | 0.033 | 7.0 | 0.019 |
| 55 | 0.169 | 0.164 | 0.130 | 0.046 | 0.142 | 0.085 | 0.154 | 0.080 | 0.030 | 7.0 | 0.018 |
| 56 | 0.189 | 0.177 | 0.121 | 0.064 | 0.133 | 0.075 | 0.129 | 0.079 | 0.032 | 7.0 | 0.019 |
| 57 | 0.168 | 0.165 | 0.133 | 0.047 | 0.138 | 0.078 | 0.150 | 0.089 | 0.031 | 7.0 | 0.018 |
| 58 | 0.146 | 0.141 | 0.092 | 0.057 | 0.132 | 0.081 | 0.185 | 0.135 | 0.031 | 5.0 | 0.018 |
| 59 | 0.166 | 0.141 | 0.118 | 0.064 | 0.142 | 0.088 | 0.165 | 0.082 | 0.033 | 7.0 | 0.020 |
| 60 | 0.175 | 0.152 | 0.131 | 0.048 | 0.143 | 0.084 | 0.157 | 0.082 | 0.029 | 7.0 | 0.017 |

| Column no. | Clay (<2 µm) | Silt (2-20 µm) | Coarse silt (20-50 µm) | Fine sand (50-63 µm) | Fine sand (63-125 µm) | Fine sand (125-200 µm) | Coarse sand (200-500 µm) | Coarse sand (500-2000 µm) | Humus | JB | Total C |
|---|---|---|---|---|---|---|---|---|---|---|---|
| | kg $kg^{-1}$ | kg $kg^{-1}$ | kg $kg^{-1}$ | kg $kg^{-1}$ | kg $kg^{-1}$ | kg $kg^{-1}$ | kg $kg^{-1}$ | kg $kg^{-1}$ | kg $kg^{-1}$ | N/A | kg $kg^{-1}$ |
| 73 | 0.156 | 0.164 | 0.116 | 0.074 | 0.141 | 0.091 | 0.158 | 0.065 | 0.035 | 7.0 | 0.021 |
| 74 | 0.155 | 0.158 | 0.148 | 0.053 | 0.149 | 0.086 | 0.156 | 0.062 | 0.033 | 7.0 | 0.019 |
| 75 | 0.176 | 0.171 | 0.143 | 0.052 | 0.141 | 0.073 | 0.147 | 0.064 | 0.033 | 7.0 | 0.019 |
| 76 | 0.162 | 0.164 | 0.116 | 0.065 | 0.141 | 0.095 | 0.157 | 0.067 | 0.031 | 7.0 | 0.018 |
| 77 | 0.162 | 0.164 | 0.124 | 0.048 | 0.141 | 0.088 | 0.160 | 0.085 | 0.029 | 7.0 | 0.017 |

# Appendix H

The two silt fractions and the five sand fractions from the texture analyses are put together in respectively the silt and sand contour maps shown in Figure 62.

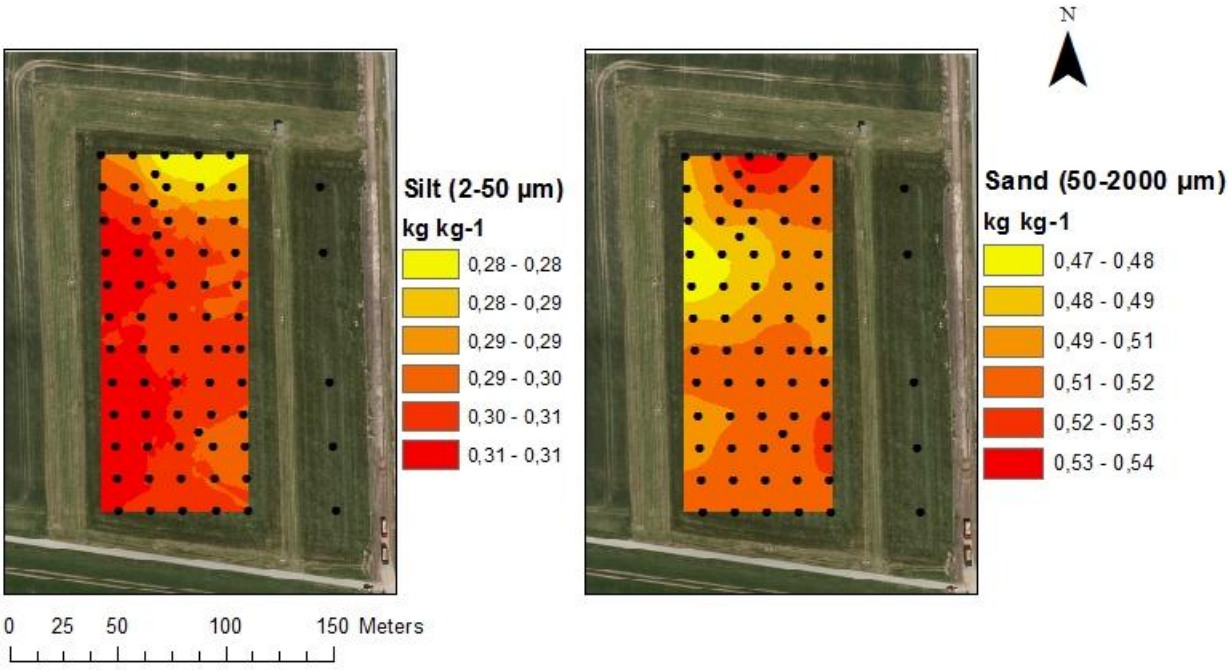


**Figure 62. Contour maps showing the contents of silt and sand (kg kg$^{-1}$).**

# Appendix I

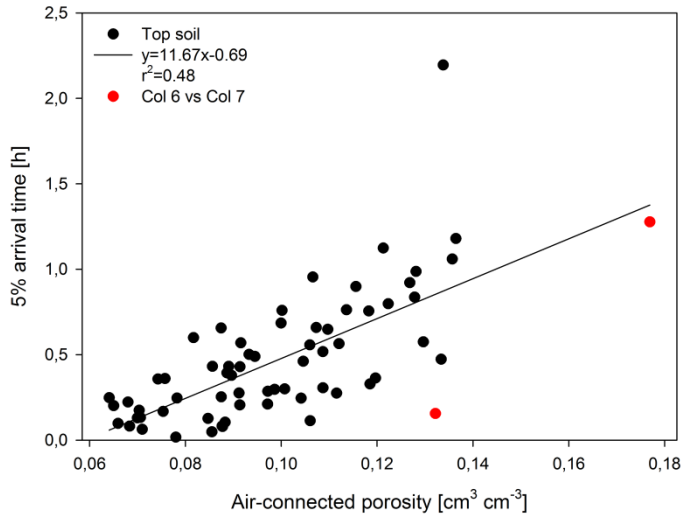


**Figure 63. 5% arrival time as a function of the air-connected porosity measured on the pycnometer.**

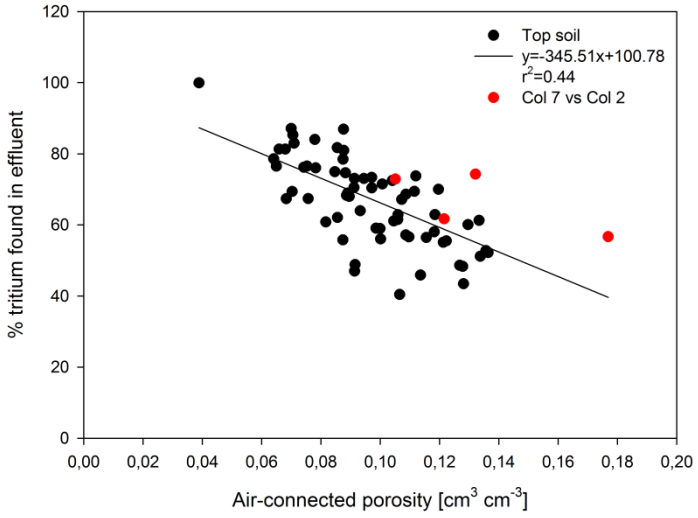


**Figure 64. Tritium recovery in the effluent as a function of the air-connected porosity measured on the pycnometer.**

# Appendix J

The phosphorus concentrations were calculated from standard curves like the one shown in Figure 65.

**Table 15. Standard row concentrations.**

| ppm [mg $L^{-1}$] | Abs |
|---|---|
| 0 | 0,002 |
| 0,025 | 0,017 |
| 0,05 | 0,0325 |
| 0,1 | 0,0625 |
| 0,2 | 0,124 |
| 0,5 | 0,3095 |
| 1 | 0,612 |

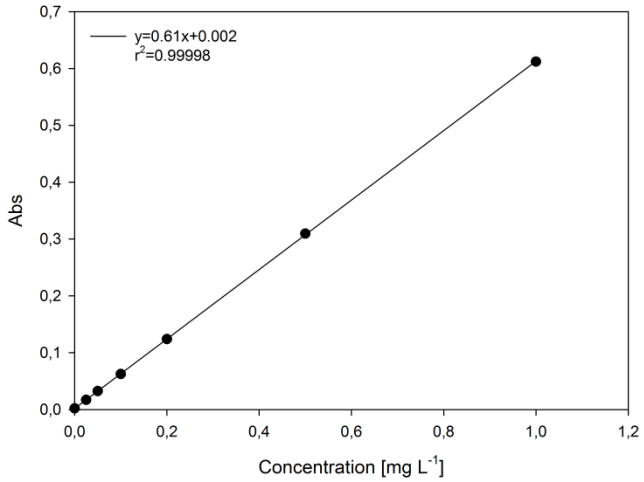


**Figure 65. Standard curve for determination of TP and TDP.**

# Appendix K

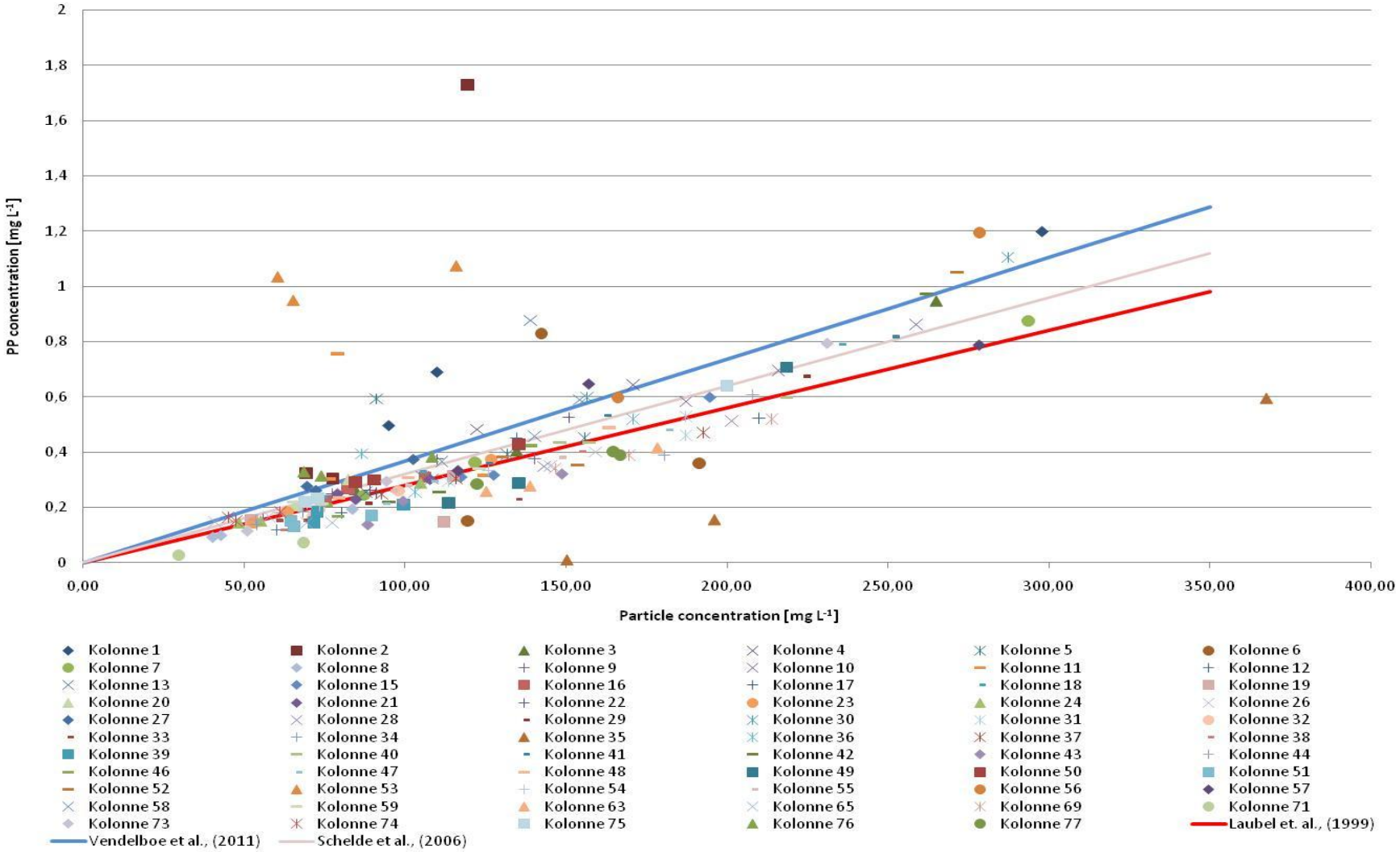


**Figure 66. Particular phosphorus concentrations as a function of particle concentration for all the columns.**

# Appendix L

**Table 16. Summary statistics of soil specific characteristics and measured parameters.**

| | Clay content[1] | Silt content (2-50 µm)[1] | OC content[1] | Bulk density | Air-connected porosity (in situ) | Air permeability (in situ) | Air-filled porosity (in situ) | Average EC | Average pH | Acc. Particle mass at 60 mm | Acc. DOC | Acc. TP | Acc. TDP | Acc. PP |
|---|---|---|---|---|---|---|---|---|---|---|---|---|---|---|
| | kg $kg^{-1}$ | kg $kg^{-1}$ | kg $kg^{-1}$ | g $cm^{-3}$ | $cm^3$ $cm^{-3}$ | $\mu m^2$ | $cm^3$ $cm^{-3}$ | mmho | - | mg | mg | mg | mg | mg |
| Min. Value | 0.14 | 0.23 | 0.02 | 1.39 | 0.04 | 1.58 | 0.06 | 0.09 | 6.72 | 30.00 | 9.73 | 0.13 | 0.07 | 0.05 |
| Max. value | 0.19 | 0.33 | 0.02 | 1.63 | 0.18 | 115.08 | 0.18 | 0.34 | 8.22 | 260.00 | 74.72 | 4.28 | 3.81 | 2.36 |
| Mean | 0.16 | 0.30 | 0.02 | 1.50 | 0.10 | 39.12 | 0.11 | 0.23 | 7.44 | 151.17 | 25.33 | 2.05 | 1.61 | 0.46 |
| Median | 0.16 | 0.30 | 0.02 | 1.49 | 0.10 | 36.80 | 0.11 | 0.23 | 7.50 | 151.50 | 22.43 | 2.04 | 1.63 | 0.43 |
| SD | 0.01 | 0.02 | 0.00 | 0.06 | 0.02 | 23.93 | 0.023 | 0.06 | 0.27 | 41.25 | 13.59 | 0.76 | 0.71 | 0.29 |
| CV(%) | 8.36 | 5.50 | 5.95 | 3.68 | 23.63 | 61.19 | 20.33 | 24.73 | 3.66 | 27.29 | 53.66 | 37.02 | 44.11 | 64.32 |
| Geometric mean | 0.16 | 0.30 | 0.02 | 1.49 | 0.10 | 31.94 | 0.11 | 0.22 | 7.44 | 144.70 | 22.94 | 1.83 | 1.37 | 0.39 |
| Skewness | 0.60 | -1.08 | -0.40 | 0.41 | 0.39 | 1.23 | 0.28 | -0.04 | -0.36 | -0.0024 | 2.56 | 0.17 | 0.37 | 4.02 |

[1] Was determined on separate soil bulk samples taken adjacent to each soil column.

# Appendix M

## Mapping Soil Physical Structure of an Agricultural Field for Assessing Potential Leaching Risk

Trine Nørgaard (1), A.L. Vendelboe (2), L.W. de Jonge (2), P. Moldrup (1), and P. Olsen (2)

(1) Dept.of Biotechnology, Chemistry and Environmental Engineering, Aalborg University, Sohngaardsholmsvej 57, DK-9000 Aalborg, Denmark. (2) Dept. of Agroecology and Environment, Faculty of Agricultural Sciences, Aarhus University, Blichers Alle 20, P.O. Box 50, DK-8830 Tjele, Denmark.

Trine.norgaard@agrsci.dk

**Summary**
The Danish Pesticide Leaching Assessment Programme (PLAP), initiated in 1998, evaluates leaching risk of pesticides and their metabolites. Until recently TPMP (5-(trifluoromethyl)-2(1H)-pyridinone), a metabolite of the pesticide fluazifop-P-butyl sold as e.g. Fusilade X-tra or Fusilade Max, was not considered a potential metabolite. However, at the PLAP field at Silstrup fluazifop-P-butyl application was linked with TFMP detections in a downstream monitoring well just 39 days after application.
The aim of this study is to identify areas within the PLAP field having high tendencies for leaching of pesticides and e.g. phosphorus, and to construct a tool that can assess the risks of pesticide leaching from vulnerable areas to the groundwater based on soil physical and hydrological properties including soil texture, contents of organic matter and clay as well as leaching experiments using intact soil columns.

**Introduction**
During the last decades, detection of pesticides and metabolites in groundwater has increased, forcing several drinking water wells to shut down (Rosenbom et al., 2010). In PLAP 41 pesticides and 40 metabolites have been investigated on 5 locations in Denmark all conventionally cultivated. One of these locations is a field in Silstrup located south of Thisted in the north-western part of Jutland. The installations on the field are shown in Figure 1.

Clay content ranges from 28% to 36% according to EM38 measurements, whereas TOC from samples in the topsoil vary between 1.9 and 2.4% (dry weight) (Lindhardt et al., 2001). Clay content increases to the North and TOC content to the South.

The pesticide Fluazifop-P-butyl was applied at Silstrup on July 1, 2008. It degrades into fluazifop-P (free acid) and later into TFMP. TFMP was first detected in a depth of 1.5 to 3.5 m in monitoring well M5 on August 7, 2008, and subsequently in other installations, see Figure 2 and Figure 3.

**Figure 1. Installations and groundwater flow of the Silstrup test field. A buffer zone (grey) surrounds the cultivated area (white) (Rosenbom et al., 2010).**

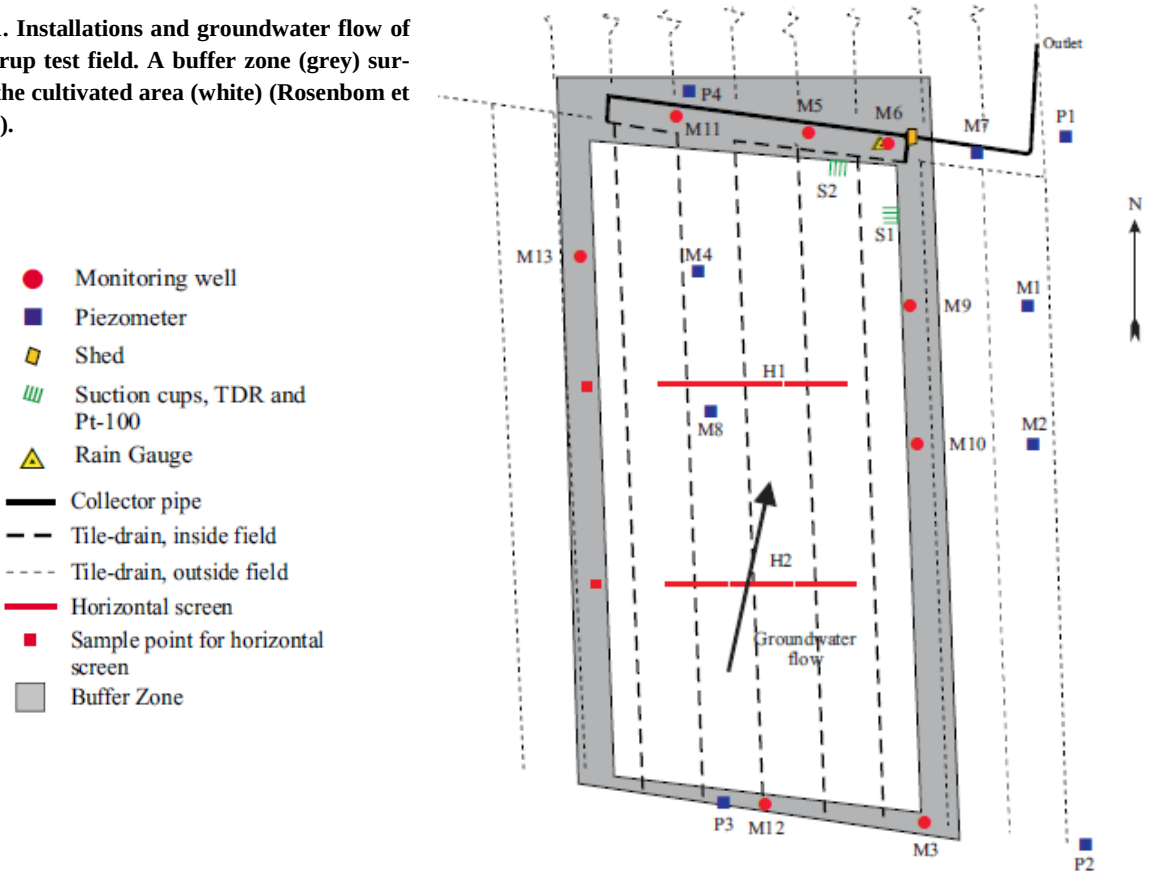


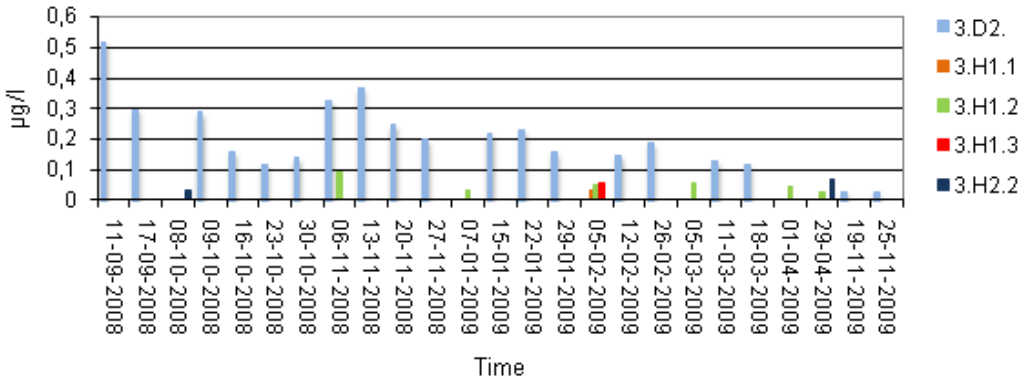


**Figure 2. TFMP concentrations in the horizontal screens (H) and drain (D). The last digits in the legends i.e. 1, 2 or 3 refer to the screen section. Each screen section is 18 m.**

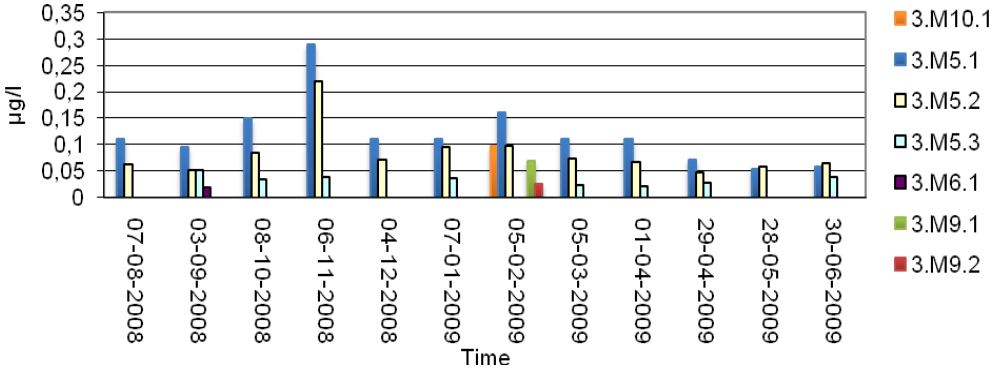


**Figure 3. TFMP concentrations in vertical screens (M). The last digits in the legends i.e. 1, 2 or 3 refer to the depths 1.5-2-5 m, 2.5-3.5 m and 3.5-4.5 m below ground surface, respectively.**

The project will evaluate the field at Silstrup based on new measurements of TOC and clay, structural parameters, and leaching of tritium, colloids and phosphorus to see if leaching of pesticides as TFMP is linked to the soil structure. Further we will construct a "risk map" showing the leaching potential from vulnerable areas.

**Methods**

In a rectangular grid of app. 15 x 15 m, 65 aluminum pipes of 20 x 20 cm was pushed into the topsoil by a hydraulic press, excavated by hand, carefully trimmed at top and bottom and sealed with plastic caps. Further, five samples were taken from areas having high TOC levels or significant TOC gradients. Sampling was done randomly from grid intersections or in random directions 1 m away from intersections.

Air permeability of the columns has been measured. Before the leaching experiments the columns will be saturated with artificial soil water and then drained and equilibrated to -20 cm from the middle of the columns. The columns will be irrigated with a free lower boundary using tritium as tracer. The effluent measurements will include turbidity, electric conductivity, pH, total P, dissolved organic P and dissolved organic C.

On bulk soil samples taken from all sampling points there will be measurements of dispersivity, texture, pH as well as clay and organic matter using near infrared spectroscopy (NIR). Additional 143 samples were taken for the NIR analyses between two grid intersections in both the South-North directions and the East-West directions as well as in each diagonal of the grid.

**Results**

The project is still in an early stage and so far there are no results besides the air permeability measurements on the columns represented in Figure 4 below.

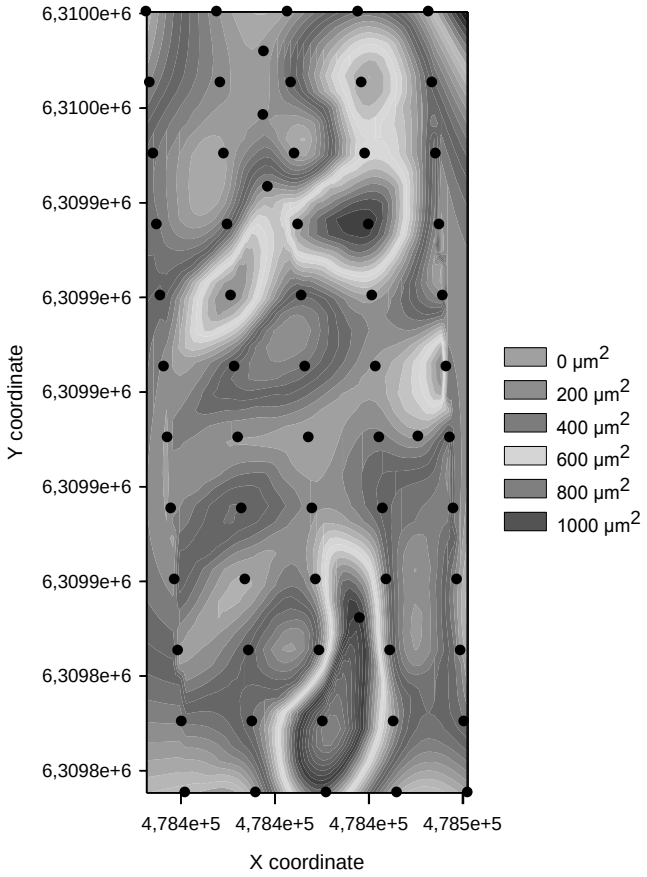


**Figure 4. Contour plot showing the air permeability measured on the columns taken across the field. The black dots indicate the sampling points.**

Air permeability tends to show low values in the North-Western corner of the field, and it is also in the Northern end of the field clay contents and thus soil structure forming potentials are the highest.

## Conclusion/expectations

The expected "risk maps" should be used as a tool for assessing the pesticide or e.g. phosphorus leaching risk from vulnerable areas down to the groundwater.

# Appendix N

## Mapping Soil Physical Structure of an Agricultural Field for Assessing Potential Leaching Risk

Aarhus University
Faculty of Agricultural Sciences

Trine Nørgaard (1), A.L. Vendelboe (2), L.W. de Jonge (2), P. Moldrup (1), and P. Olsen (2)

AALBORG UNIVERSITET

(1) Dept.of Biotechnology, Chemistry and Environmental Engineering, Aalborg University, Sohngaardsholmsvej 57, DK-9000 Aalborg, Denmark.
(2) Dept. of Agroecology and Environment, Faculty of Agricultural Sciences, Aarhus University, Blichers Alle 20, P.O. Box 50, DK-8830 Tjele, Denmark.

### Objectives

The Danish Pesticide Leaching Assessment Programme (PLAP) was initiated in 1998 with the purpose to monitor and evaluate the leaching risk of pesticides and their degradation products.
The aim of this project is to develop a "risk map" based on soil physical as well as hydrological properties. The map should be used as a tool for assessing the leaching risk from vulnerable areas to the groundwater and fresh water streams.
We hypothesize that the contents of clay and organic matter has an influence on the leaching potential.

### Location

PLAP is a monitoring program including five test fields placed at different locations in Denmark. The fields are cultivated as conventional arable fields. This study has its focus on a field in Silstrup located south of Thisted in the north-western part of Jutland.

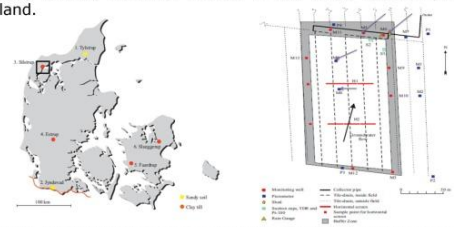

To the left, location of the six test fields in Denmark. The test field in Silstrup is shown in the upper left corner. The figure on the right shows the installation and groundwater flow on the field. Sorbicells are installed in the wells and drain pointed out with purple arrows.

Clay contents ranged from 28 % to 36 %. EM-38 mapping with 1 meter penetration depth indicate that the highest clay content is found in the Northern end of the field. Measurements of TOC contents show a gradient running in the opposite direction of the clay content as shown below.

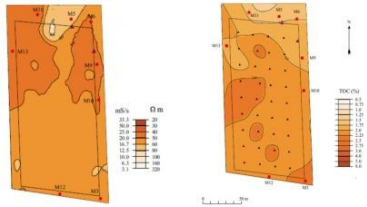

### Pesticide findings in Silstrup

Fluazifop-P-butyl was applied again on the 01-07-2008. The degradation product fluazifop-P was not detected but the degradation product TFMP was found for the first time on the 07-08-2008 and later on as shown below.

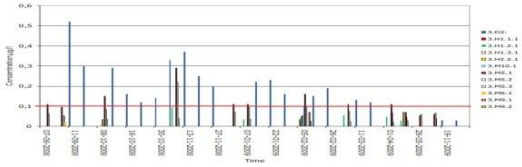

Leaching of TFMP from drains (D), horisontal screens (H) and monitoringwells (M) in Silstrup. The red line at 0.1 µg/l indicates the maximum allowable concentration in groundwater.

### Materials and methods

Seventy aluminium columns 20 cm in height and 20 cm in diameter was pushed into the topsoil in a rectangular approximately 15 x 15 m grid.
The columns were saturated with artifcial soil water and subsequently drained and equilibrated to -20 cm.
Tritium was used as a tracer. Effluent was collected for measurements of turbidity, electrical conductivity, pH, total phosphorus, total dissolved phosphorus and dissolved organic carbon.
Air permeability and pygnometer measurements were performed before saturation. Air permeability was repeated prior to the leaching experiments.

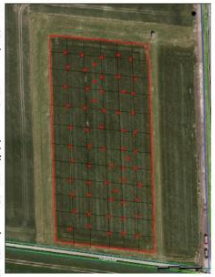

The leaching set up. The columns were irrigated with artificial rain water applied uniformly from the irrigation head.

Bulk soil samples were taken at each column sampling point for texture and dispersibility measurements. Additionally, 143 samples were taken in each grid intersect and diagonals for determination of TOC and clay content.

### Results and discussion

Contour map showing the air permeability across the field before saturation of the columns is shown to the right.
Similar maps will be produced for:
- air permeability before leaching.
- pygnometer measurements.
- clay content and
- TOC content

It would be possible to compare the contour maps for clay and TOC with the maps shown from previous analysis.

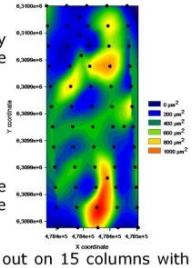

Leaching experiments have been carried out on 15 columns with the results shown below.

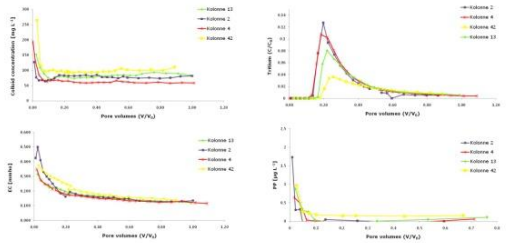

First row is colloid leaching curves and tritium breakthrough curves for four selected columns. Second row shows EC and particular phosphorus (TP-TDP) versus colloid concentration, also for the selected columns.

- The colloid leaching curves show a typical first flush effects after which the values reach a constant level different for each column.
- The skewness and tailing of the tritium curves indicate macropore flow.
- The fast decreasing tendency on the EC curves indicate macropore flow through the columns. Irrigation water has low EC.
- The amount of particular phosphor is correlated to the colloid concentrations.

### Perspective

Results from the study will be used to help explain the leaching of TFMP at Silstrup.

### References

Lindhardt, B., Abildtrup, C., Vosgerau, H., Olsen, P., Torp, S., Iversen, B. V., Jørgensen, J. O., Plauborg, F., Rasmussen, P., & Gravesen, P., 2001. The Danish Pesticide Leaching Assessment Programme - Site Characterization and Monitoring design. 74 p + appendices, Geological Survey of Denmark and Greenland, ISSN/ISBN:87-7871-094-4.
Schelde, K., Moldrup, P., Jacobsen, O. H., de Jonge, H., de Jonge, L. W. & Komatsu, T., 2002. Diffusion-Limited Mobilization and Transport of Natural Colloids in Macroporous Soil. Vadose Zone Journal 1:125-136.

**Figure 67. Poster from Cæsar.**